Wetting on heterogeneous surfaces

by

Hedieh Modaressi-Esfeh

A Thesis submitted to the Faculty of Graduate Studies and Research in partial fulfillment of the requirements of the degree of

Doctor of Philosophy

Department of Chemical Engineering

McGill University

Montréal (Québec)

July 2001

To my mother

ABSTRACT

Dynamic wetting and absorption of water droplets on heterogeneous surfaces, including paper, was studied. The objective was to elucidate the role of surface heterogeneities on wetting and absorption properties of paper. To better understand the phenomena, wetting on glass slides with a controlled level of heterogeneity was investigated. Also, partially hydrophobized glass capillaries were used to simulate capillary penetration into the pores on sized paper.

Dynamic wetting on paper followed a power law model with a lower rate than wetting on a smooth surface. The chemical composition of the paper surface did not affect the wetting dynamics, which was mainly affected by surface roughness in a micron scale. The super-hydrophobic properties of the sized papers were due to air entrapment in the micron-scale roughness on the surface.

Wetting and absorption of water droplets on sized paper occurred in different time scales. A pseudo-equilibrium contact angle was reached at the end of wetting just before absorption of water droplets. Increasing the surface coverage of the hydrophobic domains on paper by sizing increased the pseudo-equilibrium contact angle and delayed absorption into paper. This delay was related to partial dissolution of the surface sizing polymers in the water droplets on the surface.

The equilibrium contact angle of water droplets on partially hydrophobized glass slides was a linear function of a characteristic dimension of the hydrophobic domains and the length of the three phase contact line.

The dynamic rise of water in partially hydrophobized vertical capillaries followed two mechanisms. First, capillary rise was a function of the dynamic contact angle,

changing with the velocity of the contact line. Second, local changes of the advancing contact angle due to the heterogeneities on the capillary walls lowered the capillary rise velocity. The stick (pause) and jump of the contact line was another effect of the hydrophobic domains. Capillary rise dynamics was a function of the advancing contact angle of water droplets measured on a flat glass slide with the same coverage of hydrophobic domains.

RÉSUMÉ

Nous avons étudié le mouillage dynamique et l'absorption de gouttelettes d'eau sur des surfaces hétérogènes, tel que le papier. Ici, notre objectif est d'élucider le rôle des hétérogénéités de surface sur les propriétés de mouillage et d'absorption du papier. Pour mieux comprendre ces phénomènes, le mouillage des surfaces modèles (plaques en verre) est investigué en contrôlant le niveau d'hétérogénéité. Aussi, pour simuler la pénétration capillaire dans les pores du papier, on utilise les capillaires en verre partiellement hydrophobisés.

Le mouillage dynamique sur le papier suit un modèle de loi-puissance avec un taux plus bas que dans le cas du mouillage sur une surface lisse. La dynamique du mouillage n'est pas affectée par la composition chimique, mais surtout par la rugosité de la surface à l'échelle du micron. Nous avons démontré que les propriétés super-hydrophobes du papier couché sont causées par l'emprisonnement de l'air dans les rugosités de la surface à l'échelle du micron.

L'échelle de temps du phénomène de mouillage est différente de celle de l'absorption de gouttelettes sur papier couché. Un pseudo-équilibre de l'angle de contact est atteint à la fin du mouillage, juste avant l'absorption des gouttelettes d'eau. En augmentant la couverture des domaines hydrophobes du papier, l'angle de contact au pseudo-équilibre s'accroît et retarde ensuite l'absorption par le papier. Ce retard est relié à la dissolution partielle des agents de couchage dans les gouttlettes d'eau à la surface.

On a examiné le mouillage des gouttelettes d'eau sur du verre comprenant des domaines hydrophobes. L'angle de contact à l'équilibre des gouttelettes d'eau est une fonction linéaire du rapport entre une dimension caractéristique des domaines

hydrophobes et la longeur de la ligne de contact triphasique. Nous avons montré que l'équation de Cassie ne prend pas suffisamment en compte le caractère hydrophobe de la surface. L'effet de la rugosité sur l'angle de contact est en accord avec l'équation de Wenzel.

Nous avons mesuré la pénétration par capillarité de l'eau dans les capillaires verticaux hydrophobes. L'ascension dynamique suit deux mécanismes. En premier lieu, la montée capillaire est une fonction de l'angle de contact dynamique dépendant de la vitesse d'avancement de la ligne de contact. En second lieu, des variations locales de l'angle de contact se formant à cause des hétérogénéités diminuent la vitesse de la montée capillaire. Les mouvements du type "stick and jump" de la ligne de contact sont liés à la présence des domaines hydrophobes.

FOREWORD

The thesis was prepared in accordance with article B2 of the Guidelines for Thesis Preparation of McGill University. This article reads as follows:

"As an alternative to the traditional thesis format, the dissertation can consist of a collection of papers of which the student is an author or co-author. These papers must have a cohesive, unitary character making them a report of a single program of research. The structure for the manuscript-based thesis must conform to the following:

1. Candidates have the option of including, as part of the thesis, the text of one or more papers submitted, or to be submitted, for publication, or the clearly-duplicated text (not the reprints) of one or more published papers. These texts must conform to the "Guidelines for Thesis Preparation" with respect to font size, line spacing and margin sizes and must be bound together as an integral part of the thesis. (Reprints of published papers can be included in the appendices at the end of the thesis.)
2. The thesis must be more than a collection of manuscripts. All components must be integrated into a cohesive unit with a logical progression from one chapter to the next. In order to ensure that the thesis has continuity, connecting texts that provide logical bridges between the different papers are mandatory.
3. The thesis must conform to all other requirements of the "Guidelines for Thesis Preparation" in addition to the manuscripts.

The thesis must include the following:

(a) a table of contents;
(b) an abstract in English and French;
(c) an introduction which clearly states the rational and objectives of the research;
(d) a comprehensive review of the literature (in addition to that covered in the introduction to each paper);
(e) a final conclusion and summary.

4. As manuscripts for publication are frequently very concise documents, where appropriate, additional material must be provided (e.g., in appendices) in sufficient detail to allow a clear and precise judgement to be made of the importance and originality of the research reported in the thesis.
5. In general, when co-authored papers are included in a thesis the candidate must have made a substantial contribution to all papers included in the thesis. In addition, the candidate is required to make an explicit statement in the thesis as to who contributed to such work and to what extent. This statement should appear in a single section entitled "Contributions of Authors" as a preface to the thesis. The supervisor must attest to the accuracy of this statement at the doctoral oral defence. Since the task of the examiners is made more difficult in these cases, it is in the candidate's interest to clearly specify the responsibilities of all the authors of the co-authored papers.
6. When previously published copyright material is presented in a thesis, the candidate must include signed waivers from the co-authors and publishers and submit these to the Thesis Office with the final deposition, if not submitted previously.
7. Irrespective of the internal and external examiners reports, if the oral defence committee feels that the thesis has major omissions with regard to the above

guidelines, the candidate may be required to resubmit an amended version of the thesis. See the "Guidelines for Doctoral Oral Examinations," which can be obtained from the web (http://www.mcgill.ca/fgsr), Graduate Secretaries of departments or from the Thesis Office, James Administration Building, Room 400, 398-3990.
8. In no case can a co-author of any component of such a thesis serve as an external examiner for that thesis."

This thesis consists of six chapters. Chapter 1 describes the field of research pertaining to the present work and introduces previous results on research relating to the subject of the thesis. Chapter 2, 3, 4 and 5 present the principal results and research conducted, written in manuscript format. Chapter 6 gives an overview of the work and presents the claimed contributions.

The following are the manuscripts written by the author, which were used in the preparation of this thesis. Manuscripts 1, 2, 3 and 4 are included in Chapters 2, 3, 4 and 5, respectively. The co-authors are the thesis supervisors.

1. Modaressi, H. and Garnier, G., "Effect of internal and surface sizing on the wetting and absorption properties of paper", accepted for publication by *Journal of Pulp & Paper Science*, 2001.

2. Modaressi, H and Garnier, G., "Mechanism of wetting and absorption of water droplets on sized paper: Effects of chemical and physical heterogeneity", submitted to *Langmuir*, 2001.

3. Modaressi, H and Garnier, G., "Wetting on a heterogeneous surface", submitted to *Langmuir*, 2001.

4. Modaressi, H, Weber, M.E., and Garnier, G., "Spontaneous penetration of water in partially hydrophobized vertical capillaries", for *Langmuir*, 2001.

ACKNOWLEDGEMENTS

I wish to thank:

My supervisor Dr. Gil Garnier, for his guidance, understanding and support through hard times and for his commitment until the very end.

Dr. Martin Weber, who offered his help at a time when it was most needed. I am especially grateful for his time and enthusiasm and for the invaluable discussions.

Dr. Theo van de Ven, for his challenging and inspiring criticism.

Dr. Juan Vera, for his encouragements and for accepting me as a member of the group.

Dr. Bob Alince for precious advice and for his interest in my work.

Pulp & Paper Research Institute of Canada (PAPRICAN) for providing the facilities and technical assistance.

All of those who came to my oral defense; it was quite an audience! A big thank you goes to: Chris, for putting up with me all this time; Françoise, my best French interviewee, Karine for introducing me to "la culture Quebecoise", Louis for teaching me so many things in such a humble way, and Tom for being a great example!

My sister, for her understanding and unconditional kindness, and my brother, for inspiring me and showing me the way.

My parents, for their love and for encouraging me to be where I am today.

And finally, Mehdi & Persis, my little family, for enduring such a long journey and for the joy we have always shared together. I love you!

CONTENTS

ABSTRACT		iii
RÉSUMÉ		v
FORWORD		vii
ACKNOWLEDGEMENTS		ix
CONTENTS		x
LIST OF FIGURES		xiv
LIST OF TABLES		xviii

CHAPTER 1

Introduction		1
1.	GENERAL	1
2.	BACKGROUND	2
2.1.	Sizing	3
2.1.1.	Internal sizing	4
2.1.2.	Surface sizing	6
3.	RATIONALE AND SCOPE OF THIS INVESTIGATION	7
4.	REFERENCES	10

CHAPTER 2

Effect of internal and surface sizing on the wetting and absorption properties of paper		12
Abstract		12
1.	INTRODUCTION	13
2.	EXPERIMENTAL	16

2.1. Materials 16

2.2. Methods 16

3. RESULTS 20

4. DISCUSSIONS 32

5. CONCLUSIONS 40

6. ACKNOWLEDGEMENTS 41

7. REFERENCES 42

CHAPTER 3

Mechanism of wetting and absorption of water droplets on sized paper: Effects of chemical and physical heterogeneity 44

Abstract 44

1. INTRODUCTION 45

2. EXPERIMENTAL 50

2.1. Materials 50

2.2. Methods 53

3. RESULTS 56

4. DISCUSSION 63

5. CONCLUSION 73

6. ACKNOWLEDGEMENTS 73

7. REFERENCES 74

CHAPTER 4

Wetting on a heterogeneous surface 77

Abstract 77

1. INTRODUCTION 79

2. EXPERIMENTAL 84

2.1. Materials 84

2.2. Methods 84

2.2.1. Application of Polystyrene 84

2.2.2. Surface Coverage Measurements 85

2.2.3. Surface Roughness Measurements 85

2.2.4. Contact Angle Measurements 85

3. RESULTS 87

4. DISCUSSION 100

4.1. Latex Deposition 100

4.2. Wetting 101

5. CONCLUSION 109

6. ACKNOWLEDGEMENTS 109

7. REFERENCES 110

CHAPTER 5

Spontaneous penetration of water in partially hydrophobized vertical capillaries 112

Abstract 112

1. INTRODUCTION 113

2. EXPERIMENTAL 118

2.1. Materials 118

2.2. Methods 119

2.2.1. Surface Coverage Measurement 119

2.2.2 Contact Angle and Advancing Angle Measurement 119

2.2.3. Capillary Rise Measurement 120

3. RESULTS 122

4. DISCUSSION 129

5. CONCLUSION 136

6. ACKNOWLEDGEMENTS 136

7. REFERENCES 137

CHAPTER 6

Conclusions and contributions 139

1. CONCLUSIONS 139

1.1. Effect of sizing on wetting and absorption properties of paper 139

1.2. Dynamics of wetting and absorption of sized papers 139

1.3. Wetting on a heterogeneous impermeable surface 140

1.4. Capillary penetration in partially hydrophobized vertical capillaries 140

2. CONTRIBUTIONS TO KNOWLEDGE 141

LIST OF FIGURES

CHAPTER 2

Figure 1. Schematic of the experimental setup

Figure 2. Line profilometry

Figure 3. Droplet contact angle and volume vs time for ASA(0/0) paper. Delay is shown.

Figure 4. Evolution of the apparent contact angle as a function of time for different sizing treatments. A) ASA internal sizing with starch surface sizing, B) ASA internal sizing only, C) AKD internal sizing with starch surface sizing, D) AKD internal sizing only.

Figure 5. Effect of surface sizing on the pseudo-equilibrium contact angle of a droplet deposited on AKD (■) and ASA (●) internally sized papers.

Figure 6. Absorption mechanism for a water droplet on sized paper. a) Side view showing droplet spherical cap shape at successive times b) Top view showing penetration in the sheet with a motionless contact line.

Figure 7. Typical stick and jump movement of the base line of uncalendered and calendered papers.

Figure 8. Comparison of the HST and the absorption rate of a sessile droplet of water on sized papers. ■ is for AKD papers and ◆ is for ASA papers.

CHAPTER 3

Figure 1. Schematic of the experimental setup.

Figure 2. Typical scanning electron microscopy (SEM) of the paper surface. The white domains are the calcium carbonate aggregates.

Figure 3. Typical dynamics of a water droplet on sized paper. Two regimes can be distinguished. 1) Governed by wetting 2) Dominated by absorption into paper. Evaporation was kept negligible.

Figure 4. Effect of paper roughness on the apparent contact angle of water droplets. Surface chemistry is constant. The average roughness reached by calendering is indicated.

Figure 5. Wetting and absorption mechanism of a droplet on paper. a) Decrease in the apparent contact angle due to bulk absorption, b) Radial penetration of the droplet.

Figure 6. Hoffman-Tanner model for wetting dynamics of water droplets on sized paper.

Figure 7. Wetting dynamics of water droplets on sized papers. For reference, the theoretical hydrodynamic and friction regimes are also plotted.

Figure 8. Effect of the surface concentration of hydrophobic domains (SMA) on equilibrium contact angle of water. ■ is for ASA papers and ○ is for AKD papers.

Figure 9. Schematic representation of air entrapped in the valleys on paper roughness.

Figure 10. Effect of surface chemical composition and roughness on the wetting rate of water on paper. Roughness on the papers is indicated.

CHAPTER 4

Figure 1. Top view microscopy images of latex deposited glass slides. Deposition time and % coverage is shown for each picture.

Figure 2. Latex coverage on glass as a function of deposition time. ■ is for 2-hr annealed latex deposited glass slides; ◆ is for the air-dried latex deposited glass slides without any heat treatment.

Figure 3. Scanning electron microscope images of latex deposited glass slides; a) air dried latex particles with no heat treatment; b) 2-hr annealed latex particles.

Figure 4. Evolution of contact angle of water droplets on latex treated glass slides: a) 5-min annealing at 150 °C; b) 2-hr annealing at 150 °C. The % coverage of latex particles on glass is shown on each plot.

Figure 5. AFM image of latex deposited glass slide annealed for 2 hours at 150 °C.

Figure 6. Evolution of the advancing/receding contact angle with volume for 5-min annealed latex deposited glass; deposition time was 10 minutes (12% coverage). ◆ is the advancing and ■ is the receding angle.

Figure 7. Comparison between Cassie's model prediction and experiments. Dashed line shows Cassie's model for 5-min annealed and solid line shows the same model for 2-hr annealed latex particles, ■ is for the 2-hr annealed and ▲ is for the 5-min annealed latex deposited glass slides.

Figure 8. The true surface area covered by a single particle assuming the liquid doesn't remove the air from the space under the particle.

Figure 9. Comparison between experimental data, Cassie's model and the model proposed by Swain and Lipowsky. ■ is for experimental data, solid line shows Cassie's model and dashed line shows the model proposed by Swain and Lipowsky.

Figure 10. Geometry of particles after 5-min annealing and 2-hr annealing.

CHAPTER 5

Figure 1. Spontaneous penetration into a single capillary.

Figure 2. Contact angle measurement on a flat surface; a) advancing angle measured as the volume increases; b) receding angle measured as the volume decreases.

Figure 3. Scanning electron microscopy of annealed latex particles on a glass slide.

Figure 4. Size distribution of latex particles annealed on a glass slide for 2 hours. The deposition time was 10 minute and the coverage was 16%.

Figure 5. The advancing and receding contact angle of water on a glass slide with 16% surface coverage of annealed latex particles. Two replicates are shown.

Figure 6. Capillary rise dynamics in capillaries of 0.8 mm radius. The percent surface coverage of hydrophobic domains is shown on each curve.

Figure 7. Reproducibility of capillary rise dynamics in capillaries of 0.8 mm radius with 16% coverage of hydrophobic domains. The stick and jump of the contact line is shown for one replicate.

Figure 8. Capillary rise dynamics in capillaries of 0.3 mm radius and 1% coverage of hydrophobic domains. Curves: 1) Equation 5 (Washburn's model with gravity) assuming $\theta = \theta_a$ 2) Equation 13, assuming $\theta = \theta_a$

Figure 9. Mechanism of the three phase contact line advancement in presence of hydrophobic domains. a) The contact line is pinned at the contact point to the hydrophobic domains; b & c) The contact line curves around the hydrophobic domains as water proceeds; d) The sudden jump and contact line over the hydrophobic domains.

Figure 10. Capillary rise dynamics in capillaries of 0.3 mm radius and 1% coverage of hydrophobic domains. The solid line is the model.

LIST OF TABLES

CHAPTER 2

Table I. Properties of sized papers.

Table II. Surface roughness of sized papers.

Table III. Delay time before water absorption.

Table IV. Absorption rate on sized paper.

CHAPTER 3

Table I. Physical properties of papers. Pick-up, mean pore diameter, porosity and roughness.

Table II. Bond numbers for water droplets deposited on paper.

Table III. Pseudo-equilibrium contact angle (θ_e^*), advancing angle (θ_a), receding angle (θ_r) and hysteresis ($\Delta\theta$) of water droplets on sized paper. Four replicates were at least measured.

CHAPTER 4

Table I. Average height of the latex particles measured by AFM Section Analysis.

Table II. Advancing Angle (θ_a), Receding Angle (θ_r) and Hysteresis ($\Delta\theta$) for latex deposited samples annealed for 5 minutes at 150 °C.

CHAPTER 1

Introduction

1. GENERAL

Non-impact printing has the fastest growing rate in the printing industry. For instance, inkjet printing has become one of the most popular printing techniques in recent years. One of the major parameters affecting print quality is the chemical composition of paper surface. To achieve the desired print quality, chemical composition of the paper is manipulated by applying a surface treatment (sizing). This technique creates hydrophobic domains on the fibers in a paper sheet, however the mechanism by which these domains control the print quality is ambiguous. Whether the distribution or/and the size of these domains plays the major role in enhancing the hydrophobicity of a paper sheet is still unknown. Understanding the mechanism by which hydrophobic domains on a surface, in general, interact with a liquid droplet has a significant impact not only in printing industry but also in other industries such as agriculture, pharmaceutical and biotechnology.

Upon contact of a droplet of ink with the paper surface, three major phenomena occur which affect print quality: wetting, absorption and evaporation. Among these three, wetting and absorption are functions of the chemical heterogeneity of paper. Wetting is also affected by the paper surface roughness. Hence, surface treatment of paper, whether chemical or physical, affects the print quality by influencing these two phenomena. In order to elucidate the role of heterogeneity, whether chemical or physical, on these phenomena some questions should be answered:

1. How does chemical or physical heterogeneity of a surface affect the shape of a liquid droplet on a heterogeneous surface? This can be quantified by measuring the contact angle a liquid droplet forms on the surface: 1) under static conditions (the equilibrium contact angle); 2) under dynamic conditions (the apparent contact angle).
2. Does surface heterogeneity affect the dynamics of wetting and absorption? Which of the chemical and physical heterogeneities have the most significant effect on these phenomena?
3. Is wetting or absorption a function of the scale of heterogeneity? Does distribution or size of various chemical/physical domains on the surface affect these phenomena?
4. Is there a link between wetting and absorption behavior of a liquid on a porous surface with chemical and physical heterogeneity? What is the mechanism of absorption into a porous heterogeneous surface and how does it relate to capillary penetration into a tube with heterogeneous domains?

This thesis attempts to answer the above questions both experimentally and by evaluating the existing models for wetting and absorption into heterogeneous surfaces. In the first part of this chapter a general review of paper technology and sizing is presented. In the second part, the rationale and the scope of the thesis are described.

2. BACKGROUND

Paper results from the continuous drainage of a fiber suspension onto a moving screen. The fibrous suspension used as raw material for papermaking is called pulp.

Pulp fibers usually have plant origin although synthetic fibers may be used for special applications. Fibers used in papermaking should be conformable and must have a stable structure. In plant fibers, cellulose is the main substance determining the fiber character and permitting its use in papermaking. Cellulose is a polysaccharide with the chemical formula $(C_6H_{10}O_5)_n$. The degree of polymerization (DP) for most commercial wood pulps is in the range of 600-1500 (weight-averaged) [1]. Softwood fibers are generally tapered cylinders 3 mm long and about 30 μm in diameter. Hardwood fibers are about 2 mm long with a diameter of 20 μm [2].

In the papermaking process, after the pulp has been made by either chemical or mechanical means, it is diluted to a solid concentration of 0.2 to 1%. Since the dilution is done by water, the hydrophilic nature of cellulosic fibers accelerates water absorption and facilitates dispersion of fibers in the water suspension. To enhance specific sheet properties, several additives are added to the furnish at this point. These additives include: fillers (clay, talc, TiO_2), retention aids, fiber flocculants, slimicides, and sizing agents. The pulp suspension then enters to the paper machine, where it is drained and pressed to yield a paper web containing about 40-45% solids. The wet paper web is then dried and is ready for further surface treatments such as sizing, coating, and calendering. Sizing and coating change the chemical composition of the paper surface while calendering changes the fibrous network by pressing the paper to smooth the surface.

2.1. Sizing

Sizing is performed mainly to make paper more resistant to wetting and penetration by liquids. When hydrophobic colloids are added to the wet furnish (pulp suspension) before the paper machine, the process is referred to as "internal sizing".

Surface application of hydrophobic polymers or colloids to paper is known as "surface sizing". The most important variable controlling the rate of liquid penetration into paper is the contact angle formed between the liquid and paper surface. A contact angle larger than 90° inhibits wetting and penetration. The contact angle a liquid forms on a smooth surface is a function of the chemical composition of the surface. Hence, by manipulating the chemical composition of the surface, wetting and penetration of a liquid into paper may be controlled.

2.1.1. Internal sizing

Internal sizing, the most common way of sizing, was first used by Illig in 1807 [3]. The traditional internal sizing agent is a modified water soluble rosin, although a non-soluble dispersed free acid form is also used. Natural rosin, an amber-colored resin from southern pines, is an amphipathic material, i.e. it has both hydrophilic and hydrophobic parts. Rosin does not react chemically with cellulose and is categorized as a non-reactive or bulk sizing agent. Rosin is anionic and consequently has no affinity for cellulosic fibers. With the aid of aluminum sulfate (alum) the rosin is deposited and fixed on fibers. Rosin retention on fibers depends on its particle size and electrostatic attraction with fibers. The drying conditions of the paper web also affect internal sizing by rosin. The moisture content of the web affects the orientation of the deposited aluminum resinate; a more uniform distribution over fibers is achieved when the proper heat-moisture relationship is established.

Application of cellulose-reactive sizing agents started in the 1960s. These sizing systems, which are based on alkyl ketene dimers (AKD) or alkenyl succinic acid derivatives (ASA), have attracted increasing attention recently. About 50% of the North

American alkaline fine paper is sized by ASA, however ASA has been poorly accepted in Europe [3].

ASA is a yellowish oily product. Since it does not dissolve in water, prior to application, it is emulsified. Cationic starch, a small amount of activator, normally 3-6%, and a stabilizer which is normally a synthetic cationic polymer are added to ASA for emulsification. The synthetic cationic polymers induce a positive charge on the oil droplets, which improves ASA retention on fibers and increases sizing efficiency. The reaction of ASA with cellulose in the presence of water is fast and irreversible, however besides the formation of the desired covalent ester linkage, the undesirable hydrolysis of ASA also occurs. Poor emulsion stability and ASA hydrolysis are among the major obstacles to general use of ASA for internal sizing. The major advantage to its use is the rapid reaction with cellulose in the dryer sections of a paper machine.

Alkyl ketene dimers (AKD) are unsaturated lactones. AKD used for paper sizing was first developed by Hercules Inc. in the United States [3]. In the commercial synthesis of AKD waxes, technical grade saturated fatty acids are used. Examples are: palmitic acid, lauric acid, and stearic acid. AKD wax is dispersed as small particles in water before addition to the wet furnish. For emulsification (since the AKD is added to water in molten state) AKD flakes are added to a water solution containing cationic starch (stabilizer) and a small amount of surfactant. The high temperature of this solution causes the AKD flakes to melt. The mixture is then passed through microfluidizers. After cooling the resulting dispersion contains particles in the range of 0.5-2 μm. The charge of AKD varies from slightly to highly cationic depending on the amount of the cationic starch or other cationic stabilizers added. AKD reacts with cellulose to form β-

keto-esters. A hydrolysis side reaction also occurs which has been controlled in the recent years with the production of more stable AKD dispersions. Prior to the chemical reaction, the dispersed cationic AKD particles adsorb onto the fiber surfaces by electrostatic attraction. The adsorbed AKD particles melt and partially cover the fibers as the web is heated during drying. Once a certain humidity (moisture content) on the web is reached, the chemical reaction between AKD and cellulose begins. Re-arrangement of the molecules, which causes the hydrophobic tails to orient away from the surface, provides water repellency. Surface coverages of up to 5% of fibers under practical internal sizing conditions have been reported [10]. Compared to ASA, AKD is considerably less reactive [3].

2.1.2. Surface sizing

Surface sizing is as ancient as papermaking itself. In surface sizing the agent is applied to the surface of paper where it glues the surface fibers to the bulk of the paper. Surface sizing reduces the size of the pores on the surface thus, besides increasing water repellency, it increases paper resistance to wetting by oil. Surface sizing also increases surface strength.

Starch is the principal commercial surface sizing agent. Other agents used for surface sizing include: methyl cellulose, carboxymethyl cellulose, animal glue, polyvinyl alcohol, wax emulsions, and certain polymers. Surface sizing is most commonly applied at the size press, between drying sections. A size press normally consists of two rolls between which the paper passes while absorbing the sizing solution. The objective in surface sizing is to keep the sizing agents on the paper surface, although penetration of starch into paper during surface sizing is also desirable since it improves the internal properties of the sheet. Starch only partially covers the fiber surfaces yielding a non-

uniform film on the paper. Surface sizing with starch prevents loosening of the surface fibers by increasing fiber-fiber bonding. Surface sizing improves the writing quality of paper by affecting the contact angle, reducing the porosity and increasing the smoothness. It also improves the erasability of paper since it increases resistance to ink penetration and abrasion, and increases surface smoothness. Since the viscosity of native starch is too high for surface sizing, chemically modified starches like: oxidized starches, cationic starches and hydroxyethyl ether derivatives are often preferred [12].

Styrene-copolymers are another class of sizing agents used on paper. These copolymers contain carboxyl or acid anhydride groups. For instance, styrene maleic anhydride (SMA) is mixed with starch and applied to the paper surface in a size press. Hydrolyzed styrene maleic anhydride polymers are more surface active in solution than starch, hence upon sizing, SMA stays on top of starch. The hydrophobicity transferred to the paper surface is due to the styrene tails of SMA which are oriented away from the paper surface. Styrene-copolymer resins can be dissolved in water with ammonia. Ammonia evaporates in the drying stage after surface sizing and the resin reverts to its water-insoluble acidic form, which then deposits on the paper. Styrene-copolymer resins are also used in the form of water-soluble sodium salts. The ammonium salt of SMA however, is more efficient for surface sizing [15].

3. RATIONALE AND SCOPE OF THIS INVESTIGATION

Paper consists of a porous structure made of fibers of different forms and sizes. Capillary penetration of a liquid into this porous network is a function of the contact angle the liquid forms with the fibers either on the surface or in the bulk of paper.

However, due to sizing, the surface chemical composition of the fibers is heterogeneous, consisting of hydrophobic and hydrophilic domains. This heterogeneity strongly affects the dynamics of wetting and penetration of the liquid in contact with paper. Another important factor affecting liquid interactions with paper is the physical heterogeneity of paper due to the roughness of the surface. To develop effective sizing strategies, understanding the mechanisms of interactions between the sizing agents on paper and ink is essential.

In this investigation the interactions between water and a heterogeneous surface were studied. The objective was to elucidate how wetting and penetration of a liquid is affected by physical and chemical heterogeneity of the surface. To reach this objective the project was divided into four sections (Chapters 2-5):

In Chapter 2, the effects of internal and surface sizing on wetting and absorption of water droplets on paper are described. The evolution of the contact angle of water droplets on sized papers, varying in type and concentration of the sizing agents, was monitored. Conventional testing methods of sizing and the results of the contact angle measurements were compared. This chapter gives a better understanding of the mechanisms of wetting and absorption of water droplets on sized paper.

In Chapter 3 the dynamics of wetting of sized paper by water droplets are investigated. The Dynamic wetting of sized paper are compared to existing models for dynamic wetting on smooth, homogeneous surfaces. In this chapter the role of surface roughness in enhancing the hydrophobicity of paper is elucidated.

Chapter 4 presents a theoretical and experimental study of wetting of water droplets on a glass surface with controlled physical and chemical heterogeneity. With

glass as the model surface, water absorption is eliminated, so that the effect of surface heterogeneities on wetting is isolated.

In Chapter 5 a study of the effect of surface heterogeneity on capillary penetration is presented. Theoretical models for dynamics of capillary penetration are compared to the experimental measurements of water rise in partially hydrophobized glass capillaries.

The conclusions from this work and the contributions to knowledge are presented in Chapter 6.

4. REFERENCES

1. G.A. Smook, Handbook for pulp and paper technologists, Angus Wilde Publications, Vancouver, B.C., **1992**.
2. T. Asselman, Hetero-flocculation of wood fibers and fines induced by polymers and microparticles, Ph.D. Thesis, McGill University, Montreal, Canada, **1999**.
3. L. Neimo, Internal sizing of paper, in Paper making chemistry, Chapter 7, Fapet Oy., Finland, **1999**, 151-204.
4. T. Lindstrom and D. Eklund, Water penetration and internal sizing, in Paper Chemistry: An introduction, DT Paper Science Publication, **1991**, 192-222.
5. T. Lindstrom and G. Soderberg, On the mechanism of sizing with alkyl ketene dimers, Part 1: Studies on the amount of alkyl ketene dimers required for sizing different pulps, Nordic Pulp and Paper Research Journal, **1986**, 1, 26-33.
6. T. Lindstrom and H. O'Brian, On the mechanism of sizing with alkyl ketene dimers, Part 2: The kinetics of reaction between alkyl ketene dimers and cellulose, Nordic Pulp and Paper Research Journal, **1986**, 1, 34-42.
7. T. Lindstrom and G. Soderberg, On the mechanism of sizing with alkyl ketene dimers, Part 3: The role of pH, electrolytes, retention aids, extractives, sulfonates and mode of addition on alkyl ketene dimers retention, Nordic Pulp and Paper Research Journal, **1986**, 1, 31-38.
8. L. Yu and G. Garnier, Mechanism of internal sizing with alkyl ketene dimers: the role of vapors, 11th Fundamental Research Symposium, Cambridge, **1997**, 2, 1021-1046.

9. G. Garnier, J. Wright, L. Godbout, and L. Yu, Wetting mechanism of alkyl ketene dimers on cellulose films, Colloids and Surfaces, **1998**, 153-165.

10. G. Garnier and L. Yu, wetting mechanism of starch-stabilized alkyl ketene dimer emulsion: a study by atomic force microscopy, Journal of Pulp and Paper Science, **1999**, 25, No. 7, 235-242.

11. L.Yu and G. Garnier, The role of vapor deposition in internal sizing: a comparative study, Post-Graduate Research Laboratory Report, PGRLR745, Pulp & Paper Research Institute of Canada, **1999**, 1-11

12. M.L. Cushing, Surface sizing, in Pulp and Paper Chemistry and Technology, 3, 2nd ed., (J.P. Casey, editor) John Wiley & Sons, New York, **1981**, Chapter 20, 1667-1715.

13. D.E. Ekland, Review of surface application, in Fundamentals of papermaking, C.F. Baker, Mechanical Engineering Publications Limited, London, **1990**, 2, 833-870.

14. G. Garnier, M. Duskova-Smrckova, R. Vyhnalkova, T.G.M. van de Ven and J.F. Revol, Association in solution and adsorption at air-water interface of alternating copolymers of maleic anhydride and styrene, Langmuir, **2000**, 16, 3757-3763.

15. B. Sitholé and B. Ambayec, Identification and determination of surface sizing agents on sized papers, Journal of Pulp & Paper Canada, **2000**, 101, No. 9, 53-55.

16. G.L. Batten, The effects of SMA surface sizes on paper end-use properties, Tappi Journal, **1995**, 142-146.

17. W.F. Reynolds, The sizing of paper, 2nd edition, TAPPI Press, **1989**.

CHAPTER 2

Effect of internal and surface sizing on the wetting and absorption properties of paper

Hedieh Modaressi and Gil Garnier[1]
Paprican and Department of Chemical Engineering
McGill Pulp and Paper Research Center
3420 University St.
Montreal, QC H3A 2A7

Abstract

The effect of internal and surface sizing on the wetting and absorption behavior of a water droplet on paper was studied. Two individual internally sized papers were selected (AKD, ASA) and surface sized using different concentrations of a mixture of a sizing polymer (Styrene Maleic Anhydride) and starch. Measuring the apparent contact angle of water droplets on papers revealed that the wetting characteristics of the surface varied as a function of the concentration of the sizing polymer (SMA) on the surface. Wetting and absorption were found to be two sequential phenomena. The equilibrium contact angle (θ_e^*) increased with the SMA concentration. Highly hydrophobic paper surfaces (θ_e^*>110°) resulted from the combination of internal and surface sizing. The delay before bulk absorption was also a function of SMA concentration on the surface. Delay was related to some SMA dissolution into the water droplet, which produced hydrophilic channels (θ_e^*<90°) locally. Unsteady stick and jump movement of the contact line during wetting was significant and decreased upon calendering.

Keywords: wetting, absorption, paper, internal sizing, surface sizing, AKD, ASA, SMA.

[1] For correspondence: ggarni@po-box.mcgill.ca

1. INTRODUCTION

Paper is a unique material with chemical and physical heterogeneity both in the bulk and on the surface. The chemical heterogeneity of the surface is caused by a mixture of hydrophobic and hydrophilic polymers used in surface sizing. The physical heterogeneity on the surface, on the other hand, is interpreted as roughness. Internal sizing also provides a chemical heterogeneity in the bulk and at the surface. The physical heterogeneity of the porous structure is due to pores of different shapes and sizes in the complex network of fibers forming paper. Paper is highly susceptible to external factors such as moisture and external pressure; this makes the prediction of wetting and absorption on paper challenging.

In this work, we characterize the effect of internal and surface sizing on the wetting and absorption properties of paper. The behavior of water droplets on differently sized papers was monitored by measuring their apparent contact angle and their base line length (diameter) on the surface.

Two sequential phenomena of wetting and absorption occur as a water droplet comes into contact with paper [1]. A pseudo-equilibrium stage separates the two phenomena. During this stage, the droplet rests on the surface with an immobile contact line and the apparent contact angle remains constant [1]. This angle is referred to as the pseudo-equilibrium contact angle of the droplet on the paper [2].

A time delay occurs before liquid absorption into paper [3,4], but the mechanism is not clear. Aspler [3] proposed that the wetting delay is the time for the contact angle of the droplet to decrease from above 90° to below 90° because according to the Lucas-Washburn equation, this is the necessary criterion for liquid penetration into a pore.

However, according to Kent and Lyne [5], this criterion applies only to penetration into cylindrical pores. They show that penetration into a convergent pore can occur even at a contact angle above 90°. It has also been reported that wetting delay (or absorption delay) is a function of the surface tension of the liquid and disappears as the surface tension decreases [3]. Wetting delay was also attributed to natural sizing of cellulose fibers, preventing absorption [6]. Bulk absorption into paper was claimed to occur only after a monolayer of water is adsorbed on the cellulosic fibers [7]. The effect of each sizing component (AKD/ASA, starch, SMA/Latex) on wetting and absorption is still poorly understood. It was reported that starch, the hydrophilic polymer applied on paper during surface sizing, reduces penetration normal to the sheet while it has limited effects on the radial penetration [4]. No comprehensive studies describing the role of starch are available. Internal sizing with AKD is known to reduce bulk absorption of aqueous inks in paper [4]. In a recent study Wagberg and Westerlind [2] showed that internal sizing with 1 kg/t of AKD increased the equilibrium contact angle of water droplets on paper to 110°. The equilibrium contact angle for a sessile drop of water on the same paper (without sizing) was 40°.

The effect of surface roughness on the wetting properties of solids was investigated [1,8,9,10]. The grooves present on a solid surface control the wetting pattern [8]. The unsteady stick and jump movements of the contact line of a droplet often observed during wetting on a solid surface, are due to roughness [15]. Roughness also affects the equilibrium contact angle of liquid droplets on paper [1]. However, the effect of roughness is less significant for papers with higher internal sizing pick-up [2].

The primary objective of this study is to quantify the role of internal and external sizing on the wetting and absorption behavior of a water droplet on paper. As a secondary objective, a common sizing technique (Hercules Sizing Test) will be compared to the wetting and absorption rate of sessile water droplets deposited on paper.

2. EXPERIMENTAL

2.1. Materials

Two types of internally sized commercial papers were used. The first group (ASA) was internally sized with 1.0 kg/ton Alkenyl Succinic Anhydride while in the second group (AKD) 1.5 kg/ton of Alkyl Ketene Dimer was used (addition rates in the wet-end). The basis weight and thickness of the ASA paper were 82 g/m^2 and 122 μm, respectively; and that of the AKD paper, were 66 g/m^2 and 93 μm. The ash contents were of 15% and 13% for the ASA and AKD papers, respectively. Papers (AKD/ASA) were surface sized with polymer solutions varying in composition. The sizing solution consisted of different amounts of a styrene maleic anhydride derivative (SMA, Scripset 742, Solutia, Springfield, MA, USA) mixed with starch. The starch used was hydroxyethyl ether of yellow dent corn starch, Penford Gum 290 (Penford Products, Cedar Rapids, IA, USA) and had a degree of substitution of 0.057. Surface sizing was performed using a lab scale puddle type size press (Laboratory Size Press, Kumagai Riki Kogyo Co. Ltd., Nerima, Tokyo). The nip pressure was 15 kN/m and the temperature of the sizing solution was 60 °C. Samples were then dried in a photographic drier at 100 °C for 45 s on one side. The dry pick-up, defined as the mass of sizing solid per ton paper, was measured after the samples were conditioned for 24 h at 25 °C and 50 % relative humidity.

2.2. Methods

The contact angles of droplets of de-ionized distilled water on paper were measured using a *Dynamic Contact Angle Analyzer* manufactured by *First Ten*

Angstroms (Portsmouth, VA, USA). A droplet of water was placed on paper and its wetting dynamics on the surface were monitored using a CCD video camera with a 6:1 zoom microscope lens equipped with a fiber optic drop detector. An automatic forward/reverse syringe pump (10 mL) was used for liquid delivery and producing droplets of constant volumes. The syringe and the video camera were controlled by computer. Paper samples were placed individually on an adjustable platform and each sample was brought in touch with the sessile drop hanging from the tip of the syringe needle. In this way, the effect of kinetic energy on wetting were reduced. Figure 1 is a schematic of the experimental setup. The initial volume of the droplets ranged between 5-13 μL to result in a droplet of about 3-4 mm in diameter while at rest on the surface. After the touch off, the droplet behavior on paper was captured and recorded by video camera. The total recording time varied between 40 s for lightly sized samples, up to 10 min for heavily sized samples. The time interval between two consecutive frames was set at 0.017 s (60 frames per second). The recorded images were analyzed and the apparent contact angle θ(t) and the length of the base line d were measured for each frame. The volumes of the droplets were calculated from the contact angles and the base line measurements assuming the droplet was a spherical cap:

$$V_d = \frac{\pi}{3} R^3 \frac{(1-\cos\theta)(2+\cos\theta)}{\sin\theta(1+\cos\theta)} \tag{1}$$

where V_d is the volume of the droplet on the surface, R is the radius of the contact circle (base line divided by 2), and θ is the apparent contact angle between the droplet and the paper sheet.

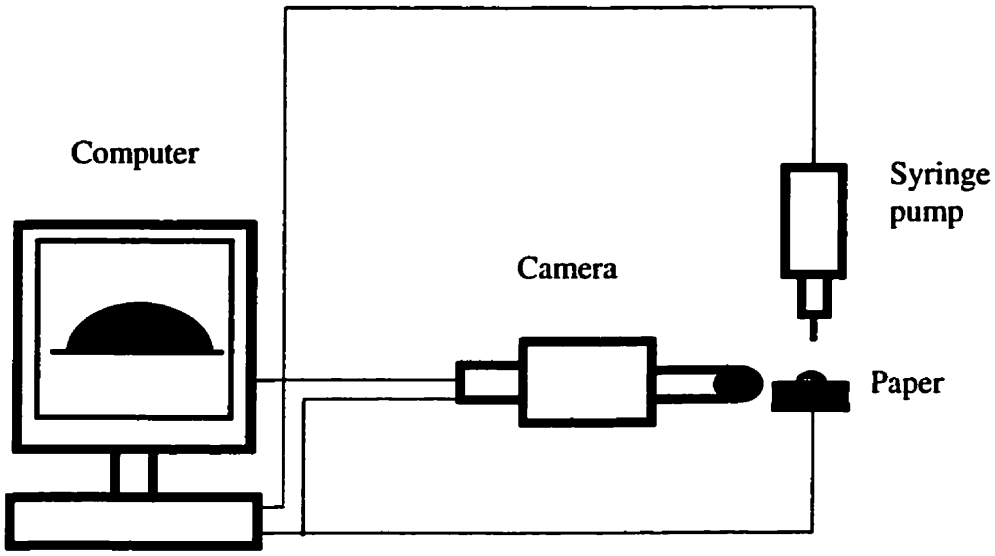

Figure 1. Schematic view of the experimental setup

The porosities of the papers and their pore size distributions were measured by the mercury intrusion method using a *Micromeritics pore sizer* (Norcross, GA, USA) capable of measuring pore sizes in the range of 0.006-300 μm. The pressure applied for intrusion was varied between 1-30000 psi. Line profilometry of the samples was performed by *AltiSurf 500* (Cotec, Evian, France), a non-contact roughness analyzer composed of an optical sensor, a motion controller, and a computer. Roughness was also measured by *Parker Print-Surf* (PPS Model M-590, TMI Canada). A hard nip laboratory calender was used for calendering papers at Paprican. The roll temperature was 50°C and the roll speed was 50 m/min. A nip load of 50 kN/m was applied.

3. RESULTS

Table I shows the surface sizing solution pick-up and some characteristic properties of the papers: mean pore diameter, porosity, and internal sizing. The mean pore diameter for the samples was only slightly affected by increasing the pick-up. Surface sizing the internally sized papers decreased porosity by a maximum decrease of 5%.

The surface roughness of all samples was measured using the Parker Print Surf technique (PPS). For each sample, ten measurements were performed at ten different locations. The average values and the standard deviations are tabulated in Table II. The average paper roughness ranged from 5.6 to 6.9 μm. For comparison, the diameter of a Kraft fiber is initially about 30 μm and typically decreases to around 10 μm upon calendering, and the diameter of precipitated calcium carbonate used as filler is about 1 μm. Thus, the roughness measured for the paper samples corresponds to the dimensions of a collapsed fiber. The Parker Print Surf measurements show that application of starch by surface sizing did not change the roughness of papers; sizing neither decreased roughness, as a result of coating, nor increased it, as a result of re-wetting and swelling of the fibers. The line profilometry measurements of the same paper unsized, sized and calendered are presented in Figure 2. Surface sizing did not affect roughness while calendering did.

Table I. Properties of Sized Papers

Sample	AKD* (kg/t)	ASA* (kg/t)	Starch (kg/t)	SMA (kg/t)	Mean Pore Size μm	Porosity (%)
$ASA_{(0/0)}$	-	1.0	-	-	1.2	50
$ASA_{(45/0)}$	-	1.0	45	-	1.0	46
$ASA_{(26/0.8)}$	-	1.0	26	0.8	1.1	48
$ASA_{(38/1.3)}$	-	1.0	38	1.3	1.1	45
$AKD_{(0/0)}$	1.5	-	-	-	1.0	44
$AKD_{(44/0)}$	1.5	-	44	-	1.0	40
$AKD_{(32/1.0)}$	1.5	-	32	1.0	1.0	43
$AKD_{(46/1.6)}$	1.5	-	46	1.6	0.9	42

* Addition rate in the wet-end

Table II. Surface Roughness of Sized Papers

Sample	Roughness (μm)	S.D. (μm)
$ASA_{(0/0)}$	6.9	0.2
$ASA_{(45/0)}$	6.9	0.2
$ASA_{(26/0.8)}$	5.8	0.2
$ASA_{(38/1.3)}$	5.7	0.2
$AKD_{(0/0)}$	5.6	0.2
$AKD_{(44/0)}$	6.4	0.4
$AKD_{(32/1.0)}$	6.0	0.2
$AKD_{(46/1.6)}$	6.8	0.3

a) Unsized

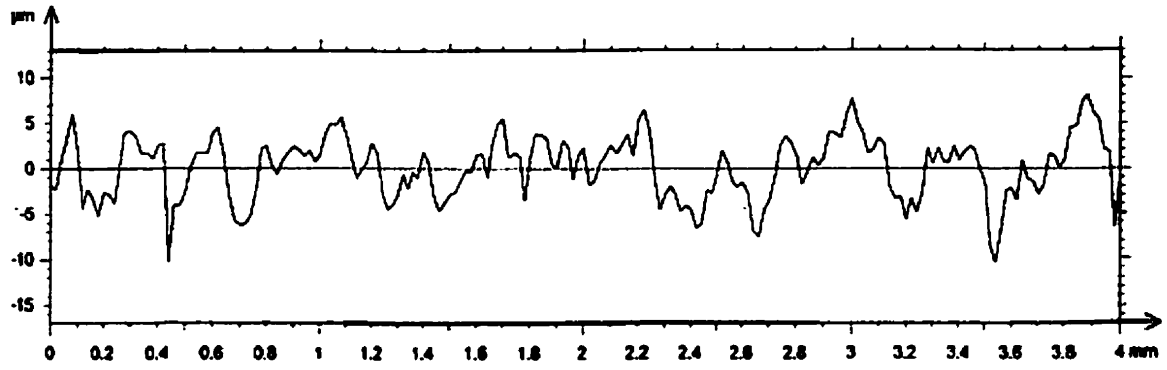

b) Surface Sized

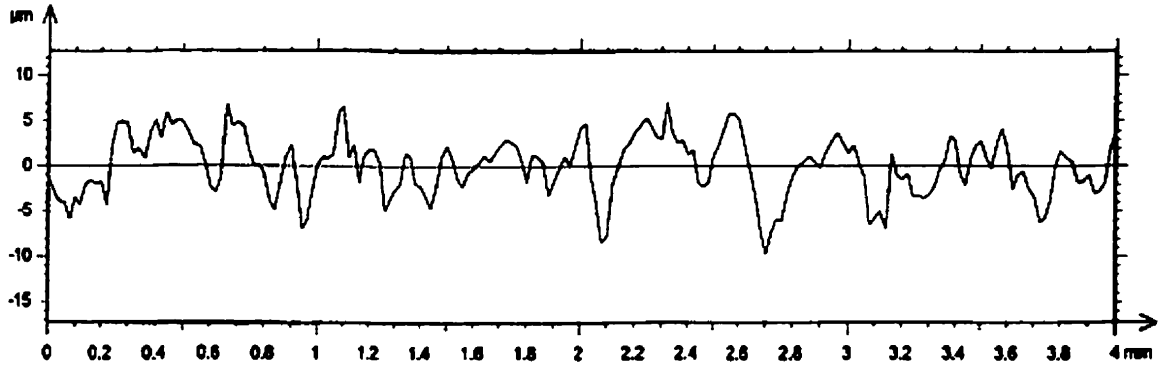

c) Calendered

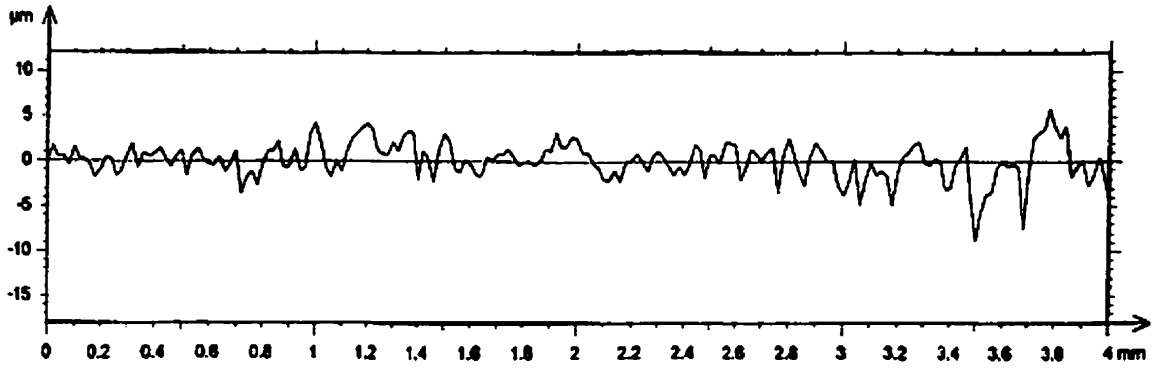

Figure 2- Line Profilometry

The typical evolution of contact angle and volume of a water droplet deposited on paper is illustrated on Figure 3. Two sequential regimes were observed as a function of time. First, the contact angle formed by the droplet decreased rapidly, while its volume remained constant. Second, the volume of the droplet decreased, while the contact angle decreased as well. The first regime represents wetting while the second corresponds to absorption. The decrease in the apparent contact angle is due to absorption into the bulk of paper [1], while the initial decrease in the apparent contact angle (until a plateau is reached) is caused by wetting. A transition time characteristic of sizing treatment was observed between the two regimes. We define *delay* as the period of time the droplet remained on the surface with an immobile contact line and constant contact angle, just before absorption starts. This definition is slightly different from the definition of the *wetting delay* reported in the literature [3]. Table III summarizes the delay times, t^*, measured between wetting and absorption. Increasing the concentration of SMA on the surface increased the delay while applying only starch onto the surface significantly decreased it (samples $ASA_{(0/0)}$ vs $ASA_{(45/0)}$ and $AKD_{(0/0)}$ vs $AKD_{(44/0)}$). The delay for papers sized only with starch lasted 2-10 s, while for papers highly sized with a hydrophobic polymer it was as high as 50 s. Increasing the SMA concentration increased the apparent contact angle of the water droplet on paper (Figure 4). In Figure 4, curves A and C correspond to ASA and AKD papers surface sized only with starch, while curves B and D represent the same papers prior to surface sizing. Surface sizing papers with starch enhanced absorption and decreased the delay before absorption.

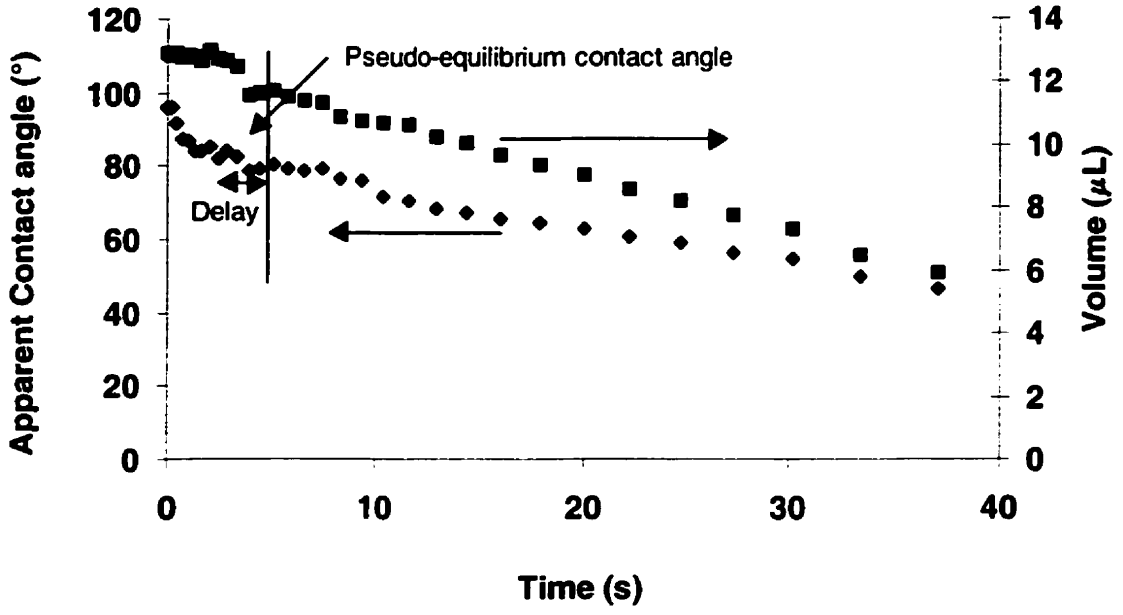

Figure 3- Droplet contact angle and volume vs time for ASA(0/0) paper. Delay is shown.

Table III. Delay Time before Water Absorption

Sample	Delay Time (t^*), s
$ASA_{(0/0)}$	5
$ASA_{(45/0)}$	2
$ASA_{(26/0.8)}$	10
$ASA_{(38/1.3)}$	15
$AKD_{(0/0)}$	40
$AKD_{(44/0)}$	10
$AKD_{(32/1.0)}$	50
$AKD_{(46/1.6)}$	50^+

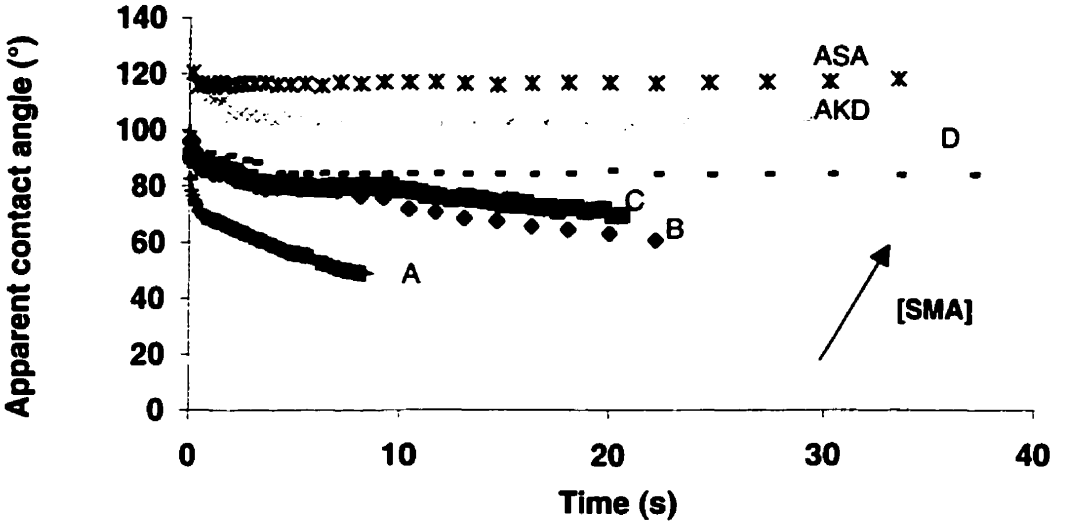

Figure 4- Evolution of the apparent contact angle as a function of time for different sizing treatment. A) ASA internal sizing with starch surface sizing B) ASA internal sizing only, C) AKD internal sizing with starch surface sizing, D) AKD internal sizing only

Figure 5 plots the pseudo-equilibrium contact angles (θ_e^*) of water droplets on papers as a function of the concentration of SMA surface sizing for AKD and ASA internally sized papers. The concentration of styrene maleic anhydride (SMA) on paper was varied with the solution pickup. By increasing the concentration of SMA in the surface sizing solution, both AKD and ASA papers became more hydrophobic. Plateaus in θ_e^* were reached at 115° and 105° at 1 kg SMA/t, for the ASA and AKD internally sized papers, respectively. Receding contact angles of 28°±5°, 60°±12° and 49°±9° were measured respectively on $ASA_{(0/0)}$, $ASA_{(26/0.8)}$ and $ASA_{(38/1.3)}$. This measurement was repeated for five replicates for each paper. The final contact angle achieved at the end of absorption for the same three papers were 18° ± 5°, 30°± 7° and 40°± 5°, respectively.

The Hercules Sizing Test (HST) was performed as a comparison to standard techniques in the paper industry. HST indicates the time required for a specific amount of ink (initially 10 mL) deposited on one side, to penetrate into paper such as to decrease the reflectance measured on the other side by 80%. The paper sheet is clamped between two rings. The diameter of the ring is 5 cm. Therefore, HST is a macro scale measurement of the absorption velocity into paper. HST was performed on six replicates in each group. The average HST values and the sample standard deviations are shown in Table IV. The standard deviation typically represents 10% of the average.

The average volumetric flow rates of water droplets into paper were derived. These results are also provided in Table IV. Increasing the concentration of SMA on paper had little effect on the rate of water absorption.

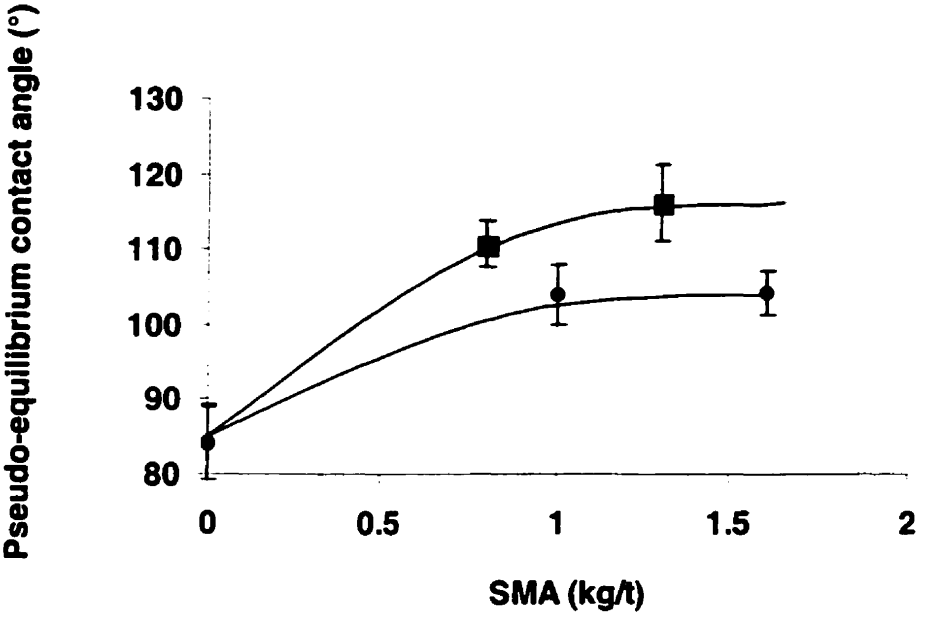

Figure 5- Effect of surface sizing on the pseudo-equilibrium contact angle of a water droplet deposited on AKD (●) and ASA (■) internally sized papers.

Table IV. Absorption Rate on Sized Paper

Sample	Flow rate (μL/s)	HST (s)
$ASA_{(0/0)}$	0.17	2.9±0.2
$ASA_{(45/0)}$	0.11	3.3±0.4
$ASA_{(26/0.8)}$	0.02	29±4
$ASA_{(38/1.3)}$	0.01	123±12
$AKD_{(0/0)}$	0.01	200±29
$AKD_{(44/0)}$	0.02	17±2
$AKD_{(32/1.0)}$	0.01	229±33
$AKD_{(46/1.6)}$	-	296±32

The contact angle of water droplets on glass slides coated with SMA and a mixture of SMA and starch was measured. For SMA coating, the glass slide was dipped into a SMA solution and air-dried. For the SMA/starch treatment the sample was dipped into a mixture of starch and SMA after the starch had been cooked and cooled to 50 °C. The equilibrium contact angle of water was 65° on SMA coated glass and 48°±1° for the starch/SMA coated glass slide. As a comparison, the contact angle of water on polystyrene ranges from 86°-91° [16]. The solubility of SMA in water was also evaluated. A second droplet was deposited on the very same position as the previous one (after the initial droplet was removed) and the contact angle was measured. A decrease of 10° in the equilibrium contact angle was measured for SMA/starch coated glass. This confirms some SMA dissolution into the water droplet during the time frame of measurements.

4. DISCUSSION

The contact angle of a water droplet deposited on sized paper follows two sequential regimes describing wetting and absorption, respectively. The wetting velocity was compared to theoretical models developed for smooth model surfaces; the complete analysis can be found elsewhere [1]. Surface roughness and chemical heterogeneity decrease the mobility of the three phase contact line formed by the wetting droplet on paper. A pseudo-equilibrium stage separates the two regimes of wetting and absorption. The duration of this stage depends on the concentration of hydrophobic domains created by sizing. In most cases the diameter of droplets remains unchanged after the first regime. In other words, absorption of the liquid into the bulk of paper only causes a change in the apparent contact angle while the droplet contact line remains motionless on the surface. Top view images of the droplet revealed that during this period liquid absorption into paper was in the radial direction (i.e. along the sheet), preferentially following the axis of fibers. Figure 6 portrays the absorption mechanism, schematically. The droplet collapses into the surface while its contact line is pinned to the surface. As a result, the apparent contact angle decreases as shown in the side view (Figure 6a). The top view (Figure 6b) represents the radial penetration of water during this period.

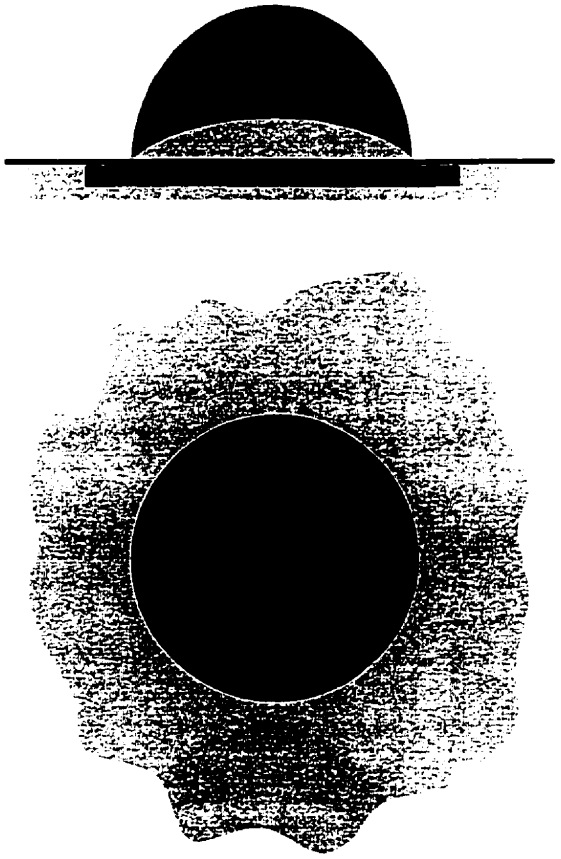

Figure 6- Absorption mechanism for a water droplet on sized paper. a) Side view showing droplet spherical cap shape at successive times b) Top view showing penetration in the sheet with a motionless contact line.

A stick and jump behavior in the contact line was observed just before the pseudo-equilibrium stage during the wetting regime (Figure 7). This stick and jump behavior results from the physical heterogeneity (roughness) on the surface [8,9]. The typical surface asperity was higher than 0.16 μm high on a single sample. According to Oliver and Mason [8] this difference is sufficient to inhibit wetting significantly and to induce non-equilibrium stick and jump movements in the contact line. The edges of the fibers on the surface induce a sudden flow of the liquid causing stick and jump movement of the contact line [15]. After calendering the papers the stick and jump was reduced (Figure 7).

The time (delay, t^*) the apparent contact angle remained constant at the pseudo-equilibrium angle ranged from 2 to 50 seconds. The more hydrophobic the surface (larger θ_e^*), the longer was the delay. Since the surfaces were extremely hydrophobic ($\theta_e^*>100°$), liquid absorption into paper could start only if the surface became hydrophilic; i.e. when $\theta_e^*<90°$. An explanation for this delay is that some of the sizing polymer on paper dissolve into the water droplet during the pseudo-equilibrium stage, thus, changing the surface chemistry up to a point where, at least locally, the surface becomes hydrophilic enough to allow liquid penetration. Two experimental results support this hypothesis. First, the receding contact angles on each paper were larger than the contact angle at the end of droplet absorption. Since the receding contact angle is theoretically the smallest angle a liquid can form on a solid surface, this difference could be due only to a change in the surface properties as a result of contact with the water droplet. However, this contact may have also caused a physical change, i.e. the swelling

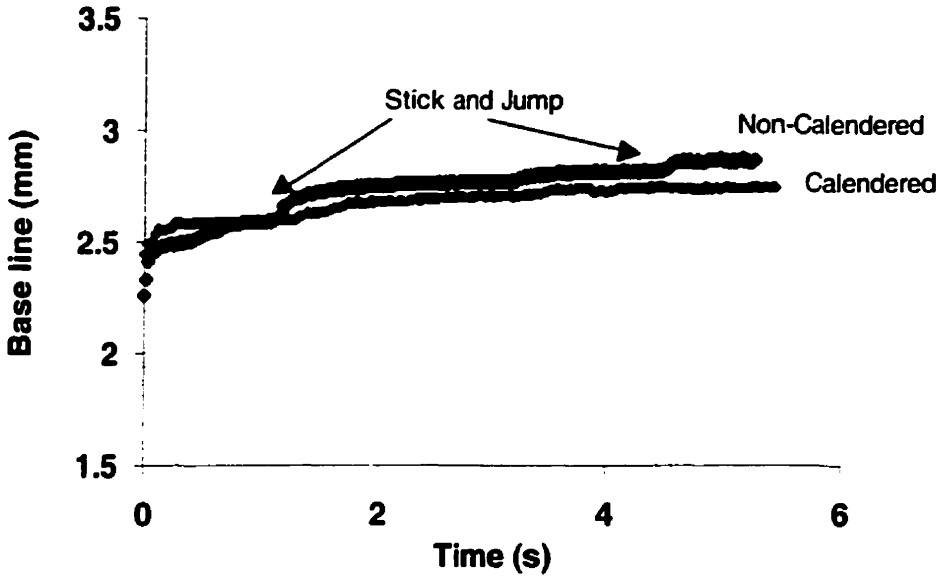

Figure 7- Typical stick and jump movement of the contact line for uncalendered and calendered papers

of fibers, which would modify porosity. The second relevant experimental result is that the contact angle of a second water droplet deposited at the same spot on a SMA/starch glass surface was smaller than the contact angle of the first droplet. The decrease of ~10° in the equilibrium contact angle (second drop) indicated that the surface became more hydrophilic; some SMA dissolved in the droplet during the pseudo-equilibrium stage.

Surface sizing with starch (45 kg/t) had no effect on HST of the ASA internally sized papers, but decreased significantly the HST value of the AKD internally sized papers. This different behavior is very likely independent of the type of internal sizing (AKD versus ASA) but is controlled by the amount of internal sizing (surface coverage). More information on the mechanism of internal sizing can be found in [13,17,18]. Furthermore, the HST value measured on AKD papers was almost an order of magnitude higher than on ASA papers, for presumably comparable internal sizing concentrations. The evolution of contact angle of water droplets as a function of time describes the same behavior as by the HST measurements (Figure 4). Sizing the AKD and ASA papers with starch not only induced a shift towards lower pseudo-equilibrium contact angles, but also accelerated the absorption process for both papers. Surface sizing with starch accelerated water absorption by 30 s for AKD papers and by 7 s for ASA papers. This difference in the absorption properties of $ASA_{(0/0)}$ and $ASA_{(45/0)}$ was not detected by the HST method. On the other hand, increasing the concentration of SMA in the starch solution transformed the paper surface into non-wetting conditions by shifting the pseudo-equilibrium contact angle to values higher than 100° (Figure 3), which delayed absorption even further. Papers with $\theta_e^* > 90°$ had higher HST values. Increasing the SMA concentration on papers increased θ_e^* more for ASA papers than it did for AKD

papers, while the corresponding HST values showed faster absorption for the ASA papers than for the AKD papers. This represents an interesting inconsistency. In the HST method, restricting the liquid inside a ring eliminates wetting. The sizing polymer domains on paper form a barrier to prevent absorption. The rate and extent of dissolution of the SMA domains into the HST ink would affect the HST values for a family of papers with different levels of sizing (same formation). The surface chemical composition controls the liquid absorption only to a limited extent; absorption is only delayed by surface sizing (SMA). The HST method reflects more precisely internal sizing than surface sizing. One of the reasons is that internal sizing chemicals (AKD, ASA) are not water soluble, while some surface sizing chemicals (SMA) are soluble to some extent.

Applying starch (hydrophilic) increased the rate of liquid absorption for AKD papers, while it caused no significant change for ASA papers. This is in agreement with the HST values; HST dropped from 200 s to 17 s by surface sizing the AKD papers with starch, while HST remained unchanged for ASA papers. The relationship between the HST and the superficial absorption velocity of a water droplet on paper can be seen in Figure 8. The superficial velocity was calculated assuming a one-dimensional absorption in the vertical direction. A linear correlation is observed for low absorption velocities corresponding to high HST values ranging from 300 s to 100 s. However, the HST measurement loses accuracy at high absorption superficial velocities (13 μm/s) corresponding to low HST values. It should be noted that since the droplet size is similar to the critical dimension of flocs (of the order of mm), measurements with droplets highlight the microscopic wetting and absorption behavior of papers, while the HST

method measures the average macroscopic liquid absorption. Formation will affect both measurements.

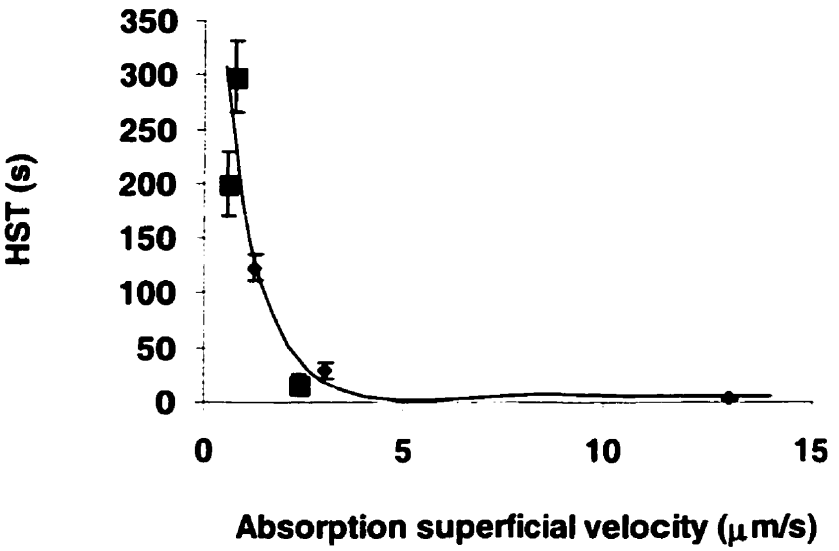

Figure 8- Comparison of the HST and the absorption rate of a sessile droplet of water on sized papers. ■ is for AKD papers and ◆ is for ASA papers.

5. CONCLUSIONS

The contact angle of water droplets deposited onto AKD/ASA internally sized papers surface sized with different SMA/starch concentrations was measured as a function of time. Surface roughness was controlled by calendering the papers. The amount of SMA polymer applied onto the paper surface affected significantly the wetting and absorption behavior of water droplets. Wetting and absorption were two sequential regimes occurring upon contact between the droplet and sized papers. The pseudo-equilibrium contact angles (θ_e^*) achieved at the end of the wetting regime increased as a function of the concentration of SMA. Addition of starch rendered the paper surface more hydrophilic and enhanced absorption. The delay at the end of the wetting regime, just before absorption, increased as a function of the concentration of SMA on the surface. During this delay, some SMA dissolution into the water droplet occurred, thus reducing θ_e^* below 90° locally and allowing absorption of the droplet into the bulk of the paper to start. Surface roughness also affected the apparent contact angle of the water droplet on the surface and induced non-equilibrium stick and jump movement of the contact line. Reducing surface roughness by calendering reduced the stick and jump. Surface chemical heterogeneity affected the rate of liquid absorption only to a limited extent. The HST method was found to be a reliable method for evaluating absorption properties of highly sized papers. HST lost preciseness for papers with low sizing.

6. ACKNOWLEDGEMENTS

This work was supported by the Natural Sciences and Engineering Research Council of Canada, and by Hercules Inc..

7. REFERENCES

1. Modaressi, H. and Garnier, G., "The dynamics of wetting and absorption of water droplets on sized paper", manuscript for Langmuir, (2000).
2. Wagberg, L. and Westerlind, C., "Spreading of droplets of different liquids on specially structured papers", submitted for publication to Nordic Pulp and paper research Journal, (2000).
3. Aspler, J.S., "Interactions of ink and water with paper surface in printing", A review, Nordic Pulp and Paper Journal, no. 1, 68-74, (1993).
4. Inoue, M., Tsai Yi-Guan and Colasurdo, T., "The effect of sizing materials on the ink absorption in water", presented at Tappi paper makers conference, Atlanta, GA, Tappi Press, 111-122, (1998).
5. Kent, H.J. and Lyne, M.B., "On the Penetration of Printing Ink into Paper", Nordic Pulp and Paper Research Journal, (2), 141-145, (1989).
6. Lyne, M.B. and Aspler, J.S., "Wetting and the sorption of water by paper under dynamic conditions", Tappi Journal, 98-101, (1982).
7. Hoyland, R.W., "Fiber-water interactions in paper making", The Div. BPBIF, London, 557-577, (1978).
8. Oliver, J.F. and Mason, S.G., "Liquid spreading on rough metal surfaces", J. Mat. Sci., 15, 431-437, (1980).
9. Huh, C., Oliver, J.F., and Mason. S.G., "An experimental study of some effects of solid surface roughness on wetting", Colloids and Surfaces, 1, 79-104, (1980).

10. Semal, S., Blake, T.D., Geskin, V., de Ruijter, M.J., "Influence of surface roughness on wetting dynamics", Langmuir, 15 (23), 8765-8770, (1999).

11. Gillespie, T., "The spreading of low vapor pressure liquids in paper", J. Col. Sci., 13, 32-50, (1958).

12. Borhan, A. and Rungta, K.K., "An experimental study of the radial penetration of liquids in thin porous substrates", J. Col. Int. Sci., 158, 403-411, (1993).

13. Yu, L. and Garnier, G., "Mechanism of internal sizing with alkyl ketene dimers: The role of vapor deposition", Fundamental Research Symposium, vol. 2, Cambrige, 1021-1046, (1997).

14. Oliver, J.F., "Wetting and Penetration of Paper surfaces", Reprographic Technology, American Chemical Society, 435-453, (1982).

15. Oliver, J.F., "Effect of surface roughness on wetting", Ph.D. Thesis, McGill University, Montreal, PQ, (1975).

16. Mark, J.E., Physical Properties of Polymers Handbook, American Institute of Physics (AIP) Press, 673, (1996).

17. Garnier, G. and Yu, L., "Wetting mechanism of a starch stabilized alkyl ketene dimer emulsion: a study by atomic force microscopy", J. Pulp Paper Sci., 25 (7), 235-250, (1999).

18. Garnier, G. and Godbout, L., "Wetting behavior of alkyl ketene dimer on cellulose and model surfaces", J. Pulp Paper Sci., 26, (5), 194-199, (2000).

CHAPTER 3

Mechanism of wetting and absorption of water droplets on sized paper: Effects of chemical and physical heterogeneity

Hedieh Modaressi and Gil Garnier[1]
Paprican and the Department of Chemical Engineering
McGill Pulp and Paper Research Center
3420 University St.
Montreal, QC H3A 2A7

Abstract

The wetting and absorption dynamics of water droplets deposited on hydrophobized paper were studied. The objective was to quantify the effect of chemical and physical heterogeneity of a porous surface on its wetting and absorption behavior. Wetting and absorption rates were calculated from the contact angle, volume and base line of the droplets on paper. Absorption started only after the drop had wetted the surface to a certain extent. There was a time delay before absorption occurred. By the end of this delay, a pseudo- equilibrium contact angle was reached, which corresponds to the thermodynamic equilibrium contact angle. Wetting on a partially hydrophobized porous surface follows a power law model with wetting rates slower than in hydrodynamic wetting by a factor H, function of surface roughness. Surface roughness also affects the equilibrium contact angle, as by entrapping air, it renders the surface more hydrophobic. The wetting dynamics was found to be independent of the chemical heterogeneity of the surface.

Keywords: wetting, absorption, paper, porous surface, roughness, heterogeneity, contact angle, surface chemistry.

For correspondence: Gil.Garnier@kcc.com or hmodar@po-box.mcgill.ca

[1] Now at Kimberly-Clark, Neenah WI.

1. INTRODUCTION

The combined dynamics of wetting and absorption of a liquid droplet deposited on a porous and heterogeneous surface are of high industrial and scientific interest. Printing, paper coating, application of lotions on skin, and spraying of pesticides are just a few of many industrial applications. The surface heterogeneity can either be of a chemical or of a physical nature. Hydrophobic domains on a hydrophilic surface such as sized paper is an example of the former type, while surface roughness (grooves, fiber orientation) highlights the latter case.

From the work of de Gennes describing dynamic wetting governed by hydrodynamics [1] and the work of Blake [2] characterizing the friction controlled wetting, de Ruijter, Voue and De Coninck [3, 4] derived a combined theory of the spreading dynamics. De Coninck et al. measured and modeled over 6 decades of time the dynamics of spontaneously spreading viscous drops on smooth surfaces. The friction regime, in which the contact angle θ scaled with time as $\theta(t) \sim t^{-3/7}$ preceded the hydrodynamic regime, where $\theta(t) \sim t^{-3/10}$. Assuming wetting to be controlled by the hydrodynamic regime, that is $\theta(t) \sim t^{-3/10}$ [1], the empirical Hoffman-Tanner equation for spreading ($\theta_e = 0$) can be used:

$$\theta^3 \propto Ca \tag{1}$$

where the Capillary number (Ca) is defined as:

$$Ca = \frac{\mu U}{\gamma} \tag{2}$$

where μ is the viscosity of the liquid, γ is the liquid-gas interfacial tension and U is the velocity of spreading.

The Hoffman-Tanner equation was shown by de Gennes to represent a particular case of the hydrodynamic regime [1]. In partial wetting, when the droplet forms a finite contact angle with the surface ($0<\theta_e<90°$), equation (1) becomes [1]:

$$\theta^3 - \theta_e^3 \propto Ca \tag{3}$$

where θ_e is the equilibrium contact angle on a homogeneous, insoluble, nonreactive and molecularly smooth surface and is predicted from the Young equation:

$$\cos\theta_e = \frac{\gamma_{sv} - \gamma_{sl}}{\gamma} \tag{4}$$

where γ_{sv} and γ_{sl} are the solid-vapor and solid-liquid interfacial tensions, respectively.

The effect of heterogeneity, physical or chemical, on the equilibrium contact angle has been known for some time [7]. The apparent contact angle on a heterogeneous solid surface equals the equilibrium contact angle if the line tension is negligible [5]. Line tension accounts for the three-phase molecular interactions at the contact line and is usually significant when the scale of roughness is of the order of a few micrometers [5,6]. However, for a smooth solid surface line tension is typically less than 5×10^{-9} N.

Cassie [10] proposed the additive nature of wetting over a chemically heterogeneous surface:

$$cos\theta_e = \sum f_i cos\theta_e^i \tag{5}$$

where f_i is the fractional area of the surface with an equilibrium contact angle of θ_e^i.

Years later, using molecular dynamics, De Coninck et al. [8] showed that the equilibrium contact angle of a sessile drop placed on a heterogeneous substrate follows Cassie's equation.

Oliver and Mason [13] studied drop advance on surfaces with physical heterogeneities. By following wetting on a porous stainless steel surface, they found Cassie's equation to be applicable to surfaces with physical heterogeneity only when the liquid spread free of non-equilibrium stick and jump movements. Non-equilibrium stick and jump movements of the contact line (pinning) mainly depend on the relative orientation of the contact line to the grooves on a rough surface. Pinning causes the immobility of the contact line not only when $\theta = \theta_e$, but for apparent contact angles between the advancing (θ_a) and receding contact angles (θ_r)[1]. Pinning on a rough surface disappears when the grooves are deep and entrap air or vapor under the liquid droplet [1].

Wenzel [14] theoretically studied the effect of roughness on the apparent contact angle using conventional thermodynamics:

$$\cos\theta = r\cos\theta_e \tag{6}$$

where θ_e is the equilibrium contact angle and r is a roughness parameter defined as the average ratio of the true to the apparent area. According to Huh et al. [15], Wenzel's equation being based on thermodynamic arguments only applies to systems with no hysteresis. This would exclude most industrial surfaces in general, and paper in particular. However, Equation (6) is valid for droplets spreading on surfaces with only radial grooves on which the contact line could move reversibly (no hysteresis) [16].

Less understood, is the effect of heterogeneity on the moving wetting line. De Coninck et al. measured and modeled the spreading of droplets on heterogeneous substrates using molecular dynamics [9]. Roughness was created at a micro-scale on Langmuir-Blodgett multi-layer substrates. The jump frequency of liquid molecules (molecular kinetic theory) was found to decrease at the wetting line with micro-scale roughness [9]. This supports the idea that surface defects induce pinning. Contact angle hysteresis also increased steadily with roughness. This confirms the earlier work of Huh et al. [15] and Oliver and Mason [13].

Liquid absorption in paper is usually modeled with the Lucas-Washburn equation derived by combining the Navier-Stokes with the Laplace equation assuming a fully developed, laminar flow of a Newtonian liquid with a constant contact angle [12]:

$$\frac{x}{R} = \left(\frac{\gamma \cos\theta}{2\mu R} t\right)^{\frac{1}{2}} \tag{7}$$

where x is the distance the liquid has advanced, R is the average radius of pores, γ is the surface tension of the liquid and μ is the viscosity. This approach has had only limited success in describing water absorption into paper [12]. Another description of liquid absorption in porous media uses Darcy's law. Gillespie [17] found a good agreement between his Darcy's law-based model and experimental observations for water absorption into paper. Borhan et al. [18] confirmed the validity of Gillespie's model for the radial absorption of ink in paper.

Very little study, if any, has simultaneously considered wetting and absorption in porous media. We raise the hypothesis that chemical heterogeneity controls the critical time scale of wetting and absorption. It is also of interest to elucidate if under certain

conditions, both phenomena can be deconvoluted. Few studies quantify the dynamics of a droplet wetting a solid surface while simultaneously absorbing into its bulk. The three dimensional and heterogeneous nature of this problem constitutes a theoretical challenge. It is not clear whether absorption into the bulk and wetting on the surface have similar time scales nor how surface heterogeneity might affect these phenomena.

In this work, we measured the wetting dynamics of a water droplet deposited on papers of different surface properties. Paper was chosen as a model porous surface, since its physical and chemical properties can be easily modified. Hydrophobic domains were introduced into paper by two processes. In the first process hydrophobic colloids were absorbed from solution onto the fibers prior to the formation of the paper web. The result is referred to as internal sizing. Two hydrophobic colloids, Alkyl Ketene Dimer (AKD) and Alkenyl Succinic Anhydride (ASA), were used. The physisorption/chemisorption of the alkyl chains of AKD and ASA onto the hydroxyl group of cellulose provided hydrophobicity. The surface coverage on fibers is typically of 1% [19]. In the second process, using a surface treatment, a polymer solution made of starch and a copolymer is applied on the paper surface. The result is referred to as surface sizing. Internal sizing provides relatively a uniform concentration of hydrophobic domains across the paper sheet while surface sizing affects the outer 20 μm.

2. EXPERIMENTAL

2.1. Materials

Two types of internally sized papers were used. The first group (ASA) was internally sized with 1.0 kg/ton alkenyl succinic anhydride while in the second group (AKD) 1.5 kg/ton of alkyl ketene dimer was used. The basis weight and thickness for the ASA paper were 82 g/m^2 and 122 μm, respectively; these properties for the AKD paper were 66 g/m^2 and 93 μm. The precipitated calcium carbonate (PCC) contents for the ASA and AKD papers were 15% and 13%, respectively. Figure 1, a SEM of the paper surface, shows the presence of $CaCO_3$ on the surface (white domains).

The two groups of papers were surface sized with polymer solutions varying in composition. The sizing solution consisted of different amounts of a styrene maleic anhydride derivative (SMA, Scripset 742, Solutia, Springfield, MA, USA) mixed with starch. The starch was a hydroxyethyl ether of yellow dent corn starch, Penford Gum 290 (Penford Products, Cedar Rapids, IA, USA) with a degree of substitution of 0.057. Surface sizing was performed on a lab scale puddle type size press. The nip pressure was set at 15 KN/m and the temperature of the sizing solution was 60 °C. Samples were dried on a photographic type drier at 100 °C for 45 s on one side only. The dry pick-up, defined as the mass of sizing solid per ton paper, was measured after the samples were conditioned 24 h at 25 °C and 50 % relative humidity. Table I shows the sizing pick-up, paper porosity and mean pore diameter.

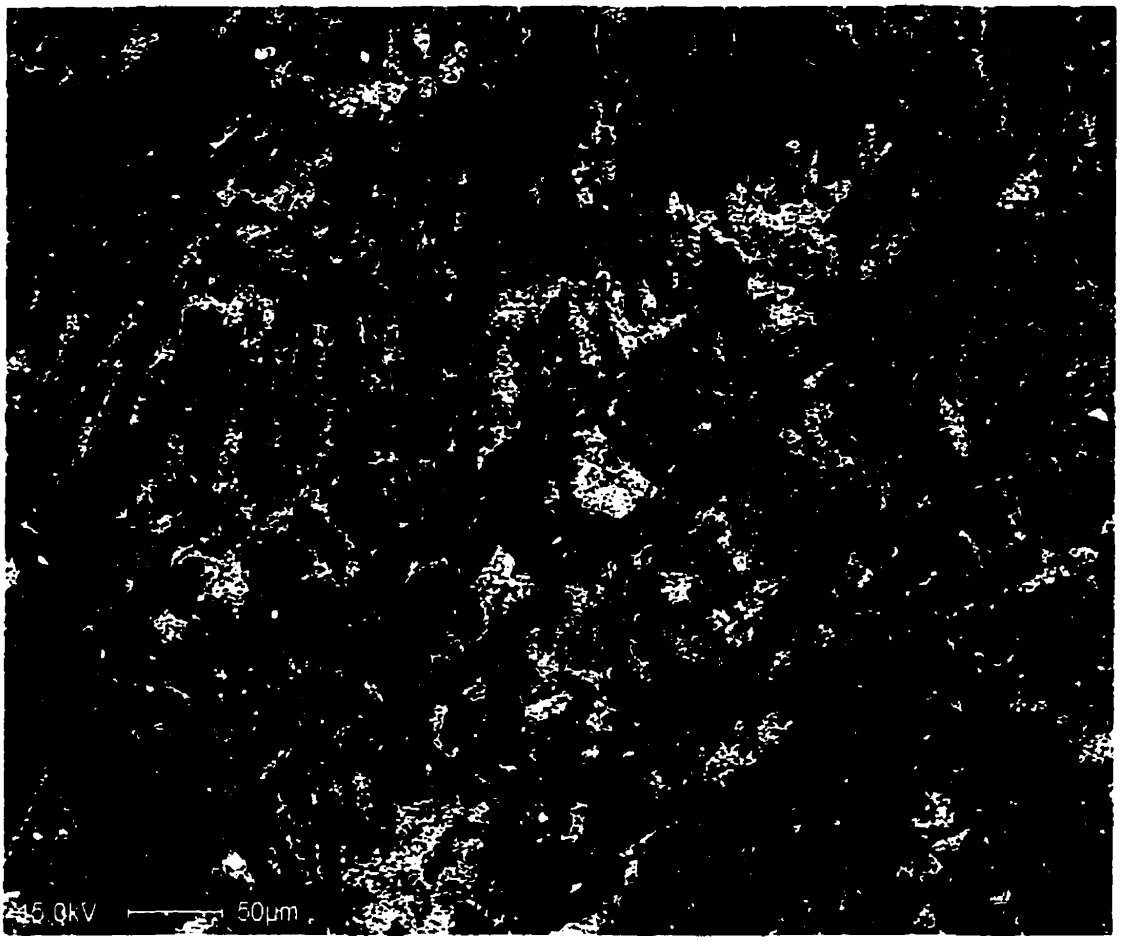

Figure 1- Typical scanning electron microscopy (SEM) of the paper surface. The white domains are the calcium carbonate aggregates.

Table I. Physical properties of papers. Pick-up, mean pore diameter, porosity and roughness

Sample[1]	AKD (kg/t)	ASA (kg/t)	Starch (kg/t)	SMA (kg/t)	Mean Pore (μm)	Porosity (%)	Roughne (μm)
$ASA_{(0/0)}$	-	1.0	-	-	1.2	50	6.9±0.2
$ASA_{(45/0)}$	-	1.0	45	-	1.0	46	6.9±0.2
$ASA_{(26/0.8)}$	-	1.0	26	0.8	1.1	48	5.4±0.2
$ASA_{(38/1.3)}$	-	1.0	38	1.3	1.1	45	5.7±0.2
$AKD_{(0/0)}$	1.5	-	-	-	1.0	44	5.6±0.2
$AKD_{(44/0)}$	1.5	-	44	-	1.1	40	6.4±0.4
$AKD_{(32/1.0)}$	1.5	-	32	1.0	1.0	43	6.0±0.2
$AKD_{(46/1.6)}$	1.5	-	46	1.6	0.9	42	6.8±0.3

1 The first number in brackets refers to the starch pick-up (kg/ton paper), while the second indicates the SMA concentration (kg/ton paper).

Glass slides (2.5 cm×2.5 cm, Fisher) were coated with SMA and a starch/SMA mixture. For the SMA coating, the glass slide was dipped into a SMA solution and air-dried. For SMA/starch treatment, the sample was dipped into a mixture of starch and SMA after the starch had been cooked and cooled to 50 °C (same conditions as in sizing). Glass slides were coated with commercial AKD from Raisio Chemicals (North America) molten on the slides at 64 °C to form a smooth layer of AKD.

2.2. Methods

The contact angles of droplets of de-ionized distilled water on paper were measured using a *Dynamic Contact Angle Analyzer* manufactured by *First Ten Angstroms* (Portsmouth, VA, USA). A water droplet was placed on paper and its wetting dynamics was monitored using a CCD video camera with a 6:1 zoom microscope lens equipped with a fiber optic drop detector (Figure 2). An automatic forward/reverse syringe pump with a 10 mL syringe was used for liquid delivery and producing droplets of constant volume. Syringe and video camera were controlled by computer. Paper samples were individually placed on an adjustable platform, and each sample was raised slowly to touch a sessile drop hanging from the tip of the syringe needle. The effects of kinetic energy on wetting were thus reduced. The initial volume of the droplets ranged from 5-13 μL yielding a droplet of about 3-4 mm in diameter while at rest on the surface. After the touch off, the droplet behavior on paper was captured by video camera and recorded. The time interval between consecutive frames was 0.02 s. The recording time varied between 40 s, for slightly sized samples, to 10 min for heavily sized samples.

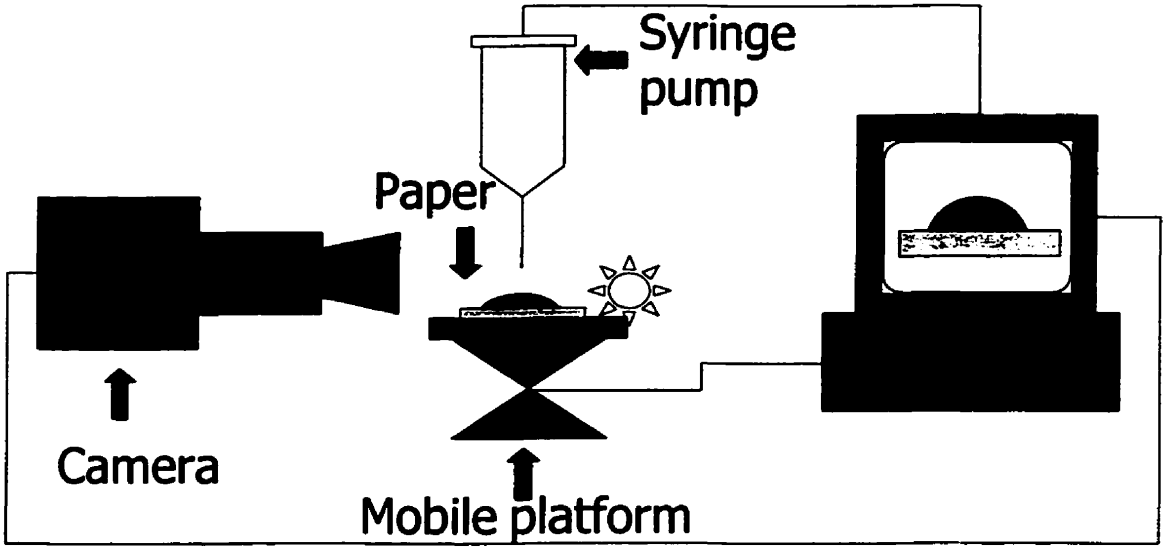

Figure 2- Schematic of the experimental setup

The apparent contact angle $\theta(t)$ and the length of the base line $d(t)$ were measured in each frame. The volume of the droplets was calculated using the experimental values for base line and contact angles, and assuming the droplet to form a spherical cap.

The advancing and receding contact angles of water droplets were measured using the same system. For measuring the advancing angles, the needle was brought close to the surface (~1mm) and the contact angle was measured as a function of time while the volume of the droplet was increased. The receding angles were measured by decreasing the volume of the droplets and measuring the contact angle as a function of time.

The porosity of the papers and their pore size distributions were measured by the mercury intrusion method using a *Micromeritics pore sizer* (Norcross, GA, U.S.A.). The pressure applied for intrusion was varied from 1-30000 psi. Line profilometry was performed by a non-contact roughness analyzer, *AltiSurf 500* (Cotec, Evian, France). A hard nip laboratory calender was used for calendering papers as described in [20]. The $ASA_{(0/0)}$ paper was calendered to two different nip pressures (10 KN/m and 60 KN/m). The roughness of papers after calendering was on average 4.8 μm and 3.0 μm, respectively.

3. RESULTS

The dynamics of wetting and absorption of water droplets deposited on paper was quantified. The variables of interest were the concentration of hydrophobic domains and their distribution across the paper. Different distribution profiles of hydrophobic domains were created within paper by using a combination of internal and surface sizing.

The typical evolution of contact angle, base line and volume of a water droplet deposited on sized paper as functions of time are shown in Figure 3. The volume of the droplet on the paper surface was calculated assuming the droplet remained spherical through out the experiment. This assumption was supported by the values of the Bond numbers ($\rho g d^2/\gamma$) which ranged from 1.3×10^{-3} to 2.2×10^{-3}, confirming the negligible effect of gravity on droplet shape (Table II) [11].

Two regimes are distinguished in Figure 3. At first, the contact angle formed by the droplet on paper decreased while the length of the base line increased rapidly. During this period, the volume of the droplet remained constant and the droplet relaxed from its initial angle to a pseudo-equilibrium value. The duration of this relaxation period was entirely dependent upon the amount and the type of polymer applied onto the surface, thus on the concentration and distribution profile of the hydrophobic domains in the paper surface [20]. In the second regime, the contact angle and the droplet volume decreased with time, roughly linearly, while the base line essentially remained stationary. This corresponds to the droplet absorption into the bulk of paper. The pseudo-equilibrium contact angles (θ_e^*) measured at the end of the first regime, and the standard deviations (four replicates) are shown in Table III.

Table II. Bond numbers for water droplets deposited on paper

Sample	Bond #
$ASA_{(0/0)}$	0.0022
$ASA_{(45/0)}$	0.0016
$ASA_{(26/0.8)}$	0.0013
$ASA_{(38/1.3)}$	0.0017
$AKD_{(0/0)}$	0.0020
$AKD_{(44/0)}$	0.0015
$AKD_{(32/1.0)}$	0.0016
$AKD_{(46/1.6)}$	0.0016

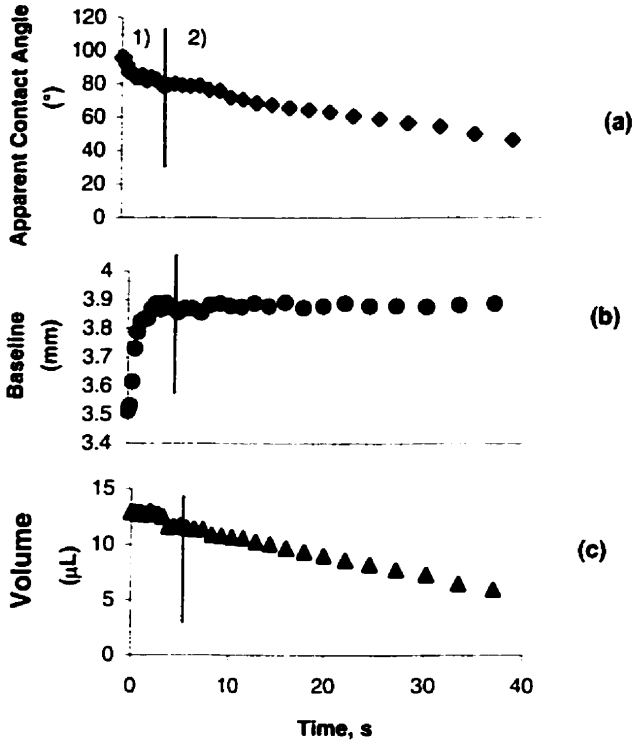

Figure 3- Typical dynamics of a water droplet on sized paper. Two regimes can be distinguished. 1) Governed by wetting 2) Dominated by absorption into paper. Evaporation was kept negligible.

Table III. Pseudo-equilibrium contact angle (θ_e^*), advancing angle (θ_a), receding angle (θ_r) and hysteresis ($\Delta\theta$) of water droplets on sized paper. Four replicates were at least measured.

Sample	θ_e^* (°)	θ_a (°)	θ_r (°)	$\Delta\theta$ (°)
$ASA_{(0/0)}$	81±5	84±6	28±5	56±8
$ASA_{(45/0)}$	71±2	76±3	-	-
$ASA_{(26/0.8)}$	110±5	129±3	60±12	69±12
$ASA_{(38/1.3)}$	120±3	130±7	49±9	81±11
$AKD_{(0/0)}$	90±4	105±3	-	
$AKD_{(44/0)}$	83±5	86±1	-	
$AKD_{(32/1.0)}$	104±5	116±8	-	
$AKD_{(46/1.6)}$	110±3	122±2	-	

Despite the significant heterogeneity among the samples, good reproducibility was achieved. Table III also regroups the advancing (θ_a) and receding (θ_r) contact angles measured for three papers. There was a fluctuation in both the advancing and receding angles. Hysteresis increased as a function of the surface sizing polymer concentration, indicating an increase in the chemical heterogeneity of the surface. All pseudo-equilibrium contact angles (θ_e^*) were bracketed by the advancing and receding angles, and ranged from 71° (wetting) to 110° (non-wetting). Surprisingly, the receding contact angles of the three papers were larger than the smallest apparent contact angle reached at the end of the absorption regime.

In most cases, the diameters of the water droplets on paper remained unchanged after the first regime, i.e. absorption of the liquid into the paper only caused a change in the apparent contact angle while the droplet contact line did not move. Top view images of the droplet revealed that during this period liquid absorption proceeded not only into the paper but also in the radial direction by preferentially following the orientation of fibers. [20]

Figure 4 shows the effect of surface roughness on the dynamics of wetting and absorption of water droplets on ASA papers. ASA paper was calendered at two different intensities to create two levels of surface roughness having different physical heterogeneity but the same chemical heterogeneity. The apparent contact angle formed by a water droplet on these calendered papers was compared to that of the initial uncalendered paper. Smoothing the surface decreased both the initial and the pseudo-equilibrium contact angles and accelerated absorption.

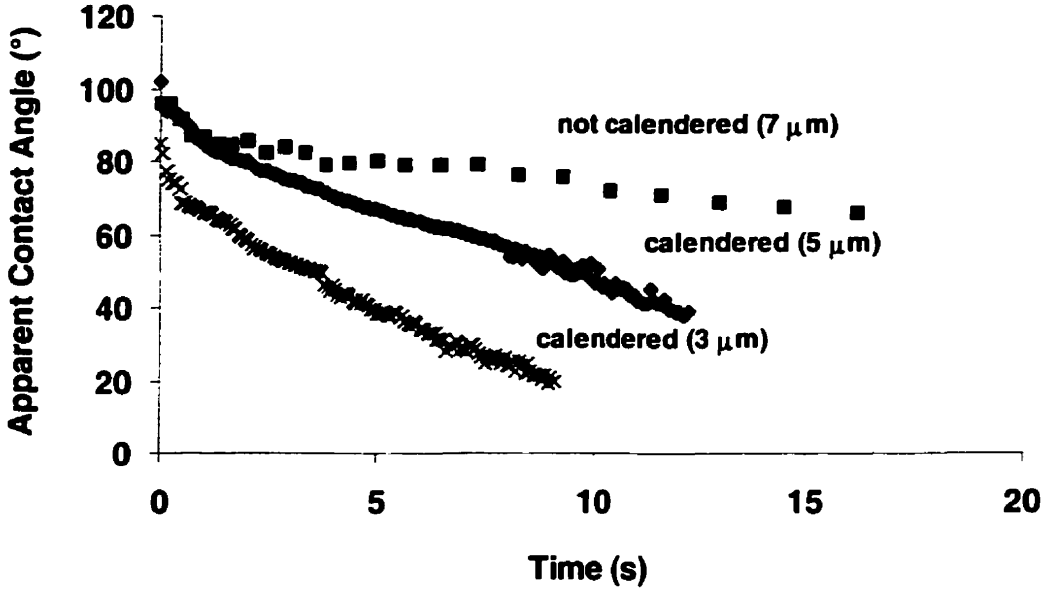

Figure 4- Effect of paper roughness on the apparent contact angle of water droplets. Surface chemistry is constant. The average roughness reached by calendering is indicated.

The contact angle of a water droplet deposited on a glass slide coated either with SMA or a mixture of SMA/starch was measured. Equilibrium contact angles of 65°±2 and 48°±1 were measured for water on the SMA and the starch/SMA coated glasses, respectively. The equilibrium contact angle of water on AKD coated glass was 108°±2.

4. DISCUSSION

Two regimes were distinguished after a droplet of water came into contact with sized paper. These regimes had different time scales corresponding to wetting and absorption, respectively. During the first regime, the droplet relaxed on the surface until a pseudo-equilibrium contact angle (θ_e^*) was reached. The volume of the droplet remained constant through out this regime. The second regime started after the pseudo-equilibrium stage. During this period, the contact line of the droplet remained stationary while its volume decreased. Figure 5 illustrates the absorption mechanism. First, the droplet diffuses into the paper while its contact line is pinned to the surface (part a). As a result, the apparent contact angle decreases as the droplet is depleting into the porous bulk of paper. Part (b) represents the radial penetration of water into paper during this period; the diameter of the droplet remains constant.

Data from the wetting regime (first ten seconds) were modeled with the Hoffman-Tanner equation. Capillary numbers (Ca) were calculated from the advancing velocity of the base line for each droplet. The cube of the apparent contact angle (θ^3) is plotted against the capillary numbers in Figure 6. The data follow almost parallel lines with different intercepts. Each intercept corresponds to the pseudo-equilibrium contact angles on the papers.

Figure 7 presents the evolution of the contact angle as a function of time on logarithmic coordinates. The linear relationships indicate that wetting follows a power-law model. Slopes of –3/7 and –3/10, representing the theoretical friction and hydrodynamic regimes [3,4], are plotted for reference.

(a) Side view

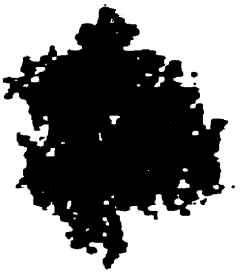

(b) Top view

Figure 5- Wetting and absorption mechanism of a droplet on paper. a) Decrease in the apparent contact angle due to bulk absorption, b) Radial penetration of the droplet.

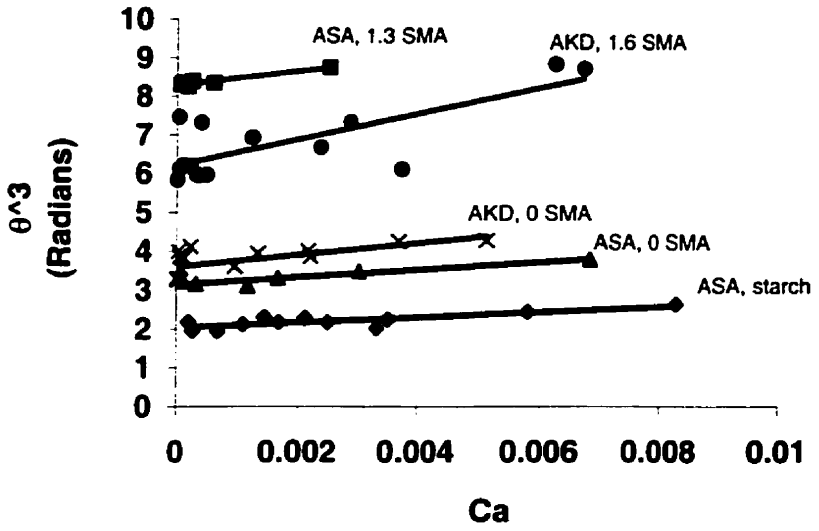

Figure 6- Hoffman-Tanner model for wetting dynamics of water droplets on sized paper.

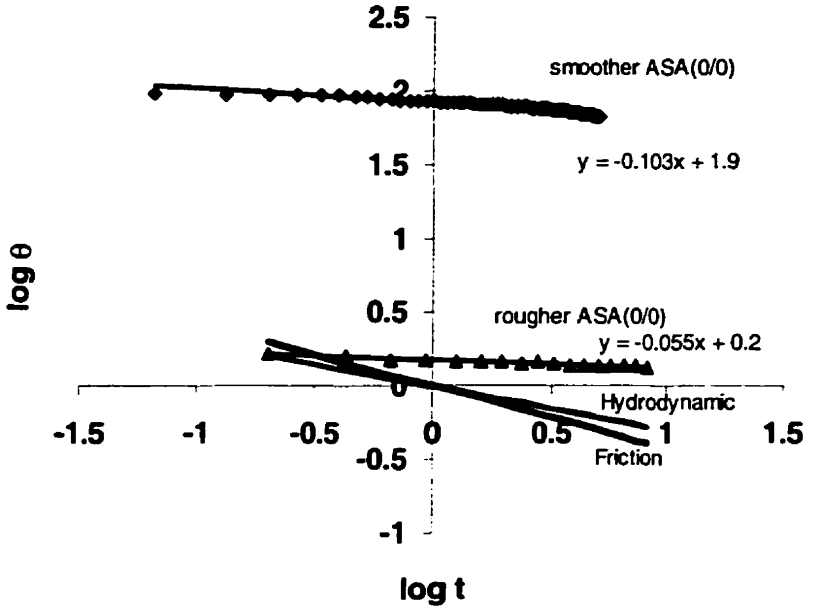

Figure 7- Wetting dynamics of water droplets on sized papers. For reference, the theoretical hydrodynamic and friction regimes are also plotted.

The experimental slopes are –0.1 and –0.06, both significantly lower than expected for the hydrodynamic or friction regimes on a smooth and homogeneous surface. These results, imply a different wetting mechanism. Two possibilities are: first, capillary penetration into paper opposes the flow. Second, surface heterogeneity, created either by hydrophobic domains or roughness, retards wetting by partially pinning the moving three-phase contact line. The average peak to valley roughness among the samples varied between 5.4 μm to 6.9 μm. Furthermore, the surface asperity was typically higher than 0.16 μm. According to Oliver and Mason [13] this difference is sufficient to slow down the wetting velocity significantly and induce non-equilibrium stick and jump movements in the contact line, as observed [20]. This stick and jump movement decreases the wetting rate while the droplet is relaxing on the surface. Another observation supporting this hypothesis is the wetting rate changing inversely proportional to roughness at a constant chemical composition (Figure 7). Therefore, surface roughness plays a significant role in lowering the wetting velocity compared to a smooth surface.

Figure 8 indicates that the equilibrium contact angle of water droplets on paper is a function of the concentration of the hydrophobic domains. Increasing the SMA concentration on paper increases the pseudo-equilibrium contact angle. However, the pseudo-equilibrium contact angles (θ_e^*) of water droplets measured on papers were significantly larger than the equilibrium contact angles measured on SMA-coated glass samples (65°), SMA/starch coated glass (48°) and even polystyrene (90°) [21]. This suggests that besides SMA and starch, another component contributes to hydrophobizing the paper surface.

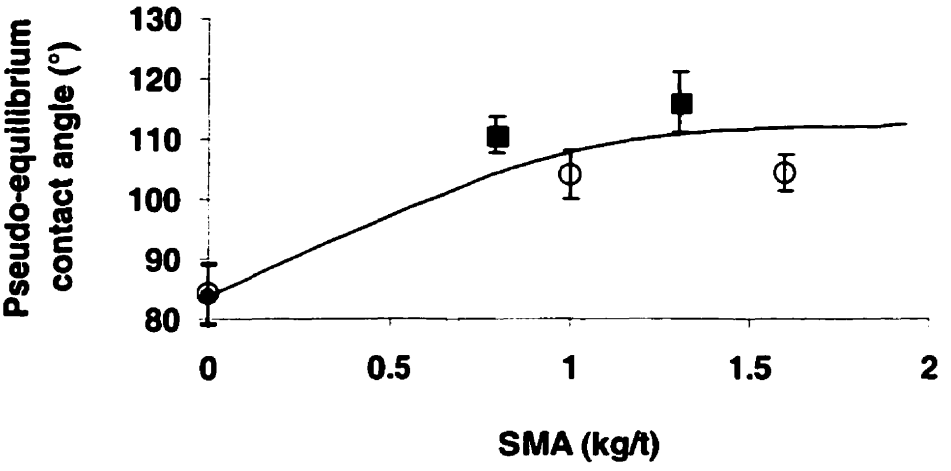

Figure 8- Effect of the surface concentration of hydrophobic domains (SMA) on pseudo-equilibrium contact angle of water. ■ is for ASA papers and ○ is for AKD papers.

We hypothesize that this is due to the air entrapped within the paper surface roughness as sketched in Figure 9. A water droplet forms a contact angle of 180° in air [22]. Hence, considering air in the Cassie's equation results in:

$$\cos\theta_e = f_1 \cos\theta_e^1 + f_2 \cos\theta_e^2 - f_3 \tag{8}$$

since: $$\cos\theta_e^3 = \cos(180°) = -1 \tag{9}$$

and: $$f_3 = 1 - f_1 - f_2 \tag{10}$$

The dynamic wetting of water droplets on papers of different roughness (Figure 4) supports this hypothesis. Decreasing roughness, thus the effective surface coverage of air in contact with the water droplet, decreases both the initial contact angle and the pseudo-equilibrium contact angles of the system. For internally hydrophobized paper with no surface treatment we assume a ternary system in contact with the water droplet consisting of 1) AKD coated fibers [21], 2) AKD vapor treated fibers [19], and 3) air. The air fraction (f_3) can be calculated by assuming: 1) surface coverage of 5% for AKD on fibers [21], 2) θ_e=108° for water on AKD, and 3) θ_e=53° for water on AKD vapor treated fibers [19]. This results in a surface coverage of 40% for air. Interestingly, this value coincides with the ratio of the total valley width to the paper width measured from line profilometry measurement [20]. Similar calculations can be made for surface treated papers.

The effect of surface chemical composition on wetting rate is shown in Figure 10 for the non-calendered papers. The slopes are not affected by surface chemistry (SMA or starch concentration) but are different for papers with different chemical composition in the bulk (ASA or AKD). The wetting rate is independent of surface chemistry and surface chemical heterogeneity. Hydrophobic domains on the surface do not reduce the wetting rate, while surface roughness does.

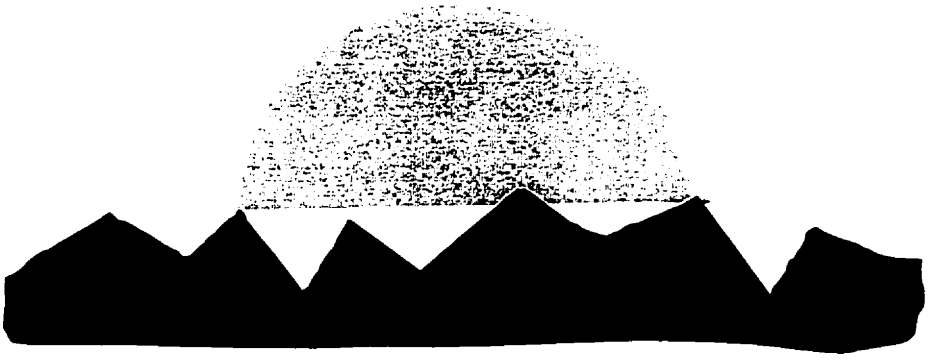

Figure 9- Schematic representation of air entrapped in the valleys on paper roughness

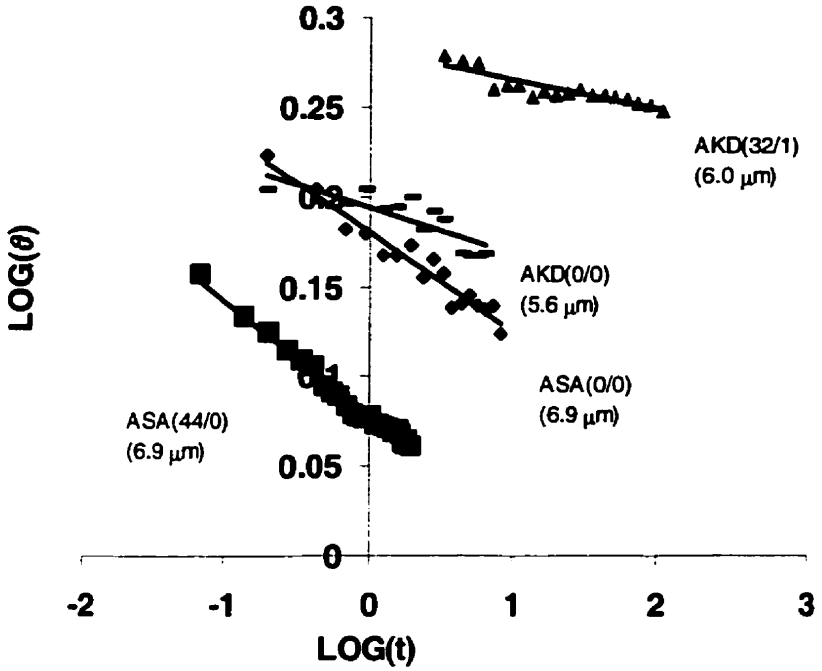

Figure 10- Effect of surface chemical composition and roughness on the wetting rate of water on paper. Roughness on the papers is indicated.

Since roughness controls the rate of wetting, we propose to modify the hydrodynamic power law by a roughness factor, H:

$$\theta(t) \propto t^{(H-\frac{3}{10})} \tag{11}$$

where H is a parameter describing roughness. For the papers tested it ranges between 0.2 for the smoothest to 0.25 for the roughest. The thorough physical meaning of this equation is yet to be explored.

6. CONCLUSION

The combined wetting and absorption dynamics of water droplets over a porous and heterogeneous surface was studied. The objective was to quantify the effect of chemical and physical heterogeneity on the wetting and absorption rates. Paper was chosen as model surface as hydrophobic domains can be easily created at the interface (outer x-y plane) and at the interphase (z-x plane).

The contact angle, volume and baseline formed by a water droplet deposited on hydrophobized paper evolve as a function of two sequential phenomena. First, the water droplet wets the surface until the pseudo-equilibrium contact angle is reached; second, the droplet absorbs into the bulk of paper.

During the first period, the dynamics of wetting follows a power law of the form $\theta(t) \propto t^{(H-3/10)}$. The wetting rate measured (slope) is smaller than that predicted by the hydrodynamic ($\theta(t) \propto t^{-3/10}$) or friction ($\theta(t) \propto t^{-3/7}$) regimes for smooth surfaces by a parameter H, function of the surface roughness. The wetting rate was found to be independent of the chemical heterogeneity of the surface. Surface roughness also affects the equilibrium contact angle as by entrapping air, it renders the surface more hydrophobic.

7. ACKNOWLEDGEMENTS

This research was funded by the Natural Sciences and Engineering Research Council of Canada, and by Hercules Inc.

8. REFERENCES

1. P.G. de Gennes, Wetting: statics and dynamics, Reviews of Modern Physics, **1985,** No. 3, Part 1.
2. T. Blake, "Wetting", J.Berg (Ed), **1993**.
3. M.J de Ruijter, J. De Coninck, G. Oshanin, Droplet spreading: Partial wetting regime revisited, Langmuir, **1999**, 15 (6), 2209.
4. M.J. de Ruijter, M. Charlot, M. Voué, J. De Coninck, Experimental evidence of several time scales in drop spreading, Langmuir, **2000**, 16 (5), 2363.
5. G. Wolansky, A. Marmur, The actual contact angle on a heterogeneous rough surface in three dimensions, Langmuir, **1998**, 14, 5292.
6. A. Marmur, Line Tension and the intrinsic contact angle in solid-liquid-fluid systems, J. Colloid and Interface Science, **1997**, 186, 462.
7. A. Marmur, Thermodynamic aspects of contact angle hysteresis, Advances in Colloid and Interface Science, **1994**, 50, 121.
8. M.H. Adao, M.J. de Ruijter, M. Voué, and J. De Coninck, Droplet spreading on heterogeneous substrates using molecular dynamics, Physical Review E, **1999**, 59 (1), 746.
9. S. Semal, T.D. Blake, V. Geskin, M.J. de Ruijter, Influence of surface roughness on wetting dynamics, Langmuir, **1999**, 15 (23), 8765.
10. A.B.D. Cassie, S. Baxter, Wettability of porous surfaces, Trans. Farad. Soc., **1944**, 40, 546.

11. G. Garnier, M. Bertin, M. Smrckova, Wetting dynamics of alkyl ketene dimer on cellulosic model surfaces, Langmuir, **1999**, 15 (22), 7843.

12. S. Middleman, "Modeling Flows in Films, Jets, and Drops", Chemical Engineering Education, Award Lecture, **1995**, 210.

13. J.F. Oliver, S.G. Mason, Liquid spreading on rough metal surfaces, J. Mat. Sci., **1980**, 15, 431.

14. R.N. Wenzel, Resistance of solid surface to wetting by water, Ind. Eng. Chem., **1936**, 28, 988.

15. C. Huh, J.F. Oliver, S.G. Mason, An experimental study of some effects of solid surface roughness on wetting, Colloids and Surfaces, **1980**, 1, 79.

16. C. Huh, S.G. Mason, , Effects of surface roughness on wetting (theoretical), J. Col. Int. Sci., 60, **1977**, 11-38.

17. T. Gillespie, The spreading of low vapor pressure liquids in paper, J. Col. Sci., 13, **1958**, 32.

18. A. Borhan, K.K. Rungta, An experimental study of the radial penetration of liquids in thin porous substrates, J. Col. Int. Sci., **1993**, 158, 403.

19. L. Yu, G. Garnier, Mechanism of internal sizing with alkyl ketene dimers: The role of vapor deposition, Fundamental Research Symposium, vol. 2, Cambridge, **1997**, p. 1021.

20. H.Modaressi and G. Garnier, Effect of internal and surface sizing on the wetting and absorption properties of paper, (submitted to JPPS **2000**).

21. Mark, J.E., Physical Properties of Polymers Handbook, American Institute of Physics (AIP) Press, **1996**, 673.

22. Adamson, A.W., Physical Chemistry of Surfaces, 2nd edition, **1967**, 358.

CHAPTER 4

Wetting on a heterogeneous surface

Hedieh Modaressi and Gil Garnier[1]
Paprican and the Department of Chemical Engineering
McGill Pulp and Paper Research Center
3420 University St.
Montreal, QC H3A 2A7

Abstract

The effect of surface heterogeneity on wetting behavior of water droplets on model surfaces was studied. Cationic polystyrene latex particles from an aqueous suspension were deposited on glass slides to generate surfaces with chemical heterogeneity. Deposition was achieved by the electrostatic attraction between the cationic polystyrene particles and the anionic glass. The latex particles were deposited as individual particles while at higher surface coverages, clusters were formed on glass. The latex particles and clusters provided hydrophobic sites on hydrophilic glass. Physical heterogeneity was manipulated by annealing the adsorbed latex particles above their glass transition temperature (T_g =108°C). The apparent contact angle of water droplets on surfaces with two levels of physical heterogeneity and six levels of chemical heterogeneity was measured. Wetting of water droplets was affected not only by the surface coverage, but also by the distribution of the hydrophobic domains on the surface.

The effect of roughness on wetting followed Wenzel's equation. Chemical heterogeneity had a more significant effect on wetting than the physical heterogeneity of the surface. The contact angle of water droplets on chemically heterogeneous surfaces did not follow Cassie's equation. Instead, the equilibrium contact angle of water droplets

was a function of a fraction of the perimeter of the water droplet in contact with the hydrophobic domains.

Keywords: contact angle, wetting, roughness, chemical heterogeneity, surface chemistry, hydrophobic, hydrophilic, modeling.

For correspondence: Gil.Garnier@kcc.com or hmodar@po-box.mcgill.ca

[1] Now at Kimberly-Clark, Neenah, WI.

1. INTRODUCTION

The wetting behavior of composite surfaces with chemical heterogeneity is of great scientific interest and has many industrial applications. For instance, in inkjet printing the presence of hydrophobic domains on the surface affects the wetting and the penetration of ink into the paper. Another application is in textile industry where controlling the degree of hydrophobicity of fabrics is of interest. In all these cases, the wetting characteristics of surfaces are controlled by the chemistry and physical heterogeneity (roughness) of the surface.

The concept of wetting on heterogeneous surfaces has been studied for a long time [1,2,3]. Cassie [1,2] first proposed a theoretical correlation for the contact angle of a liquid on a two-component surface. In his derivation, E, the energy gained when a liquid wets a unit area of a two-component composite surface is:

$$E = f_1(\gamma_{s_1v} - \gamma_{s_1l}) + f_2(\gamma_{s_2v} - \gamma_{s_2l}) \tag{1}$$

where f_1 is the fractional area of the surface with contact angle θ_1 and f_2 is the area of the surface with contact angle θ_2 and γ_{sv} and γ_{sl} are the interfacial solid-vapor and solid-liquid tensions for each of the areas with the corresponding chemical compositions.

From the Young equation in the absence of gravity, the equilibrium contact angle θ_e between a liquid droplet and a flat and homogeneous solid surface is given by:

$$\cos\theta_e = \frac{\gamma_{sv} - \gamma_{sl}}{\gamma_{lv}} \tag{2}$$

Equation (2) shows that the cosine of the equilibrium contact angle is the ratio of the energy gained in forming a unit area of solid-liquid interface to that required to form a

unit area of liquid-air interface. Using the same analogy the equilibrium contact angle for a liquid droplet on a 2-component composite surface was derived as:

$$\cos\theta_e = \frac{E}{\gamma_{lv}} = f_1 \cos\theta_1 + f_2 \cos\theta_2 \tag{3}$$

Equation (3), known as Cassie's equation, is still the most commonly used model for predicting the equilibrium contact angle of a liquid droplet on a composite surface with chemical heterogeneity.

The contact angle of a liquid on a rough solid surface is predicted using Wenzel's equation, which is a modified form of the Young equation [3, 5]:

$$\cos\theta = r\frac{(\gamma_{sv} - \gamma_{sl})}{\gamma_{lv}} \tag{4}$$

The roughness factor (r) in Wenzel's equation is the average ratio of the actual rough surface to the geometric projected area; hence, r is always greater than one. According to Wenzel's equation, roughness enhances the hydrophobicity of a hydrophobic surface and also increases hydrophilicity of a hydrophilic surface.

The combined effect of chemical and physical heterogeneity of a surface on the equilibrium contact angle has been predicted by combining Cassie's equation with Wenzel's equation [4]. Hashimoto and Watanabe et al. [4] performed wetting experiments on highly hydrophobic surfaces with various roughness. Based on AFM images of their model surfaces, they assumed the surface to consist of a series of uniform needles with constant height and spacing. Their combined Cassie and Wenzel model for a rough surface with air entrapped between the roughness on the surface has the form:

$$cos\theta = rf\, cos\theta_e + f - 1 \tag{5}$$

where θ is the equilibrium contact angle on a rough surface, θ_e is the equilibrium contact angle on a flat surface, r is the ratio of the side area to the bottom area of the needle and f is the area fraction of the surface in contact with the droplet. Their experimental values were in good agreement with the model. However, for super hydrophobic surfaces (θ~ 160°) where air entrapment was significant, r was close to 1. This indicates that water droplets were only touching the top portions of the needles (roughness) hence smoothening the surface, when a significant amount of air was entrapped in roughness [4,7].

Both Cassie's and Wenzel's equations are independent of the local heterogeneities and assume a "uniform" distribution of heterogeneities on the surface. Equilibrium contact angle of a droplet on a heterogeneous surface with non-uniform distribution of heterogeneity is a function of the location of the contact line. The contact line and the contact angle of the droplet at each point on the contour change to satisfy a local minimum free energy. For a flat and heterogeneous surface with non-uniform distribution of i chemical domains, Swain and Lipowsky [5] derived the following equation:

$$\cos\theta_{eff} = \sum_i l_i \cos\theta_i \tag{6}$$

where l_i is the fraction of the total perimeter of the drop which is on the surface composed of material i, and θ_{eff} is the effective contact angle defined as an average contact angle of the drop around the three-phase contact line at equilibrium:

$$\cos\theta_{eff} = \frac{\oint_{\partial\Gamma} ds \cos[\theta(s)]}{\oint_{\partial\Gamma} ds} \tag{7}$$

where $\partial\Gamma$ is the position of the contact line, ds is the unit arc length on the contact line and $\theta(s)$ is the local equilibrium contact angle.

Hysteresis of the contact angle is another parameter used for quantifying surface heterogeneity. The equilibrium contact angle of a liquid droplet on a heterogeneous surface depends on the manner the droplet has reached its static position [6]. For a heterogeneous surface, an advancing angle is always larger than a receding angle. Hysteresis is the difference between the advancing and receding contact angle of a droplet on a surface. Hysteresis has been mainly attributed to adsorption of liquid molecules ahead of the contact line on the solid surface, and to roughness [1,6,8]. Shuttleworth and Bailey [6] showed that hysteresis is merely due to roughness unless for specific liquids at certain conditions. For a liquid droplet advancing perpendicular to the direction of grooves on a rough surface, they showed that the apparent contact angle evolves into its first metastable equilibrium state when:

$$\theta_a = \theta_e + \psi_{\max} \tag{8}$$

where θ_a is the advancing contact angle, θ_e is the equilibrium contact angle and Ψ_{max} is the maximum slope of roughness on the surface. A receding droplet will reach its first metastable equilibrium value when:

$$\theta_r = \theta_e - \psi^*_{max} \tag{9}$$

where θ_r is the receding contact angle and Ψ^*_{max} is the maximum slope of roughness on the surface. Hysteresis on such a surface is then equal to [6]:

$$H = \psi_{max} + \psi^*_{max} \tag{10}$$

However, hysteresis was shown to be also a function of the surface chemical heterogeneity [8]. Johnson and Dettre [8] modeled the behavior of a liquid droplet at rest

on a chemically heterogeneous solid surface. In their model, they assumed the solid surface to consist of alternating circular bands of different surface energies. Between each two positions of metastable equilibrium there is an energy barrier which the drop should overcome. These energy barriers control the contact angle hysteresis.

In this study, the objective was to elucidate the effect of chemical and physical heterogeneity on the wetting properties of a surface. Latex particles were deposited on glass in order to produce hydrophobic domains on a hydrophilic surface. Changing the deposition time varied the surface coverage of the hydrophobic domains. The deposited latex particles were annealed above T_g on the surface for two different times. Annealing was performed to enhance the adhesion between the latex particles and glass [9] and to vary the roughness.

2. EXPERIMENTAL

2.1. Materials

Cationic polystyrene latex from a 200 ppm suspension was deposited on glass. Latex particles were spherical and consisted of a hydrophobic core (polystyrene) surrounded by a hydrophilic copolymer on the surface which provided the positive charge on the particles. The cationic polystyrene suspension was provided by *Hercules Inc.* (Wilmington, Delaware, USA). The suspension had 28.15% total solids with a particle size of 620 nm.

2.2. Methods

2.2.1. Application of Polystyrene

The polystyrene suspension was diluted to 200 ppm with de-ionized distilled water. Prior to each experiment, pre-cleaned glass slides (Fisher, 75×25 mm^2) were dipped in a nitric acid bath for two hours and rinsed with de-ionized distilled water. The glass slides were then air-dried. The glass slides were then immersed into the cationic polystyrene suspension for deposition. During deposition the suspension was constantly stirred at a low speed using a magnetic stirrer. Six time intervals were chosen for deposition: 1 minute, 2 minute, 10 minute, 20 minute, 1 hour and 2 hour. Upon latex deposition, the glass slides were rinsed in de-ionized distilled water. One side of the glass slide was wiped only to keep latex particles on one side of the surface. The prepared samples were hung to dry in air. One set of glass slides was placed into the oven at 150°C for two hours (T_g=108°C). A second set of glass slides was placed in the oven at the same temperature for five minutes only to secure the latex particles on glass.

2.2.2. Surface Coverage Measurement

After deposition, each glass slides was examined under a reflectance microscope with a 50x-magnifying lens. Images were analyzed with the image analysis software *Image Pro Plus* (Media Cybernetics, version 3.0). After adjusting the contrast, particles were counted and their surface area was measured. Glass slides were also examined using scanning electron microscopy (SEM). The diameter of the particles in the suspension as measured by light scattering was 620±15 nm. The polydispersity was 0.32. The electrophoretic mobility of the cationic polystyrene particles, in de-ionized distilled water was 1.4 $m^2s^{-1}V^{-1}$.

2.2.3. Surface Roughness Measurement

Atomic force microscopy (AFM, Digital Instruments Nanoscope II system) was used to measure the height of the latex particles after deposition and annealing on glass slides. A silicon nitride pyramidal tip (Digital Instruments model NP-20) was used for scanning in contact mode with AFM. AFM was also used to measure the average roughness on latex deposited glass slides after annealing.

2.2.4 Contact Angle Measurement

The contact angles of de-ionized distilled water droplets on the polystyrene-deposited glass samples were measured using a *Dynamic Angle Analyzer* manufactured by *First Ten Angstroms* (Portsmouth, VA, USA). The droplets were formed with an automatic forward/reverse syringe pump with a 10 mL syringe controlled by computer. The volume (~5 μL) was selected to achieve droplets with base line lengths of about 3- 5 millimeters while at rest on the surface. The glass samples were placed on a mobile platform. Each sample was brought into contact with a sessile drop hanging from the tip

of the syringe, thereby reducing the effects of kinetic energy on wetting. A CCD video camera with a 6:1 zoom microscope lens captured the droplet behavior. The recording time was set at 7.5 seconds with a time interval between two consecutive frames of 0.017 seconds. The recorded images were then analyzed and the apparent contact angle $\theta(t)$ and the baseline (d) of the droplets on the surface were measured for each frame. The advancing contact angle and the receding contact angle of water droplets were also measured. The advancing angles and receding angles were measured while increasing and decreasing the volume of the droplet, respectively.

3. RESULTS

The wetting behavior of water droplets on latex deposited glass slides was investigated. Cationic polystyrene latex particles were deposited onto glass to provide chemical heterogeneity. The latex particles produced hydrophobic domains on the hydrophilic glass. Since the deposited latex particles were spherical they also provided a physical heterogeneity on the surface. Surface chemical heterogeneity was varied with the deposition time of cationic polystyrene onto the surface. After latex deposition, the glass slides were examined using a reflectance microscope (Figure 1). Varying the deposition time between 1 min to 2 hours increased the surface coverage of latex particles on the surface between 1.2% and 21.3%. The rate of deposition slowed down after 20 minutes deposition (Figure 2). Preliminary wetting experiments showed that adhesion of the latex particles on glass was not strong enough to resist the shear induced by washing or even the wetting experiments. Hence, the deposited latex particles were secured onto the surface by annealing. A maximum latex surface coverage of 29±2% was achieved. Annealing in the oven for 2 hours increased the surface coverage of the hydrophobic domains to 49.5% of the surface (Figure 2). Figure 3-a and 3-b show the SEM images of the latex deposited glass slides before and after annealing. Latex particles formed clusters on the surface (Figure 3-a). Clustering was enhanced by increasing the deposition time. Annealing transformed the clusters into semi-spherical domains of various sizes. A 5-minute annealing treatment only secured the particles on glass without affecting their shape or surface coverage.

1 minute, 1.2% coverage

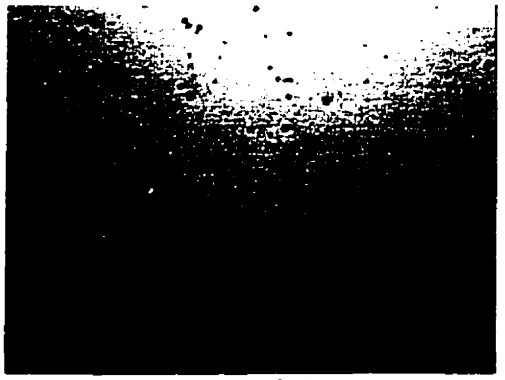

2 minutes, 2.6% coverage

10 minutes, 12.2% coverage

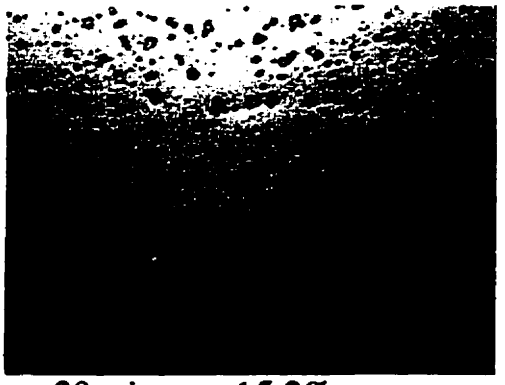

20 minutes, 15.2% coverage

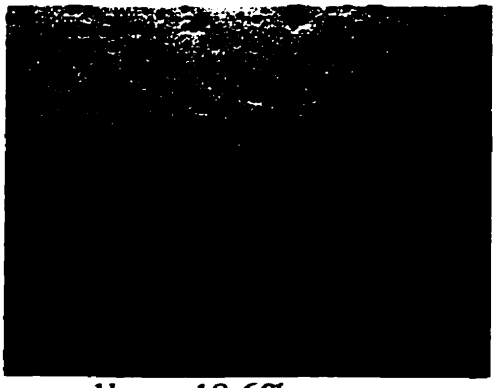

1hour, 18.6% coverage

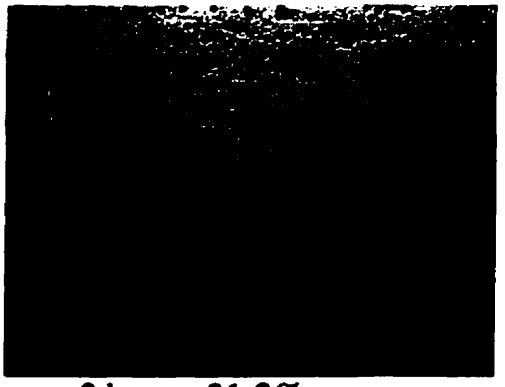

2 hours, 21.3% coverage

Figure 1- Top view microscopy images of latex deposited glass slides. Deposition time and coverage (%) are shown for each picture.

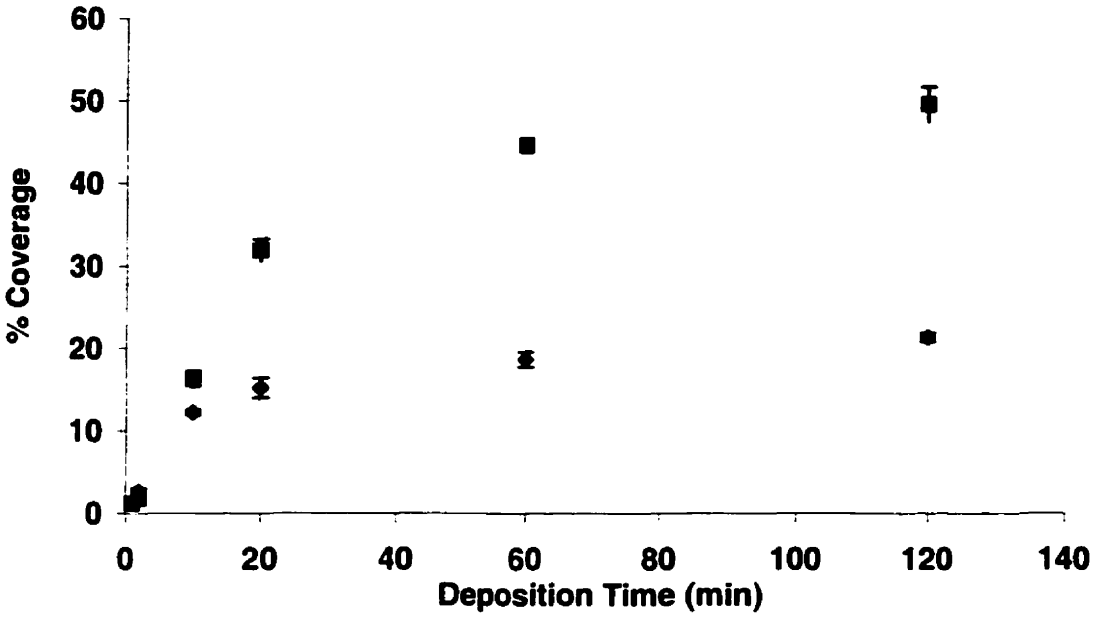

Figure 2- Latex coverage on glass as a function of deposition time. ■ is for 2-hr annealed latex deposited glass slides; ◆ is for the air-dried latex deposited glass slides without any heat treatment.

Figure 3-a Scanning electron micrograph of air-dried latex deposited glass slides (no heat treatment).

Figure 3-b- Scanning electron micrograph of 2-hr annealed latex deposited glass slides.

The evolution of the contact angle of a water droplet with time on a heterogeneous glass slide is shown in Figure 4-a and b for 5 minute and 2 hour annealing, respectively. Increasing the surface coverage of latex particles on glass increased hydrophobicity. The equilibrium contact angle of water droplets on surfaces with latex surface coverages ranging from 1% to 50% varied from 18° to 71°. Increasing the surface coverage of hydrophobic domains from 32% to 50% did not significantly increase the equilibrium contact angle.

Atomic Force Microscopy was used to evaluate the roughness and the height of the latex particles annealed on glass slides (Figure 5). Table I lists the average height of the latex particles annealed for 5 minutes and 2 hours. Annealing for 5 minutes did not affect the diameter of the spherical particles from their original size (~600 nm), while annealing for 2 hours decreased the height of the spheres to less than half of their original diameter. This is in agreement with the increase in the surface coverage. The AFM measurements also show that the clusters were only formed on the x-y plane and particles were not stacked on top of each other.

To further characterize the surface heterogeneity, advancing and receding contact angles of water droplets were measured on the latex deposited glass slides. The advancing contact angle remained constant as the volume of the water droplet increased, while decreasing the volume decreased the receding angle (Figure 6). Hysteresis ($\Delta\theta$) for a 5-min annealed glass slide with ~17% latex coverage (1-hr deposition) was 37° while for a 2-hr annealed glass slide with the same latex coverage was 33°. The advancing angle for the 2-hr annealed sample was $\theta_a = 65° \pm 3°$ while the receding angle was $\theta_r = 32° \pm 1°$.

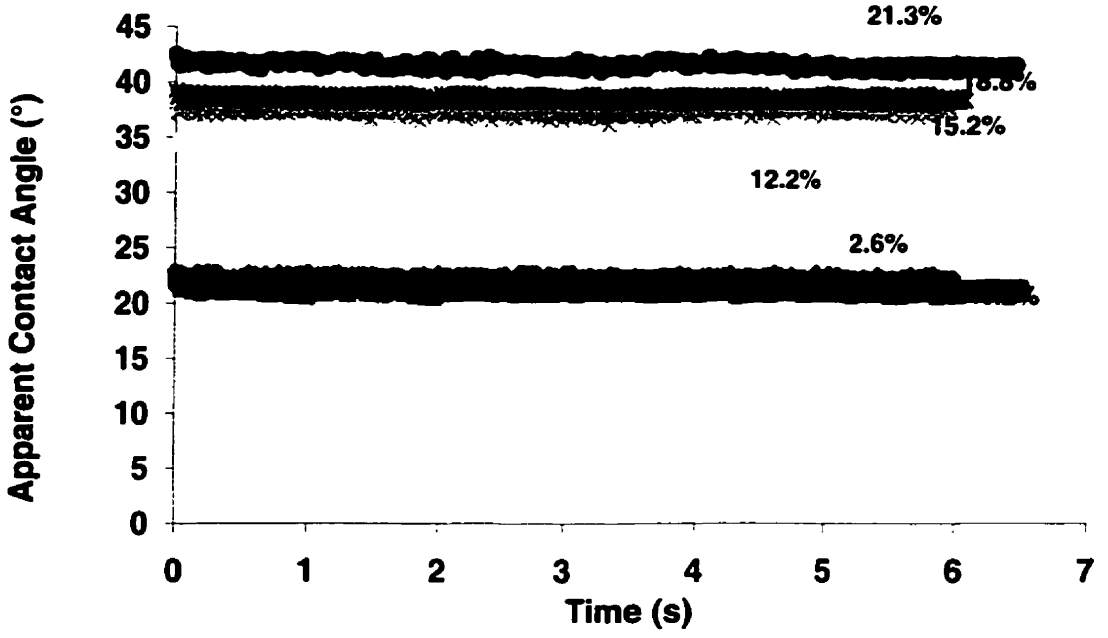

Figure 4-a- Evolution of contact angle of a water droplet on latex treated glass slides (5-min annealing at 150 °C). The coverage (%) of latex particles on glass is shown on each plot.

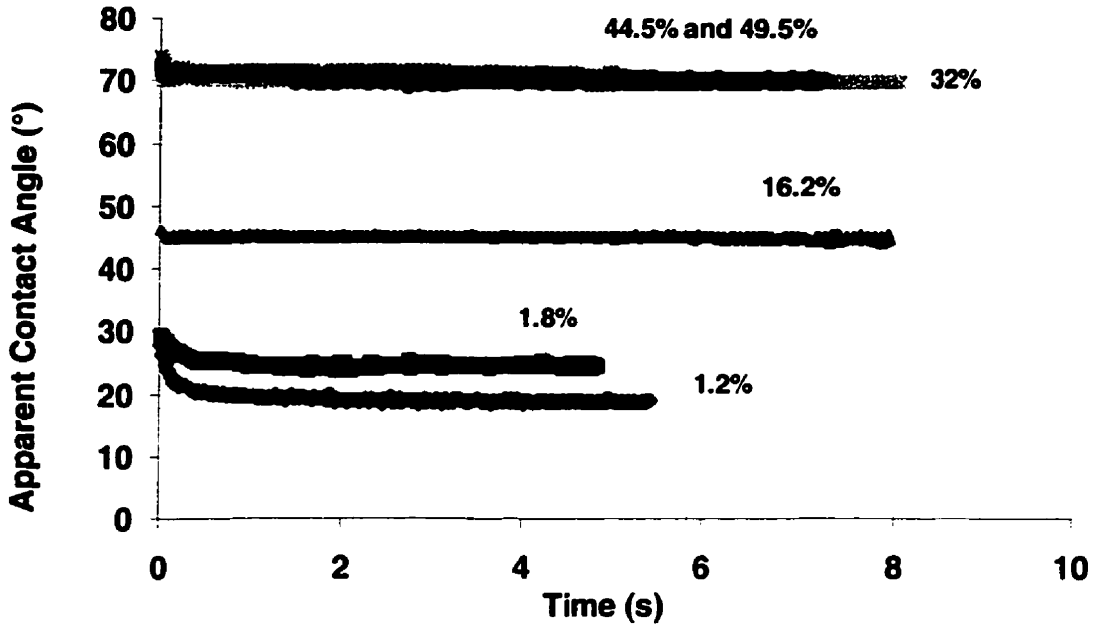

Figure 4-b- Evolution of contact angle of water droplets on latex treated glass slides (2-hr annealing at 150 °C). The coverage of latex particles on glass is shown on each plot.

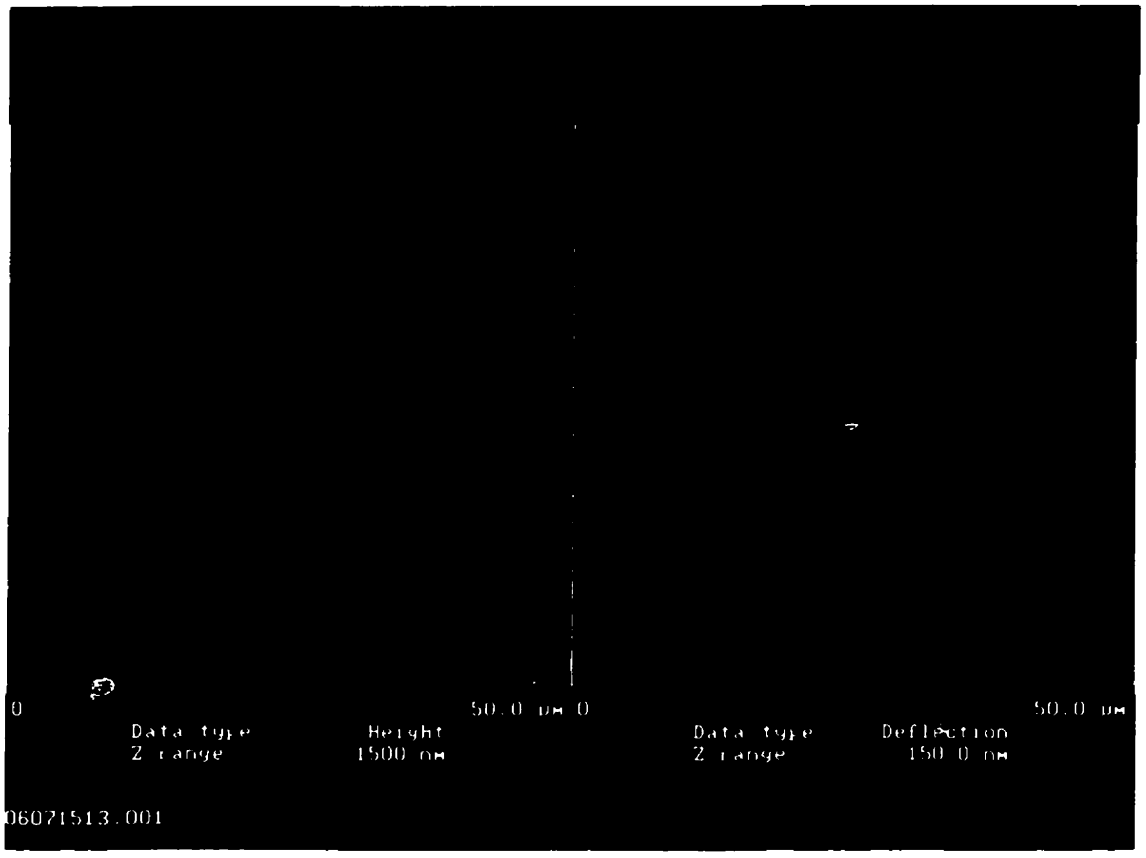

Figure 5- AFM image of latex deposited glass slide annealed for 2 hours at 150 °C.

Table I- Average height of the latex particles measured by AFM Section Analysis

Deposition (min)►	**2**	**20**	**120**
Annealing time ▼			
5 min (nm)	630±93	574±116	606±115
2 hrs (nm)	122±48	242±97	238±89

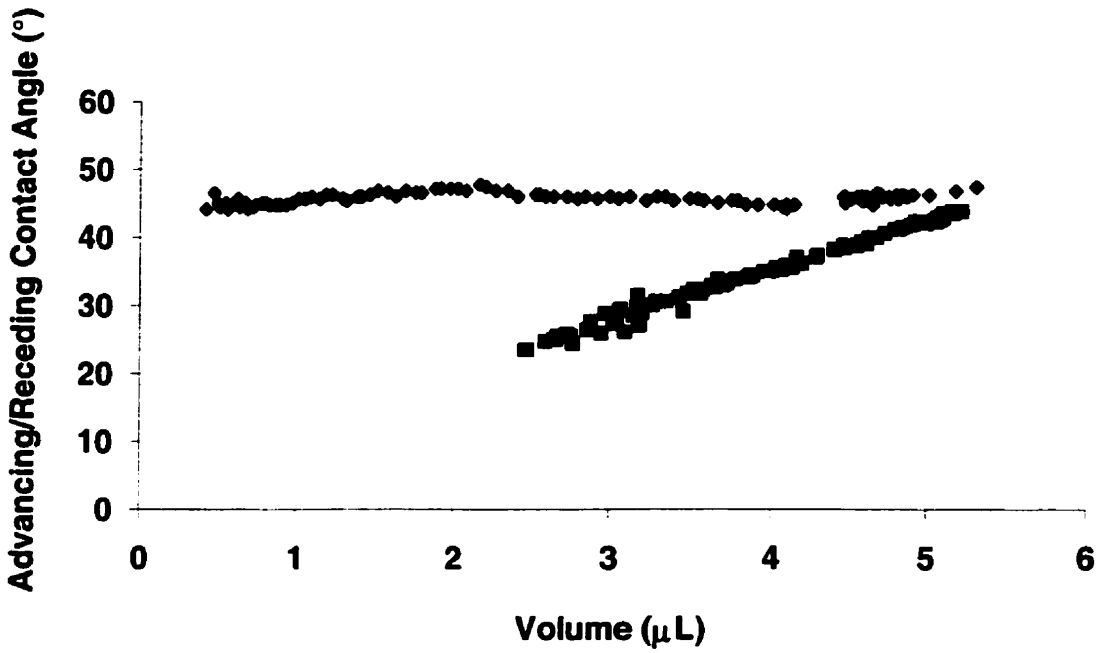

Figure 6- Evolution of the advancing/receding contact angle with volume for 5-min annealed latex deposited glass; deposition time was 10 minutes (12% coverage). ◆ is the advancing and ■ is the receding angle.

Table II compares the change in hysteresis as a function of latex surface coverage. The average of three replicates is shown. Advancing angles, receding angles and hysteresis all increased with increasing latex coverage.

Table II- Advancing Angle (θ_a), Receding Angle (θ_r) and Hysteresis ($\Delta\theta$) for latex deposited samples annealed for 5 minutes at 150 °C

	% Coverage					
	4	**4.5**	**11.5**	**13.6**	**16.9**	**17.4**
θ_a (°)	32±5	31±6	45±6	53±3	66±5	57±7
θ_r (°)	8±1	10±3	21±4	27±7	29±3	21±5
$\Delta\theta$ (°)	24±5	21±7	24±7	26±8	37±6	36±9

4. DISCUSSION

4.1. Latex Deposition

The surface coverage of latex particles on glass is expected to increase with deposition time. Increasing deposition time should allow more positively charged particles to adhere to the negatively charged glass surface. However, there was a limit to deposition and a maximum surface coverage of about 22% was reached after 20 minutes exposure of glass slides to the 200 ppm latex suspension. Two explanations could account for the maximum surface coverage. First, since the driving force for deposition is the electrostatic forces between the particles and the surface, deposition may stop when the total charges of the cationic particles deposited on the surface compensate the total negative charge of glass [12]. Second, electrostatic repulsion between the positively charged latex particles causing desorption of cationic particles from the surface might limit further deposition. Therefore, the electrostatic repulsion between the cationic particles will reduce the adsorption rate once certain spacing between the adsorbed particles is achieved.

Even though deposition was due to the electrostatic forces between the cationic latex particles and anionic glass, only a weak adhesion was achieved. A water film may form on the surface of the particles during deposition. At the same time, during deposition, a water layer is also formed on glass (hydrophilic). These two layers might prevent direct contact between the cationic polystyrene latex particles and glass and poor adhesion might result. The clusters formed on the surface after drying were due to the capillary forces acting on the particles during drying (water evaporation in the interstitial

region between two adjacent latex particles) [13]. Poor adhesion of the latex particles to the surface made the latex particles more susceptible to move under the shear due to capillary forces and hence, form clusters on the surface [7].

4.2. Wetting

Assuming a two-component system of glass and polystyrene with the measured corresponding surface coverage, the equilibrium contact angles of water droplets were calculated using Cassie's equation. Figure 7 compares the predicted equilibrium contact angles with the actual equilibrium contact angles measured on the surface. The equilibrium contact angles as predicted by Cassie's equation are consistently lower than the actual angles measured on latex deposited glass slides and annealing did not affect this deviation. Hence, roughness is not the cause of this deviation. Deviation from Cassie's equation for the samples annealed for 5 minutes is in the range of 20-40% while it is 20-50% for the particles annealed for 2 hours. In the latter case, deviation from Cassie's equation is more pronounced at lower deposition times. Distribution of hydrophobic domains on the surface at lower coverage (< 5%) is expected to have a more pronounced effect on the contact line and hence on the contact angle than at higher coverage. In the case of 5-min annealed particles it should be noted that since the particles are spherical, the surface coverage measured for these samples are higher than the actual surface coverage. In fact the actual surface area covered per spherical particle is πa^2 if we assume that the liquid does not remove the air under the particle and that the contact line is pinned by a particle at its footstep (Figure 8). The ratio of a/R_p is always less than 1 unless the water droplet forms a contact angle of 90° on the surface where $a=R_p$.

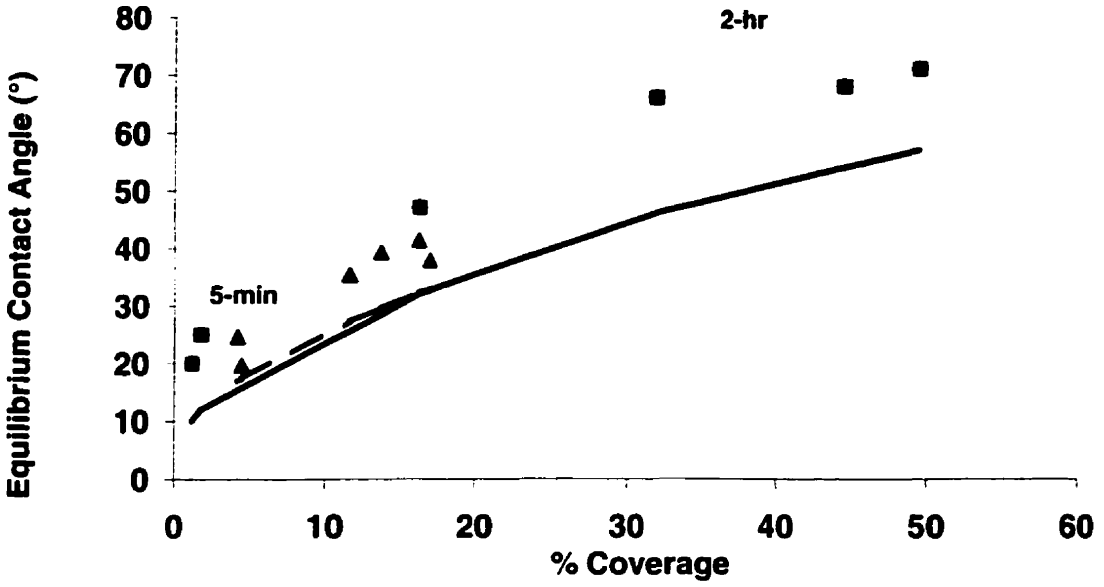

Figure 7- Comparison between Cassie's model prediction and experiments. Dashed line shows Cassie's model for 5-min annealed and solid line shows the same model for 2-hr annealed latex particles, ■ is for the 2-hr annealed and ▲ is for the 5-min annealed latex deposited glass slides.

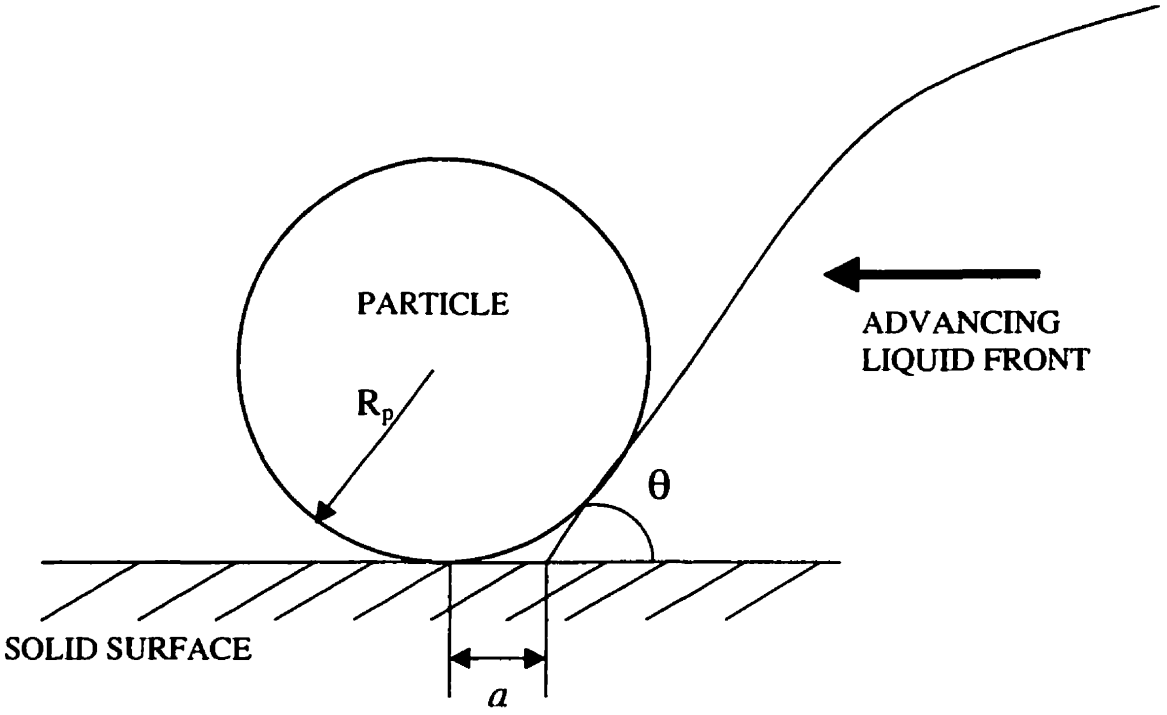

Figure 8- The true surface area covered by a single particle assuming the liquid doesn't remove the air from the space under the particle.

This argument suggests that even though the actual coverage of latex particles is over estimated in our calculations, Cassie's equation fails to explain the wetting characteristics of the surface. Again, non-uniform distribution of the hydrophobic domains on the surface may be a reason for this deviation [5]. Figure 1 clearly shows the non-uniform distribution of latex particles at all deposition times. It is evident that the probability of the three phase contact line to meet any of the hydrophobic domains is not the same on all locations on the surface. Hence, relying on an average surface coverage for predicting the contact angle of a droplet on such a surface is not optimal. Instead, the approach proposed by Swain and Lipowsky [5] and presented in equation 6 was preferred. Assuming all the latex particles to be of uniform size (d_i), the fraction of the total perimeter of the drop in contact with the latex particles (l_i) in equation 6 can be estimated as:

$$l \propto \frac{d}{R_d} \tag{11}$$

where R_d is the radius of the water droplet on the surface. For the same surface, the surface coverage (f_i) in Cassie's equation is estimated as:

$$f \propto (\frac{d}{R_d})^2 \tag{12}$$

Therefore l can be estimated as the square root of the surface coverage. Figure 9 shows that with these assumptions equation 6 is in good agreement with the experimental data. This suggests that only the hydrophobic particles at the three-phase contact line dictate the shape of the droplet and the contact angle it forms on the surface.

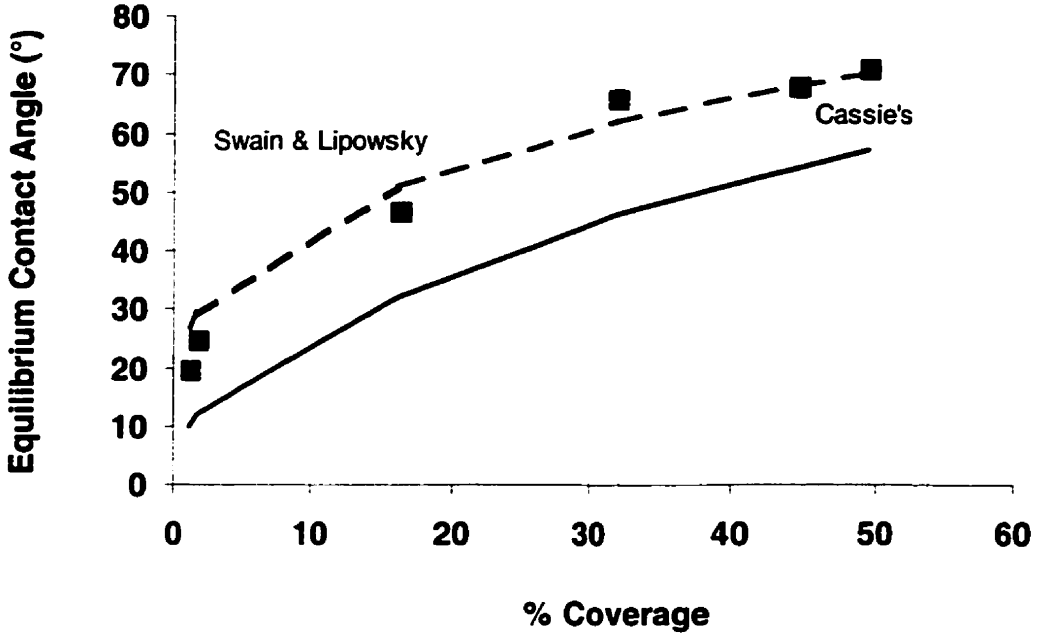

Figure 9- Comparison between experimental data, Cassie's model and the model proposed by Swain and Lipowsky. ■ is for experimental data, solid line shows Cassie's model and dashed line shows the model proposed by Swain and Lipowsky.

The effect of surface roughness was investigated by comparing the equilibrium contact angles of water droplets measured on 5-min annealed and 2-hr annealed glass slides with the same surface coverage of latex particles. Both samples chosen had 16% coverage of latex particles. Assuming Wenzel's equation to be valid, the relationship between the equilibrium contact angle of water droplets on 5-min (θ_5) and 2-hr (θ_m) annealed sample can be written as:

$$\cos\theta_5 = r\cos\theta_m \tag{13}$$

The average height of the particles measured by AFM sample were h_5 = 575 nm and h_m = 240 nm for the 5-min and the 2-hr annealed samples, respectively. Figure 10 schematically compares the particles at both conditions. The 5-min annealed particle was assumed to be a sphere while the 2-hr annealed particle was a spherical cap with the volume: (parameters as defined in Figure 10)

$$V = \frac{1}{6}\pi h_m(3r_2^2 + h_m^2) \tag{14}$$

Assuming an equal volume for the two particles, r_2 was calculated from:

$$\frac{h_m}{r_2} = \frac{1-\cos\alpha}{\sin\alpha} \tag{15}$$

$$R = \frac{r_2}{\sin\alpha} \tag{16}$$

The surface area of the spherical cap (Sa_{cap}) was then calculated:

$$Sa_{cap} = 2\pi R^2 - 2\pi Rh \tag{17}$$

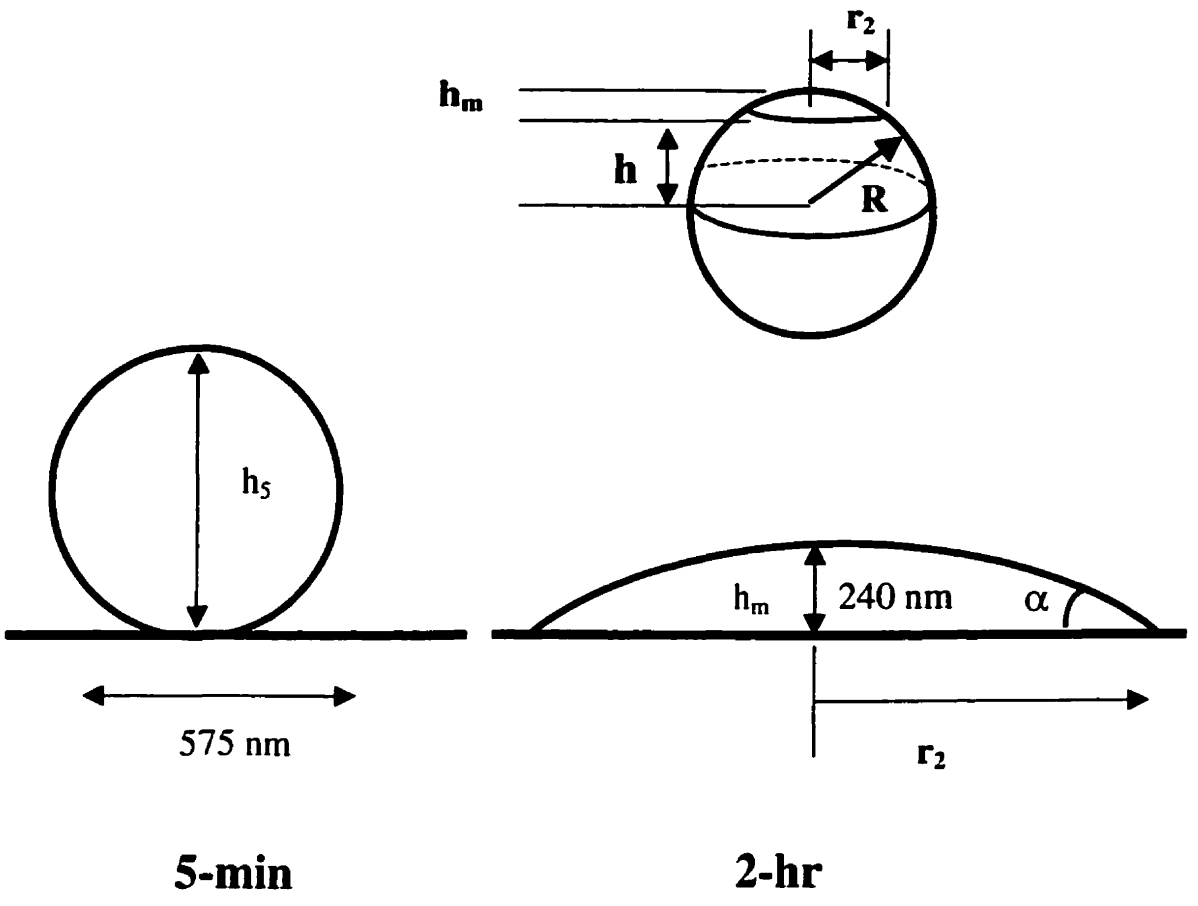

Figure 10- Geometry of particles after 5-min annealing and 2-hr annealing.

Assuming the samples to consist of latex particles of the same size, the roughness factor (r) in Wenzel's equation was calculated as the ratio of the surface area of the spherical particle in the 5-min sample to the surface area of the spherical cap in the 2-hr sample. This resulted in an r value of 1.08. This value only differs by 4% from the r value calculated from equation 13. Hence, roughness affected the wetting properties of the surface as predicted by Wenzel's equation.

Finally, our observations showed that hysteresis was more a function of chemical heterogeneity of the surface than roughness.

5. CONCLUSION

The wetting behavior of water droplets deposited on glass slides with chemical and physical heterogeneity was studied. Cationic polystyrene latex particles were deposited on glass to provide hydrophobic domains on a hydrophilic surface. Surface coverage of latex particles was a function of deposition time. Roughness was controlled by annealing.

Roughness affected wetting in accordance with Wenzel's equation. The roughness factor r in Wenzel's equation quantified from the wetting experiments was similar to that calculated from the geometry of the surface.

Cassie's equation was found to underestimate the hydrophobicity of the surface. Changing the roughness of the surface did not affect this deviation. The average equilibrium contact angle of a water droplet on latex deposited glass slides was a function of the fraction of the contact line in contact with the hydrophobic domains.

Hysteresis was mainly affected by chemical heterogeneity. Changing the surface roughness did not significantly affect hysteresis.

6. ACKNOWLEDGEMENTS

The authors thank Drs. M.E. Weber and B. Alince for inspiring discussions and valuable advice.

This research was funded by the Natural Sciences and Engineering Research Council of Canada, and by Hercules Inc.

6. REFERENCES

1. A.B.D.Cassie, Contact Angles, Discussion of Faraday Society, **1948**, 3, 11-16.
2. A.B.D. Cassie and S. Baxter, Wettability of porous surfaces, Trans. Faraday Soc., **1944**, 40, 546-551.
3. W.R. Wenzel, Resistance of solid surface to wetting by water, Ind. Eng. Chem., **1936**, 28, 988-994.
4. M. Miwa, A. Nakajima, A. Fujishima, K. Hashimoto and T. Watanabe, Effects of the surface roughness on sliding angles of water droplets on superhydrophobic surfaces, Langmuir, **2000**, 16, 5754-5760.
5. P.S. Swain and R. Lipowsky, Contact angles on heterogeneous surfaces: a new look at Cassie's and Wenzel's laws, Langmuir, **1998**, 14, 6772-6780.
6. R. Shuttleworth and G.L.J. Bailey, The spreading of a liquid over a rough solid, Discussion of Faraday Society, **1948**, 16-22.
7. P.G. de Gennes, Wetting: statics and dynamics, Reviews of Modern Physics, 57, part 1, **1985**, 827-863.
8. R.E. Johnson and R.H. Dettre, Contact angle hysteresis. III. Study of an idealized heterogeneous surface, The Journal of Physical Chemistry, **1963**, 68, 1744-1750.
9. V. Granier and A. Startre, Ordering and adhesion of latex particles on model inorganic surfaces, Langmuir, **1995**, 11, 2179-2186.
10. C.C. Ho and M.C. Khew, Surface free energy analysis of natural and modified natural rubber latex films by contact angle method, Langmuir, 16, **2000**, 1407-1414.

11. T. Serizawa, S. Kamimura, M. Akashi, Electrostatic adsorption of polystyrene particles with different surface charges onto the surface of an ultrathin polymer film, Colloids and Surfaces A: Physicochemical and Engineering aspects, **2000**, 164, 237-245.

12. K.U. Fulda, A. Kampes, L. Krasemann, B. Tieke, Self assembled mono- and multilayers of monodisperse cationic and anionic latex particles, Thin Solid Films, 327-329, **1998,** 752-757.

13. F. Lin and D.J. Meier, A study of latex film formation by atomic force microscopy. A. A comparison of wet and dry conditions, Langmuir, 11, no. 1, **1995**, 2726-2733.

14. R.K. Iler, Multilayers of colloidal particles, Journal of Colloid and Interface Science, 21, **1966**, 569-594.

CHAPTER 5

Spontaneous penetration of water in partially hydrophobized vertical capillaries

Hedieh Modaressi, Martin Weber and Gil Garnier
Paprican and the Department of Chemical Engineering
McGill Pulp and Paper Research Center
3420 University St.
Montreal, QC H3A 2A7

Abstract

Capillary penetration of water into glass tubes with chemical heterogeneity on the tube walls was measured. Hydrophobic domains inside the tube walls consisted of polystyrene latex particles. The combination of these hydrophobic domains and glass created a heterogeneous surface

The rate of water penetration into latex deposited tubes was measured. The maximum penetration height was a function of surface coverage of hydrophobic domains inside the tubes. Capillary rise was not smooth and a stick and jump movement of the three-phase contact line was observed. Experimental results were compared to two models. The capillary rise dynamics for the heterogeneous capillaries were slower than model predictions. The slower dynamics were due to local changes in the static advancing contact angle. At small times, when the velocity was large, surface heterogeneity did not affect the dynamics of capillary rise. Capillary rise in the initial stages did not follow Bosanquet's model.

Keywords: capillary rise, capillary penetration, contact angle, advancing angle, receding angle, wetting, heterogeneous surface.

1. INTRODUCTION

The concept of capillary penetration has attracted considerable scientific attention over the years [1-12]. Capillarity has a significant role in many industrial and natural processes. Dying of fabrics in textile industry, ink printing, water motion in soils, and the capillary rise of water in plants are only a few examples.

Capillary penetration occurs only if the liquid wets the material of which the capillary is made i.e. when an equilibrium contact angle of less than 90° is achieved. The driving force for capillary penetration is the capillary pressure difference, which is predicted by the Laplace equation:

$$P_L = \frac{2\gamma}{R}\cos\theta \tag{1}$$

where θ is the apparent contact angle, γ is the liquid-gas interfacial tension and R is the radius of the capillary tube. For a vertical capillary, the effect of gravity is included:

$$\Delta P = \frac{2\gamma}{R}\cos\theta - \rho g x \tag{2}$$

where ρ is the density of the liquid, g is the acceleration of gravity, and x is the distance the liquid has risen above the surface of the reservoir (Figure 1). The maximum height of the liquid rise in the capillary at equilibrium is then:

$$h_{\max} = \frac{2\gamma\cos\theta_e}{\rho g R} \tag{3}$$

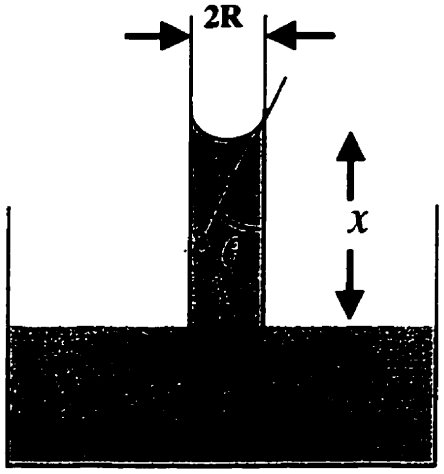

Figure 1- Spontaneous penetration into a single capillary

For a fully developed, laminar flow of a Newtonian liquid the average velocity of the liquid U can be calculated using Poiseuille's law:

$$U = \frac{dx}{dt} = \frac{R^2 \Delta P}{8\mu x} \tag{4}$$

Combining equations 2 and 4 yields:

$$T = -H^2 \left[\frac{X}{H} + \ln\left(1 - \frac{X}{H}\right) \right] \tag{5}$$

with

$$T = \frac{t}{\tau}, \tau = \frac{\mu R}{4\gamma \cos\theta}, X = \frac{4x}{R}, H = \frac{8\gamma \cos\theta}{\rho g R^2} \tag{6}$$

Assuming the effect of gravity to be negligible (a horizontal capillary of small x) and the contact angle to be constant, equation 5 gives Washburn's equation:

$$\frac{x}{R} = \left(\frac{\gamma \cos\theta}{2\mu R} t\right)^{1/2} \tag{7}$$

Hence the capillary rise is proportional to the square root of time, a relationship found for intermediate stages of penetration into long capillaries [2,3,7].

Experimental results show that Washburn's equation does not precisely predict the liquid penetration at small times. The initial penetration velocity according to Washburn's equation equals infinity while in practice it has a finite value [1,2,3,7]. Bosanquet [2] accounted for the inertia of the liquid at small times and derived a finite initial penetration velocity:

$$U_B = \left(\frac{2\gamma \cos\theta}{\rho R}\right)^{1/2} \tag{8}$$

Thus in the initial stages of penetration the liquid rises linearly with time. Equation 8 gives a rough estimate for the initial penetration velocity into wide capillaries [2].

Although equation 7 is widely used, it is known that the contact angle of a liquid while wetting a solid surface is a function of velocity of the contact line [1,4,5,8]. Hoffman [4] studied the shape of the advancing liquid-air interface in a glass capillary for a system where the viscous and interfacial forces were dominant. He argued that when the interfacial forces between the liquid and the solid during the flow remain constant, the dynamic contact angle was a function of the capillary number plus the equilibrium contact angle between the liquid and the solid surface. Many other investigators have proposed empirical models for the change in the dynamic contact angle as a liquid penetrates inside a capillary [5]. Joos et al. [6] proposed that since under advancing conditions the dynamic contact angle is a function of velocity, which is not constant, the driving force for penetration in the Laplace equation (equation 1) should be a function of a dynamic contact angle and not the static (or equilibrium) contact angle. The empirical model they found for the dynamic contact angle θ_d of a liquid rising in a capillary has the form:

$$\cos\theta_d = \cos\theta_0 - 2(1+\cos\theta_0)Ca^{1/2} \tag{9}$$

where θ_0 is defined as the static advancing contact angle and Ca is the capillary number defined as:

$$Ca = \frac{\mu U}{\gamma} \tag{10}$$

Substituting equation 9 for the cosine of the contact angle in equation 2 and assuming the static advancing contact angle (θ_0) to be zero (at equilibrium the liquid completely wets

the capillary) Joos et al. [6] developed the following dimensionless model for capillary rise:

$$X\frac{dX}{dT}+4(\frac{dX}{dT})^{1/2}=1-\frac{X}{H} \tag{11}$$

with

$$T=\frac{t}{\tau},\tau=\frac{\mu R}{4\gamma},X=\frac{4x}{R},H=\frac{8\gamma}{\rho gR^2} \tag{12}$$

Subject to at $T = 0$, $X = 0$. Joos et al. found good agreement between their experimental measurements of capillary rise for three types of silicon oils in glass tubes and numerical solutions of equation 11.

The problem of capillary rise in capillaries with chemical heterogeneity, to the best of our knowledge, has not been directly addressed in the literature. However, sticking of a small liquid column in dirty capillaries has been attributed to contact angle hysteresis [9]. In this study, the objective was to elucidate the effect of chemical heterogeneity of the solid surface on the dynamics of capillary rise. Latex particles (cationic polystyrene) were deposited on glass capillaries in order to produce hydrophobic domains on a hydrophilic surface (glass). Changing the deposition time varied the surface coverage of the hydrophobic domains. The deposited latex particles were annealed above T_g to secure the particles on the surface. Capillary rise experiments with water were then carried on these partially hydrophobized capillaries.

2. EXPERIMENTAL

2.1. Materials

A cationic polystyrene latex suspension was used to create hydrophobic domains inside the capillaries and on the glass slides used for the wetting experiments. The glass transition temperature for these particles was T_g=108°C. The cationic polystyrene suspension was provided by *Hercules Inc.* (Wilmington, Delaware, USA). The suspension had 28.15% total solids with a mean particle size of 620 nm. Before use, the polystyrene suspension was diluted to 200 ppm with de-ionized distilled water.

Glass capillaries from *Drummond Scientific Company* (Broomall, PA, USA) (radii: 0.3 and 0.8 mm) were used. Before deposition, the capillaries were cleaned in nitric acid for at least three hours, rinsed with de-ionized distilled water and air-dried. The clean capillaries were then dipped into a 200 ppm cationic polystyrene suspension for latex deposition. During deposition the suspension was constantly stirred at a low speed. Deposition time was varied between 1 minute and 1 hour. After deposition, the capillary tubes were rinsed in de-ionized distilled water and annealed for 2 hours at 150°C.

For the wetting experiments, pre-cleaned glass slides (*Fisher*, 75×25 mm^2) were re-cleaned using the method described above. The same method was also used for latex deposition. After deposition, one side of each glass slide was wiped in order to have particles only on one side of the surface for microscopy and surface coverage measurements. The prepared samples were then hung to dry in air. Finally, the glass slides were placed into an oven at 150°C for two hours.

2.2. Methods

2.2.1. Surface Coverage Measurement

After deposition, each glass slide was examined under a reflectance microscope at 50x-magnification. Images were analyzed with the image analysis software *Image Pro Plus* (Media Cybernetics, version 3.0). The background of each image was adjusted to achieve a good contrast between the particles and the background. The particles were then counted and their projected surface area was measured. Glass slides were examined using scanning electron microscopy (SEM). Atomic force microscopy (AFM, Digital Instruments Nanoscope II system) was used to measure the height of the latex particles after annealing on the glass slides. The surface coverage of the hydrophobic domains inside the capillaries was assumed to be equal to the surface coverage measured on a glass slide for the same deposition times.

2.2.2. Contact Angle and the Advancing Angle Measurement

The contact angles of de-ionized distilled water droplets on the polystyrene-deposited glass samples were measured using a *Dynamic Angle Analyzer* manufactured by *First Ten Angstroms* (Portsmouth, VA, USA). The system consisted of an automatic forward/reverse syringe pump, a mobile platform, a CCD video camera equipped with a 6:1 zoom microscope lens, and a computer. The details of measurement are described elsewhere [18,19]. Sixty images per second were captured by the camera for these measurements. The apparent contact angle $\theta(t)$ and the location of the contact line d of the droplets while at rest on the surface were measured for each captured image. The advancing contact angle and the receding contact angle of water droplets were also measured on the latex deposited glass slides. To measure the advancing angles θ_a, the

syringe needle was brought very close to the glass surface and the contact angle was measured while the volume of the droplet was increased. For these measurements the droplet was in contact simultaneously with the needle and the glass surface at the same time- see Figure 2. The receding contact angles were measured subsequently while decreasing the volume of the droplet on the surface.

2.2.3. Capillary Rise Measurement

The partially hydrophobized capillaries were used for capillary rise experiments. Capillary tubes were put in contact with de-ionized distilled water and the capillary rise dynamics were captured using a CCD video camera. De-ionized distilled water was placed in a cylindrical glass dish on an adjustable platform. The capillaries were suspended vertically from the top and the glass dish was raised until the capillaries just touched the water surface. The video images were analyzed by *Image Pro Plus*.

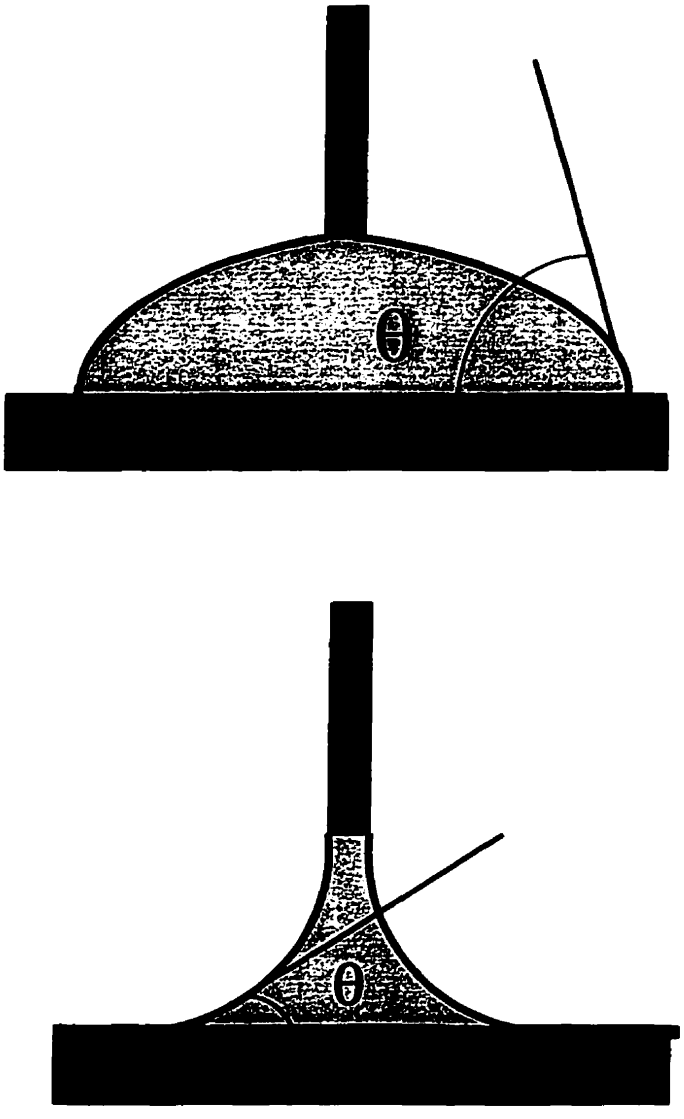

Figure 2- Contact angle measurement on a flat surface; a) advancing angle measured as the volume increases; b) receding angle measured as the volume decreases.

3. RESULTS

The surface coverage of the hydrophobic domains measured on glass slides varied between 1 and 45% [18]. Figure 3 is a SEM image of the hydrophobic domains on a glass slide after annealing. After annealing, most of the spherical latex particles attained a spherical cap shape. The average peak height measured by AFM for the annealed particles was 240±95 nm for 30 particles. The size distribution of the hydrophobic domains on a glass slide after 10 minutes exposure to the latex suspension is shown in Figure 4. The hydrophobic domains have a unimodal size distribution with more than 80% of the hydrophobic domains being in the range of 1.2-2.2 μm in diameter.

The advancing, receding and equilibrium contact angles of water droplets on glass slides with different surface coverage of the hydrophobic domains were measured [18]. An example of contact angle hysteresis on a glass slide with 16.2% coverage of latex particles is shown in Figure 5. Two replicates are shown for each of the advancing and receding contact angles measured. The smoothness of the curves in each case may indicate that roughness has a negligible effect on wetting. The receding contact angle for one replicate starts at a higher contact angle and eventually drops to an equilibrium lower value. This type of behavior is typically seen on heterogeneous surfaces were a stick and jump movement of the contact line is observed.

The dynamic rise of water in capillaries partially hydrophobized to different coverages is shown in Figure 6. The maximum capillary rise was a strong function of the surface coverage of hydrophobic domains, while the rate of capillary rise for the first 0.5 s was not. Three replicates were run for each surface coverage.

Figure 3- Scanning electron microscopy of annealed latex particles on glass slide

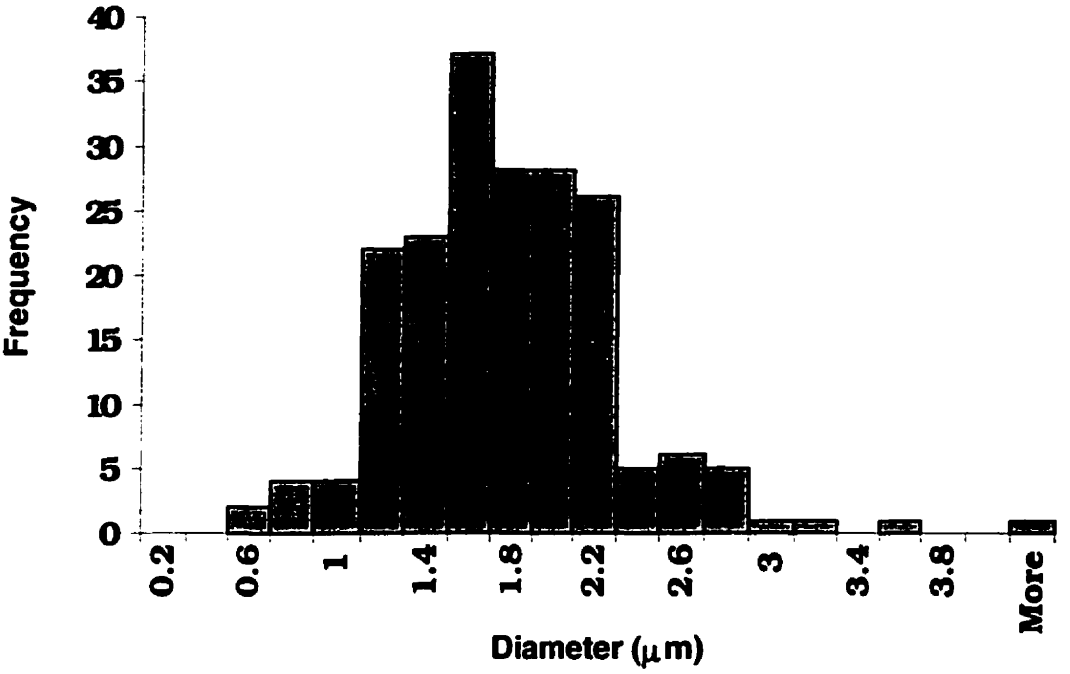

Figure 4- Size distribution of latex particles annealed on a glass slide for 2 hours. The deposition time was 10 minutes and the coverage was 16%.

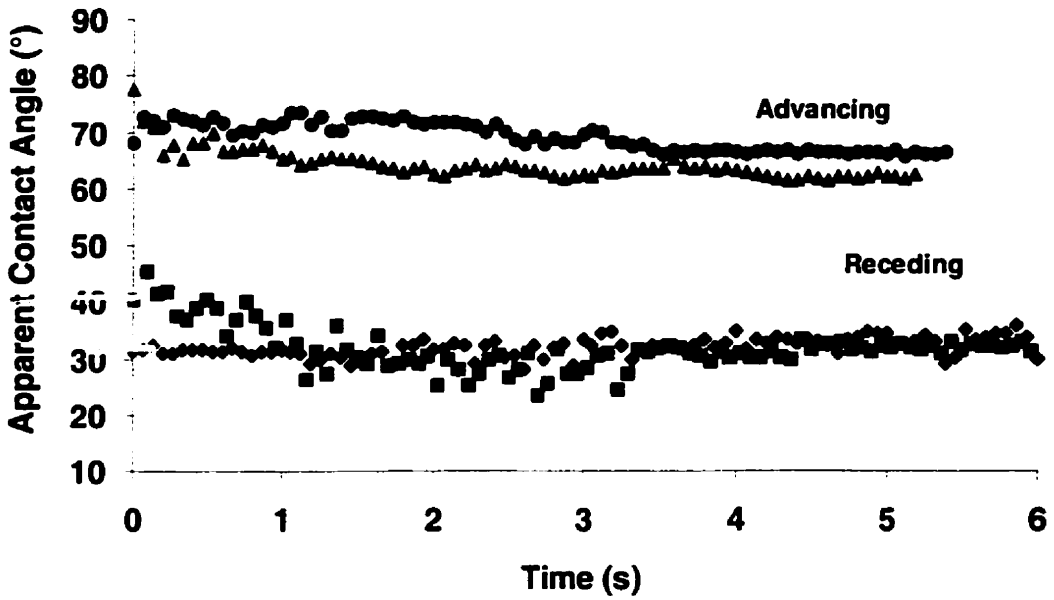

Figure 5- The advancing and receding contact angles of water on a glass slide with 16% surface coverage of annealed latex particles. Two replicates are shown.

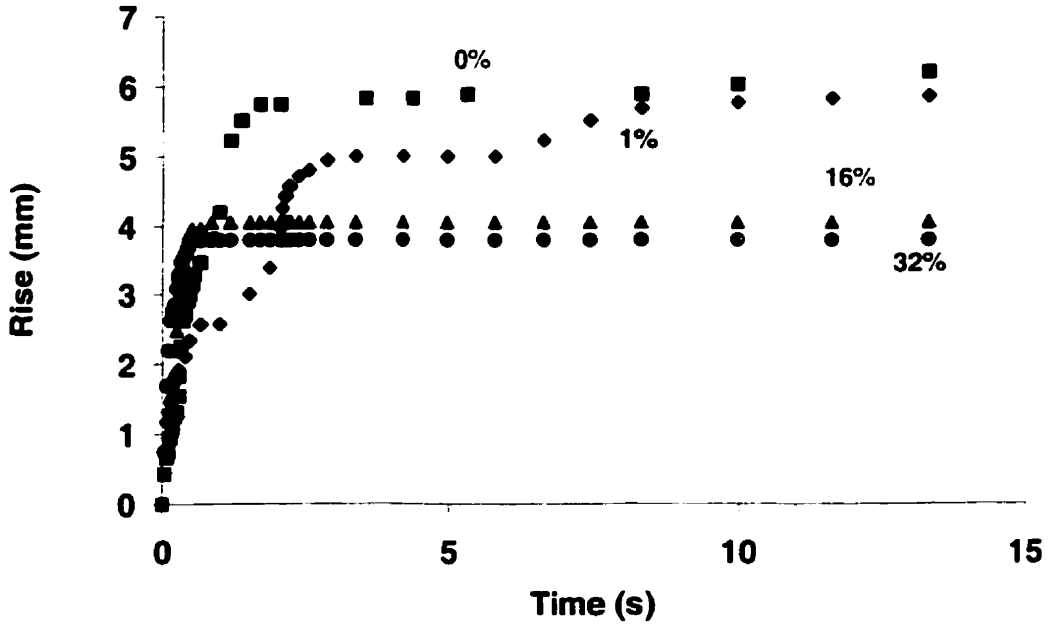

Figure 6- Capillary rise dynamics in capillaries of 0.8 mm radius. The percent surface coverage of hydrophobic domains is shown on each curve.

Figure 7 shows that for one replicate capillary penetration was smooth while for another there was a stick and jump movement of the water meniscus (three phase contact line). This stick and jump movement of the contact line was more noticeable for lower surface coverages of hydrophobic domains. The poor reproducibility of the dynamics of capillary rise for medium to long times was related to the stick and jump movements of the contact line.

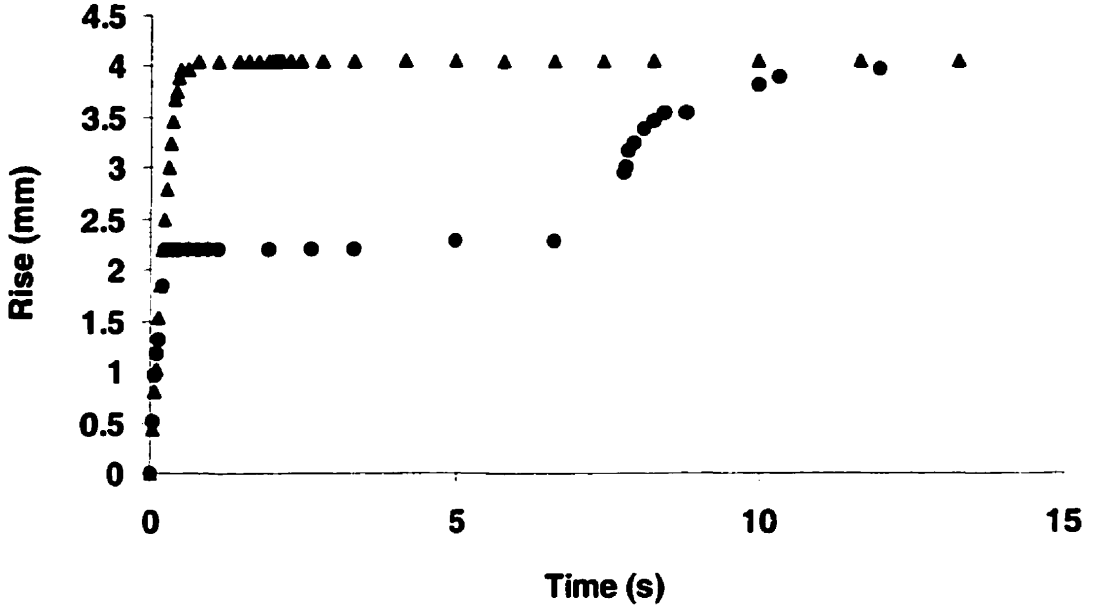

Figure 7- Reproducibility of capillary rise dynamics in capillaries of 0.8 mm radius with 16% coverage of hydrophobic domains. The stick and jump of the contact line is shown for one replicate.

4. DISCUSSION

The approach proposed by Joos et al. [6] for modeling the capillary rise by introducing a dynamic contact angle in equation 2 was used. Capillary rise following Washburn's model with a constant contact angle under the effect of gravity (equation 5) was also compared to the experimental data.

Figure 8 compares the experimental data obtained for the capillary rise with two models. These two models are: 1- Equation 5 (Washburn's model including the effect of gravity) and assuming that water rises in the capillary with the advancing angle measured on a glass slide with the same latex coverage ($\theta=\theta_a$) 2- A new model based on equation 11 (Joos's model) modified for $\theta_0=\theta_a$.

The second model was found by combining equations 2, 4, and 9 and then solving the following differential equation numerically:

$$X\frac{dX}{dT}+2(1+\cos\theta_a)\left(\frac{dX}{dT}\right)^{1/2}=\cos\theta_a-\frac{X}{H} \qquad (13)$$

From this comparison it is evident that the dynamic contact angle has a significant role in the dynamics of capillary penetration. Equation 13 makes a better prediction than Washburn's model for the capillary rise by including the change in the contact angle due to velocity. Since water did not completely wet the capillary ($\theta_0 \neq 0$), Joos's model (equation 11) was not applicable to our experimental data. The better agreement between the experimental data and equation 13 shows the sensitivity of the dynamics of capillary rise to the value of the static advancing angle (θ_0). In this model, θ_0 is taken from the measurements of the advancing contact angle on a glass slide which was exposed to the latex suspension for the same time as the capillary.

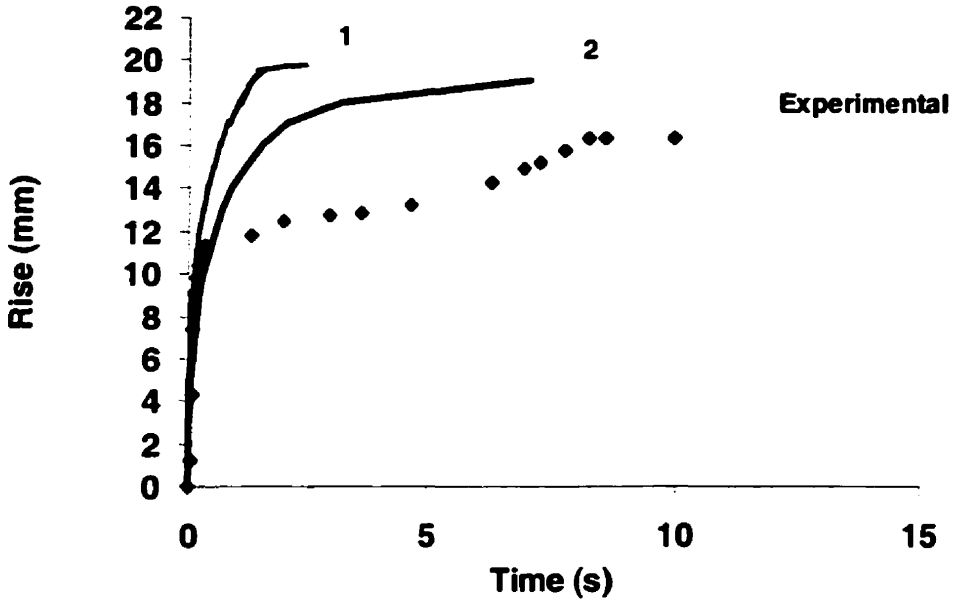

Figure 8- Capillary rise dynamics in capillaries of 0.3 mm radius and 1% coverage of hydrophobic domains. Curves: 1) Equation 5 (Washburn's model with gravity) assuming $\theta = \theta_a$; 2) Equation 13, assuming $\theta = \theta_a$

This was based on the assumption of having the same surface coverage of the hydrophobic domains inside the capillary as on the flat surface for the same deposition time. Considering the size proportion of the particles to the radius of the capillary tubes this assumption is justified.

Although this modification improves the agreement between the model and actual data, the real system has slower dynamics. Previous studies on dynamics of wetting on heterogeneous surfaces [15,19] show that surface heterogeneity reduces the wetting rate when the three phase contact line has non-equilibrium stick and jump movements. During advancement, the three phase contact line encounters high energy and low energy domains on the surface. The metastable stick and jump movements are due to the energy barriers existing between these domains [14] which cause local pinning of the contact line to the hydrophobic domains on the surface. In fact due to these pinning sites the contact line curves around each hydrophobic domain until it completely surrounds them (Figure 9). A sudden advance (jump) of the contact line occurs when the angle the liquid forms at the edge of the hydrophobic domain surpasses a critical angle defined by the geometry. This type of behavior has been referred to as the edge effect in the literature [15].

Curve fitting the capillary rise experimental data (Figure 10) shows that agreement with equation 9 can be improved by changing the static advancing angle (θ_0). The agreement between the model and experimental data shows that the static advancing contact angle during the water rise inside a heterogeneous capillary is not constant.

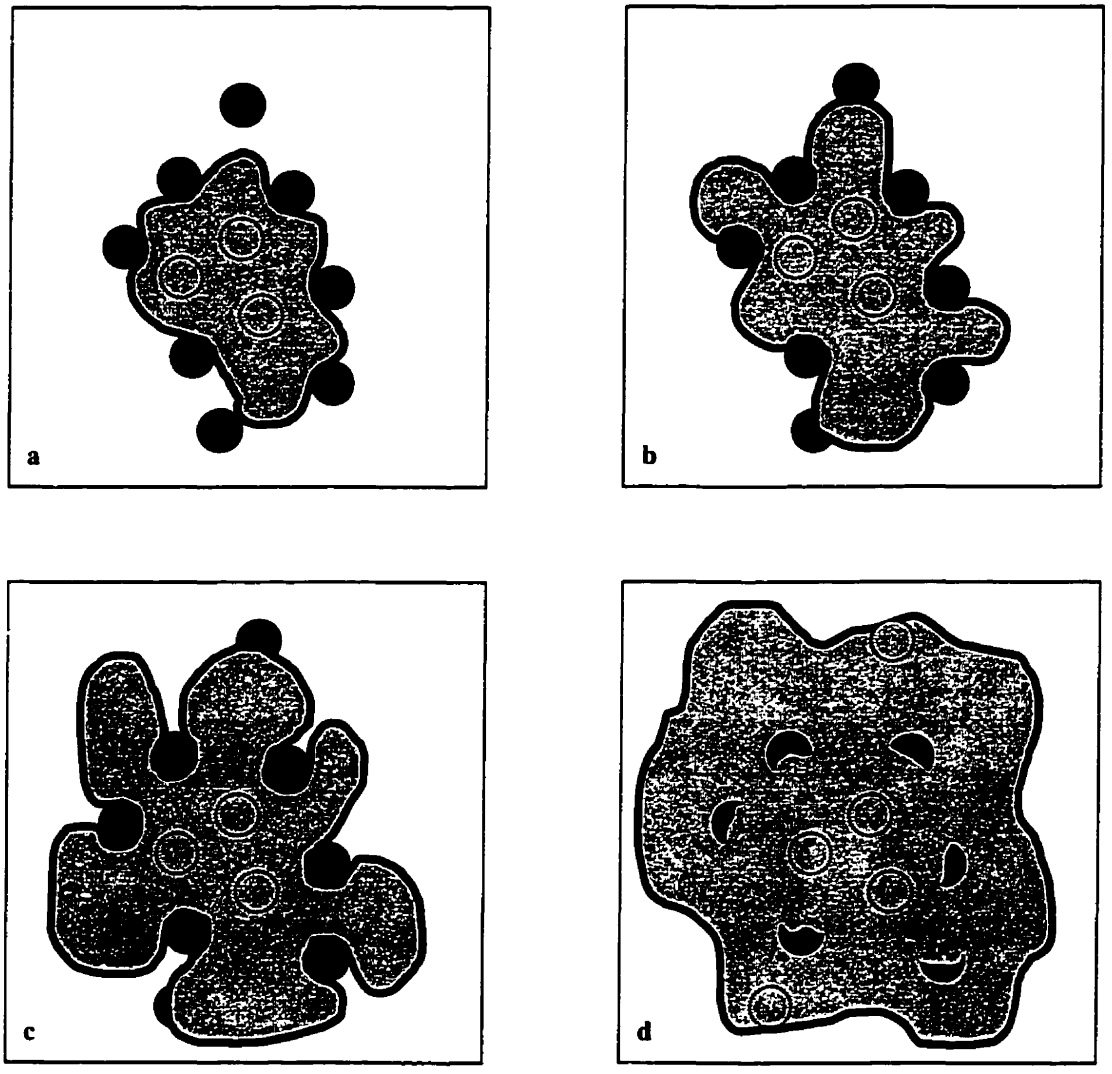

Figure 9- Schematic representation of the three phase contact line advancement in presence of hydrophobic domains. a) The contact line is pinned at the contact point to the hydrophobic domains; b & c) The contact line curves around the hydrophobic domains as water proceeds; d) The sudden jump of contact line over the hydrophobic domains.

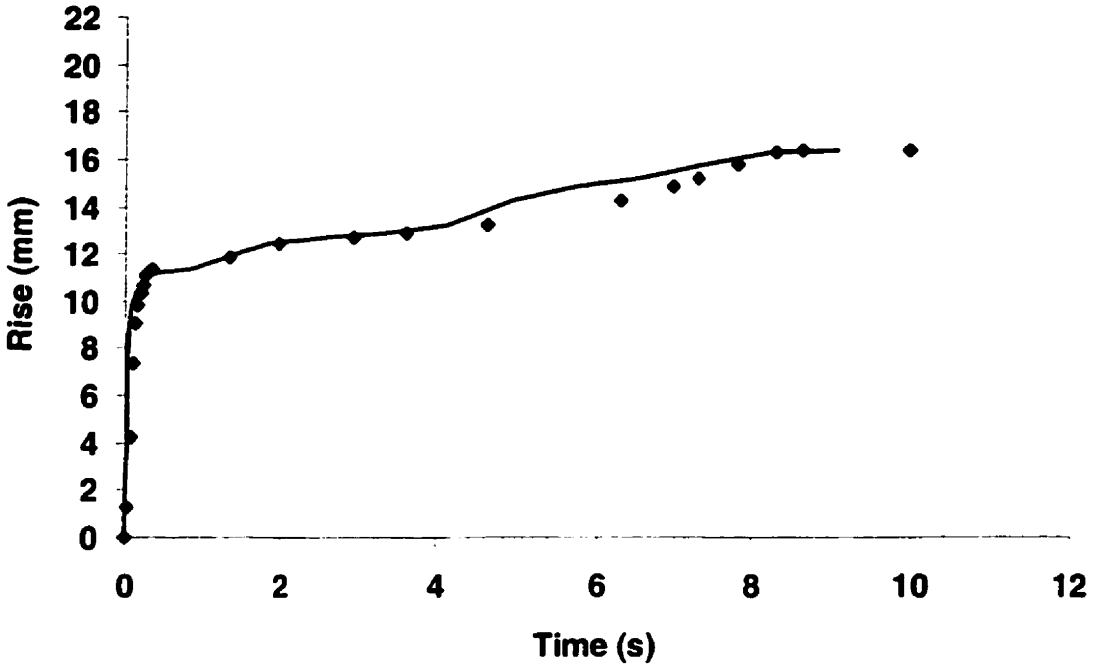

Figure 10- Capillary rise dynamics in capillaries of 0.3 mm radius and 1% coverage of hydrophobic domains. The solid line is the model.

In fact, since there is a non-uniform distribution of the hydrophobic domains inside the capillaries, the local static advancing contact angle should be a function of the location of the point of contact ($\theta_0 = f(z, \theta)$ where z, θ are the cylindrical coordinates). Therefore, for a heterogeneous surface equation 9 should be modified to account for the local change in the static advancing angle:

$$\cos\theta_d = \cos\theta_0(z,\theta) - 2(1+\cos\theta_0(z,\theta))Ca^{1/2} \qquad (14)$$

The contact angle a liquid forms on a heterogeneous surface in theory, is known to be proportional to the surface coverage of the heterogeneous domains [16,17]. The wetting experiments performed on latex deposited glass slides showed that the equilibrium contact angle measured on these surfaces is in fact an average contact angle around the three phase contact line (θ_{eff}) which is a function of the linear fraction of the drop perimeter that is in contact with different domains [18]. Hence, the effective static advancing contact angle is only a function of the location of the three-phase contact line ($\theta_0 = f(z)$) in the direction of flow.

Due to the large hysteresis, there are infinite number of possible equilibrium angles between the receding and the advancing angle that can be formed between the water and the capillary wall [14,15]. Hence, the static advancing angle can change within a wide range limited by the advancing and receding angles as water rises inside the capillaries. However, the significance of change in the static advancing angle on the dynamics of capillary rise is not the same in all stages. In the initial stages, when the velocity of liquid is high the capillary number is large and it is the second term in equation 14 that is significant. Hence, at small times, dynamic contact angle is more sensitive to the change in velocity and surface heterogeneity has a negligible effect. In

the final stages, when capillary rise is slower, the first term in equation 14 is more significant. Hence the capillary rise dynamics is controlled by the surface heterogeneity.

Bosanquet's model (equation 8) combined with the dynamic contact angle from equation 9 was also compared to the experimental data at the early stages of penetration. The experimental data did not agree with Bosanquet's model even at the very early stages of penetration for either of the capillaries used. One explanation is that our measurements were not taken at small enough times.

5. CONCLUSION

The dynamics of capillary rise of water in partially hydrophobized capillaries were investigated. Increasing surface coverage of the hydrophobic domains decreased the maximum equilibrium rise of water inside the capillaries. Presence of the hydrophobic domains reduced the rate of capillary penetration by inducing metastable stick and jump movements of the contact line. The hydrophobic domains provided local pinning sites on the contact line which affected the static advancing angle.

The model proposed by Joos et al. [6] was modified by replacing θ_0 (=0 in Joos's model) with the advancing contact angle (θ_a) measured for water on a glass slide with the same coverage of the hydrophobic domains. The model was improved further when the static advancing angle was varied as a function of the position of the three phase contact line in the final stages of capillary rise. However, in the initial stages the effect of surface heterogeneity on the capillary rise was insignificant.

6. ACKNOWLEDGEMENTS

This research was funded by the Natural Sciences and Engineering Research Council of Canada, and by Hercules Inc.

7. REFERENCES

1. S. Middleman, Modeling axisymmetric flows, dynamics of jets, films and drops, Academic Press Inc., **1995**.
2. K.G. Kornev and A.V. Neimark, Spontaneous penetration of liquids into capillaries and porous membranes revisited, Journal of Colloid and Interface Science, **2001**, 235, 101-113.
3. B.V. Zhmud, F. Tiberg and K. Hallstensson, Dynamics of capillary rise, Journal of Colloid and Interface Science, **2000**, 228, 263-269.
4. R.L. Hoffman, A study of advancing interface, I. Interface shape in liquid-gas systems, Journal of Colloid and Interface Science, **1975**, 50, No. 2, 228-241.
5. P.G. de Gennes, Wetting: statics and dynamics, Reviews of Modern Physics, **1985**, No. 3, Part I.
6. P. Joos, P. Van Remoortere and M. Bracke, The Kinetics of wetting in a capillary, Journal of Colloid and Interface Science, **1990**, 136, No 1, 189-197.
7. E.W. Washburn, The dynamics of capillary flow, The Physical Review, **1921**, 17, 273-283.
8. J. Szekely, A.W. Neumann, and Y.K. Chuang, The rate of capillary penetration and the applicability of the Washburn equation, Journal of Colloid and Interface Science, **1971**, 35, No. 2, 273-278.
9. P. Van Remoortere and P. Joos, The kinetics of wetting: the motion of a three phase contact line in a capillary, Journal of Colloid and Interface Science, **1991**, 141, No. 2, 348-359.

10. A. Marmur, Penetration of a small drop into a capillary, Journal of Colloid and Interface Science, **1988**, 122, No 1, 209-219.

11. A. Borhan and K.K. Rungta, Lucas-Washburn kinetics for capillary penetration between periodically corrugated plates, Journal of Colloid and Interface Science, **1993**, 155, 438-443.

12. E. Chibowski and L. Holysz, On the use of Washburn's equation for contact angle determination, Journal of Adhesion Science Technology, **1997**, 11, No. 10, 1289-1301.

13. A. Marmur and R.D. Cohen, Characterization of porous media by the kinetics of liquid penetration: The vertical capillaries model, Journal of Colloid and Interface Science, **1997**, 189, 299-304.

14. R.E. Johnson and R.H. Dettre, Contact angle hysteresis. III. Study of an idealized heterogeneous surface, The Journal of Physical Chemistry, **1963**, 68, 1744-1750.

15. J.F. Oliver, Effect of surface roughness on wetting, Ph.D. thesis, **1975**, McGill University, Montreal, Quebec, Canada.

16. A.B.D. Cassie, Contact Angles, Discussion of Faraday Society, **1948**, 3, 11-16.

17. P.S. Swain and R. Lipowsky, Contact angles on heterogeneous surfaces: a new look at Cassie's and Wenzel's laws, Langmuir, **1998**, 14, 6772-6780.

18. H. Modaressi and G. Garnier, Wetting on a heterogeneous surface, manuscript for publication, **2001**.

19. H. Modaressi and G. Garnier, Mechanism of wetting and absorption of water droplets on sized paper: Effects of chemical and physical heterogeneity, submitted to Langmuir, **2001**.

CHAPTER 6

1. CONCLUSIONS

The phenomenon investigated in this thesis is the effect of surface heterogeneities on the wetting of paper and partially-hydrophobized glass surfaces by water droplets. The conclusions from this work for each of the individual chapters is summarized as follows.

1.1. Effect of sizing on wetting and absorption properties of paper

The effect of sizing on wetting and absorption of water droplets onto paper was investigated. Wetting and absorption were found to be two sequential phenomena. At the end of wetting, a water droplet exhibited a pseudo-equilibrium contact angle, which was a function of the concentration of the hydrophobic surface sizing polymers on papers. The delay before absorption was a function of the chemical composition of the surface sizing polymers used. During this delay (at the end of the wetting period) the water-soluble sizing polymers on the paper surface partially dissolved into the droplet. This reduced the pseudo-equilibrium contact angle of water droplets below 90°, which then allowed absorption to start.

Surface sizing affected the rate of water absorption into paper to a limited extent. The Hercules sizing test (HST), a conventional technique used to quantify sizing of a paper sheet, was found to be a reliable method for highly sized papers.

1.2. Dynamics of wetting and absorption of sized papers

The effect of physical and chemical heterogeneity of a paper surface on the dynamics of wetting and absorption was quantified. Micron-scale roughness reduced the

rate of wetting by locally pinning the three-phase contact line to the paper surface, hence the three phase contact line moved with a stick and jump behavior. Reducing the roughness by calendering the papers reduced the stick and jump behavior. The dynamic contact angle of water droplets on paper agreed with the Hoffman-Tanner equation, modified for roughness. The wetting rate was not affected by the chemical composition of the surface sizing agents. Surface roughness also enhanced the hydrophobicity of paper by entrapping air within the roughness valleys.

1.3. Wetting on a heterogeneous impermeable surface

Wetting experiments with water droplets on glass slides with hydrophobic domains revealed that contact angle increased with increasing surface coverage of the hydrophobic domains. Cassie's equation underestimated the hydrophobicity of the surface This deviation was not due to roughness. The contact angle of water droplets was a function of the fraction of the three phase contact line in contact with the hydrophobic domains on glass slides. The effect of roughness on the contact angle agreed with Wenzel's equation.

1.4. Capillary penetration in partially hydrophobized vertical capillaries

Capillary rise was a function of the surface coverage of hydrophobic domains inside the capillaries. The rate of rise was reduced by a stick and jump behavior due to pinning of the contact line to the hydrophobic sites on the surface.

Maximum capillary rise (equilibrium height) predicted by using the advancing contact angles measured for water droplets on flat glass slides with the same level of hydrophobicity, agreed with actual measurements. Two mechanisms controlled the capillary rise dynamics. First, at higher velocities the dynamic contact angle changed as

a function of the velocity of the three phase contact line. Second, at lower velocities, the capillary rise dynamics was a function of the change in the static contact angle due to local heterogeneities on the surface.

2. CONTRIBUTIONS TO KNOWLEDGE

The main contributions to knowledge are:

1. When a water droplet is placed on surface-sized paper, wetting and absorption occur consecutively.

2. The duration of the delay before absorption is a function of the chemical composition of the paper surface after surface sizing. During this time the water-soluble polymers on the surface dissolve into the droplet, changing the contact angle to below 90° before absorption begins.

3. Micron-scale roughness on paper reduces the wetting rate significantly. The Hoffman-Tanner model for the dynamics of wetting on smooth surfaces, when modified by a roughness factor, predicts wetting dynamics on paper.

4. Cassie's equation underestimates the hydrophobicity of the glass/polymer surface. Roughness effect on the contact angle agrees with Wenzel's equation.

5. The final height of rise of water in a partially hydrophobized glass capillary is a function of the surface fraction of heterogeneities.

6. Using the advancing contact angle of water measured on a flat surface, the equilibrium height of water inside a capillary with the same level of heterogeneity can be predicted.